COO-2262-5
MITNE-171

FINITE ELEMENT SYNTHESIS METHOD

by
Shi-tien Yang, Allan F. Henry

May 1975

Department of Nuclear Engineering
Massachusetts Institute of Technology
Cambridge, Massachusetts

AEC Research and Development Report
Contract AT(11-1)-2262
U.S. Atomic Energy Commission

MASSACHUSETTS INSTITUTE OF TECHNOLOGY

DEPARTMENT OF NUCLEAR ENGINEERING

Cambridge, Massachusetts 02139

FINITE ELEMENT SYNTHESIS METHOD

by

Shi-tien Yang, Allan F. Henry

May 1975

COO - 2262 - 5

MITNE - 171

AEC Research and Development Report

Contract AT(11-1)2262

U.S. Atomic Energy Commission

FINITE ELEMENT SYNTHESIS METHOD

by

Shi-tien Yang

Submitted to the Department of Nuclear Engineering on May 2, 1975 in partial fulfillment of the requirements for the degree of Doctor of Philosophy

ABSTRACT

A coarse mesh approximation method is presented for the solution of the two-dimensional spatial neutron flux in multigroup diffusion theory. This so-called finite element synthesis method is consistent in that it is systematically derived as an extension of the finite element method by utilizing general variational techniques. Detailed subassembly solutions, found by imposing zero current boundary conditions over the surface of each subassembly, are modified by piecewise continuous Hermite polynomials of the finite element method and used directly in trial function forms.

The finite element synthesis method differs substantially from the finite element method in which homogeneous nuclear constants, homogenized by flux weighting with detailed subassembly solutions, are used. However, both schemes become equivalent when the subassemblies themselves are homogeneous.

The application of this method to some representative one-dimensional PWR configurations has been shown to be successful. However, the extension of two-dimensional problems is not as straightforward as it might appear to be, because there are flux discontinuities at subassembly boundaries. Thus, some additional terms, representing the contribution of the flux (and current) discontinuities, has to be added to the difference equations of the approximation method.

Two-dimensional, two-group numerical calculations using representative nuclear material constants for fuel, absorber and moderator and 18 cm x 18 cm subassemblies were performed using entire subassemblies as coarse mesh regions. The results indicate that the finite element synthesis method can yield accurate criticality predictions and detailed flux shapes throughout a core composed of heterogeneous subassemblies.

Thesis Supervisor: Allan F. Henry
Thesis Reader: Kent F. Hansen
Titles: Professors of Nuclear Engineering

ACKNOWLEDGEMENTS

I would like to thank and express my deep appreciation and sincerest gratitude to Prof. Allan F. Henry, my thesis supervisor, for the constant guidance, consultation and encouragement provided during the course of this study. Appreciation must also be extended to my thesis reader, Prof. Kent F. Hansen, for his assistance in reviewing the final manuscript and providing many helpful discussions.

The work was performed under USAEC Contract AT(11-1)2262, with the computations performed at the M.I.T. Information Processing Center and the Laboratory of Nuclear Science.

Special appreciation is extended to my wife, Yu-fen. Without her encouragement and understanding, this work would be impossible.

Finally, special thanks are expressed to Mrs. Stephanie Demeris who typed this thesis with skill and patience.

TABLE OF CONTENTS

LIST OF FIGURES

LIST OF TABLES

CHAPTER 1

INTRODUCTION

1.1 Introduction

This thesis is concerned with the numerical solutions for static neutron diffusion problems using finite element piecewise polynomials combined with synthesis techniques in space variables.

The study of the solutions for the neutron diffusion problem is important, both in reactor economics and reactor safety. One major concern of the reactor physicist is that the prediction of the behavior of a reactor after any foreseeable nuclear accident. A detailed safety analysis can only be obtained if all the physical processes occuring within the reactor can be fully understood and related to each other. Since all these processes can be shown to be independent on the neutron flux distribution throughout the reactor, a detailed and accurate solution of the spatial neutron flux is vital [1].

A sufficiently detailed description of the physical process occurring within a nuclear reactor is the Boltzmann neutron transport equation [2]-[3]. It is essentially a neutron balance equation in any point, any angle within a reactor system at any time and is very difficult to solve. The P-1 and diffusion theory approximation [4] greatly simplifies the transport equation into more tractable forms and has been found to give an adequate approximation for the

flux distribution for most large-core reactors.

Because of the complexity of reactor geometries and nuclear cross sections, numerical methods have been widely used to solve the neutron diffusion problems and have been shown to be more powerful than analytical methods. The most widely used method is the finite difference method [5]-[6], which is quite simple in principle but which requires relatively small meshes and hence a large number of unknowns. Thus, if hundreds of thousands of mesh points are desired, it is extremely expensive to obtain the solution today. For this reason, finite difference methods have generally been limited to kinetic problems involving only a few thousand mesh points or to relatively coarse mesh three-dimensional problems, and alternate methods have been developed which require determination of a smaller number of unknowns and yet which can be applied to complex multidimensional problems.

During the past fifteen years or so a class of approximation methods known as "synthesis methods" have been developed. The theoretical basis of modern flux synthesis methods was introduced into reactor physics by Selengut [7] within the context of variational analysis. Calame and Federighi [8] and Kaplan [9]-[10] were among the first to exploit these methods for synthesizing the spectral and spatial dependences, respectively, of the neutron flux distribution. Other workers [11]-[19] have subsequently extended and tested these techniques until today there exists a sizable

literature on these methods.

The central idea of the synthesis methods is to express the soltuion in terms of a small number of functions chosen to represent various transient states of the problem. The advantage of this method is that the expansion functions may be based on the knowledge of a particular system. However, the selection of proper expansion functions for various systems is difficult particularly if feedback effects of a priori, unknown magnitude are involved. Poor selection of expansion functions can misrepresent the solution to an extent that is not determinable in a systematic way. Therefore, there is a need to improve on the synthesis procedure, particularly for space dependent kinetic problems for complex geometrical systems.

Another computational technique which has been most highly developed in structural mechanics [20]-[21] and fluid flow [22]-[23] is the finite element method. Its application to the neutron diffusion equation made a few years ago has been shown to be quite successful [24]-[26]. Briefly, it is a process by which, given the defining equation of a problem, one seeks to discretize the equation by dividing the problem domain into a substantial number of sub-domains, referred to as elements. Interpolation functions (usually piecewise polynomials) are formulated within each element in terms of parameters associated with nodes on the element boundaries. Then these nodal parameters are related by the use of some continuity conditions across the interfaces of adjacent elements. The

variational method or weighted residual method is then applied to yield a set of simultaneous algebraic equations for the nodal parameters. Finally, the approximate solution to the problem is obtained by the use of a computer.

The advantage of the finite element method is that for a given degree of accuracy, it requires a smaller number of mesh points and thus hopefully less computational time relative to the conventional finite difference method. Also, (in distinction to the synthesis method) an error analysis can be performed to find the error bounds of the approximate solution [27]-[29]. However, when this coarse mesh method is applied to reactor systems with very complex geometrical complications, the important flux dips and peaks in small control rods and water holes, respectively, cannot be accurately predicted unless a considerable number of meshes are placed in these regions. Thus, the problem comes back to that of reducing the number of unknowns while retaining the accuracy of the flux distribution in highly heterogeneous regions.

The idea of combining finite element basis functions with the synthesis technique in solving the neutron diffusion problems was first advanced by Bailey and Henry [30]. They used both linear and cubic Hermite piecewise polynomials multiplied into detailed subassembly solutions to describe the neturon flux and current and then used a variational principle to derive the desired set of difference equations. This method was applied to some

representative one-dimensional PWR configurations, consisting of many cells and showed good results compared with those of coarse mesh finite element methods. However, because the problems were one-dimensional, there were no continuities at cell boundaries. Thus it is not possible on the basis of this preliminary work to provide a reliable evaluation of the potential of the idea.

The purpose of this thesis is to extend the aforementioned finite element-synthesis scheme to two-dimensional problems by using a variational technique. Such an extension is not as straightforward as it might appear to be since, in the two dimensional case, there are flux discontinuities at cell boundaries. For example, consider two adjacent subassemblies in a square lattice. If one cell contains a cross-shaped control rod and the other has its control rod out resulting in a large cross-shaped water hole, the flux found by stitching two, zero-current subassembly solutions together will be discontinuous at the interface. Since potential errors in overall neutron balance and detailed flux shape are the matters of chief concern in extending to two dimensions, the thesis deals only with the spatial approximation for static cases. Extension to time dependent problems is left for future study.

1.2 The Time-independent, Multigroup Diffusion Theory Equations

In this section, the time-independent, energy-discretized multigroup P-1 approximation to the Boltzmann neutron transport

equation is introduced. The derivation can be found in Glasstone [31] and elsewhere [4], [32].

The standard form of the P-1 equations for each energy group g is as follows:

$$\underline{j}_g(\underline{r}) + D_g(\underline{r})\underline{\nabla}\phi_g(\underline{r}) = 0 \tag{1.1a}$$

$$\underline{\nabla}\cdot\underline{j}_g(\underline{r}) + \Sigma_g(\underline{r})\phi_g(\underline{r}) - \sum_{\substack{g'=1 \\ g'\neq g}}^{G} \Sigma_{gg'}(\underline{r})\phi_{g'}(\underline{r}) = \frac{1}{\lambda}\phi_g \sum_{g'=1}^{G} \nu\Sigma_{fg'}(\underline{r})\phi_{g'}(\underline{r}) \tag{1.1b}$$

where the group index g runs from the highest energy group, 1, to the lowest energy group, G. The symbols and notations used throughout this thesis are summarized in Appendix A. The net current vector $\underline{j}_g(\underline{r})$ may be eliminated via Fick's Law, Equation 1.1a, to obtain the multigroup diffusion equations:

$$-\underline{\nabla}\cdot D_g(\underline{r})\underline{\nabla}\phi_g(\underline{r}) + \Sigma_g(\underline{r})\phi_g(\underline{r}) - \sum_{\substack{g'=1 \\ g'\neq g}}^{G} \Sigma_{gg'}(\underline{r})\phi_{g'}(\underline{r}) = \frac{1}{\lambda}\chi_g \sum_{g'=1}^{G} \nu\Sigma_{fg'}(\underline{r})\phi_{g'}(\underline{r}) \tag{1.2}$$

Both Equations 1.1 and 1.2 can be written in matrix form as

$$\underline{J}(\underline{r}) + \mathbb{D}(\underline{r})\underline{\nabla}\Phi(\underline{r}) = 0 \tag{1.3a}$$

$$\underline{\nabla}\cdot\underline{J}(\underline{r}) + [\mathbb{M}(\underline{r}) - \mathbb{T}(\underline{r})]\Phi(\underline{r}) = \frac{1}{\lambda}\mathbb{F}(\underline{r})\Phi(\underline{r}) \tag{1.3b}$$

and

$$-\underline{\nabla}\cdot\mathbb{D}(\underline{r})\underline{\nabla}\Phi(\underline{r}) + [\mathbb{M}(\underline{r}) - \mathbb{T}(\underline{r})]\Phi(\underline{r}) = \frac{1}{\lambda}\mathbb{F}(\underline{r})\Phi(\underline{r}) \tag{1.4}$$

respectively, where $\mathbb{D}(\underline{r})$, $\mathbb{M}(\underline{r})$, $\mathbb{T}(\underline{r})$, and $\mathbb{F}(\underline{r})$ are GxG matrices defined by

$$\mathbb{D}(\underline{r}) = \text{Diag}[D_1(\underline{r}), D_2(\underline{r}),---, D_G(\underline{r})] \tag{1.5a}$$

$$\mathbb{M}(\underline{r}) = \text{Diag}[\Sigma_1(\underline{r}),\Sigma_2(\underline{r}),---,\Sigma_G(\underline{r})] \tag{1.5b}$$

$$\mathbb{T}(\underline{r}) = \begin{bmatrix} 0 & -\Sigma_{12}(\underline{r})---- & -\Sigma_{1G}(\underline{r}) \\ -\Sigma_{21}(\underline{r}) & 0 \text{ -------} & -\Sigma_{2G}(\underline{r}) \\ \vdots & \vdots & \vdots \\ -\Sigma_{G1}(\underline{r}) & -\Sigma_{G2}(\underline{r}) --- & 0 \end{bmatrix} \tag{1.5c}$$

$$\mathbb{F}(\underline{r}) = \begin{bmatrix} \chi_1 \\ \chi_2 \\ \\ \chi_G \end{bmatrix} [\nu\Sigma_{f1}(\underline{r}), \nu\Sigma_{f2}(\underline{r}),---\nu\Sigma_{fG}(\underline{r})] \tag{1.5d}$$

and $\underline{J}(\underline{r})$ is the group current vector

$$\underline{J}(\underline{r}) = \text{Col}[\underline{j}_1(\underline{r}), \underline{j}_2(\underline{r}),\ldots,\underline{j}_G(\underline{r})] \tag{1.5e}$$

and $\Phi(\underline{r})$ is the group flux vector

$$\Phi(\underline{r}) = \text{Col}[\phi_1(\underline{r}),\ \phi_2(\underline{r}),\ldots,\phi_G(\underline{r})] \tag{1.5f}$$

It is also convenient to define the GxG group absorption, scattering the production matrix $\mathbb{A}(\underline{r})$

$$\mathbb{A}(\underline{r}) = \mathbb{M}(\underline{r}) - \mathbb{T}(\underline{r}) - \frac{1}{\lambda}\mathbb{F}(r) \tag{1.5g}$$

so that Equations 1.1 and 1.2 may be written simply as

$$\underline{J}(\underline{r}) + \mathbb{D}(\underline{r})\underline{\nabla}\Phi(\underline{r}) = 0 \tag{1.6a}$$

$$\underline{\nabla}\cdot\underline{J}(\underline{r}) + \mathbb{A}(\underline{r})\Phi(\underline{r}) = 0 \tag{1.6b}$$

and

$$-\underline{\nabla}\cdot\ \mathbb{D}(\underline{r})\underline{\nabla}\Phi(\underline{r}) + \mathbb{A}(\underline{r})\Phi(\underline{r}) = 0 \tag{1.7}$$

respectively. These forms of the group diffusion equations will be used throughout this thesis. The boundary conditions on $\Phi(\underline{r})$ accompanying these equations are of the homogeneous Dirichlet or Neumann type [33], namely

$$a_1\frac{\partial\Phi(\underline{r}_b)}{\partial\underline{n}} + a_2\,\Phi(\underline{r}_b) = 0$$

$$\text{if } a_1 = 0, \quad \text{then} \quad \Phi(\underline{r}_b) = 0, \quad \text{Dirichlet type} \tag{1.8a}$$

$$\text{if } a_2 = 0, \quad \text{then} \quad \frac{\partial\Phi(\underline{r}_b)}{\partial\underline{n}} = 0, \quad \text{Neumann type} \tag{1.8b}$$

where $\underline{r}_b$ denotes the spatial vector on the boundary surface and $\underline{n}$ is the unit vector normal to the boundary surface.

The continuity conditions imposed on the solution require that $\Phi(\underline{r})$ be continuous throughout the problem domain and the normal component of $\underline{J}(\underline{r})$ be continuous across internal interfaces separating two different material media.

1.3 Hermite Piecewise Polynomials and Basis Functions

Piecewise polynomials are polynomials defined only over subregions of the problem domain, rather than over the entire domain. The piecewise constants used in finite difference approximation can be thought of as a special case of the piecewise polynomials. Piecewise polynomials yield high accuracy for approximations of functions and their derivatives. Furthermore, besides the simplicity of differentiation and integration for practical computations, they have the following convenient features:

1) Piecewise polynomials permit flexibility in imposing the continuity or jump conditions at the joints of subregions. Also, boundary conditions can be easily imposed.
2) They provide local approximations and are thus suitable for approximating the physical behavior of the problems in which variations occur locally. In our case, for example, the reactor system is characterized by local variations of the materials and neutron cross sections, and the use of a few piecewise polynomials is more convenient than use of polynomials defined over the

entire reactor.

3) The values of functions and their derivatives can be directly incorporated into the expansion coefficients if proper piecewise polynomial basis functions are used.

There are many varieties of piecewise polynomials used in numerical analysis [34]-[36]. In this section we limit the discussion to Hermite interpolating functions because of their simplicity. For the convenience of the discussion, we shall use dimensionless variables.

Let us divide a one-dimensional problem domain [0,Z] into K adjoining regions. Each region k is bounded by nodes z_k and z_{k+1} and has width $h_k = z_{k+1} - z_k$. In general, the h_k's are different. It is convenient to define the dimensionless variable x within each region k as

$$x = \frac{z-z_k}{h_k} \tag{1.9a}$$

so that region k can be described in terms of z as

$$z_k \leq z \leq z_k + h_k = z_{k+1} \tag{1.9b}$$

or equivalently in terms of x as

$$0 \leq x \leq 1 \tag{1.9c}$$

for each of the regions k, k=1, K. This kind of dimensionless variables will be used interchangeably with the original length variables.

Now the Hermite interpolating polynomials, which are polynomials of degree (2m-1), can be expressed in terms of a set of basic functions, $u_k^{p+}(x)$ and $u_k^{p-}(x)$. These basic functions are defined by the following rules:

1) They are polynomials of degree (2m-1) in x.
2) The highest value of p is (m-1)
3) The $u_k^{p+}(x)$ are zero except in the interval h_k on the (+) side of z_k; similarly the $u_k^{p-}(x)$ are zero except in the interval h_{k-1} on the (-) side of z_k.
4) The p-th derivatives of $u_k^{p\pm}(x)$ are unity at z_k and zero at all other mesh interfaces.
5) Derivatives of $u_k^{p\pm}(x)$, lower than the p-th derivatives, are zero at all mesh interfaces.

Using these rules, we can construct the basic functions for Hermite interpolating polynomials of any odd degree. Specifically, for m=1 (p=0 only), we have linear Hermite basic functions:

$$u_k^{0-}(x) = \begin{cases} x, & z_{k-1} \leq z \leq z_k \\ 0, & \text{all other } z \end{cases} \tag{1.10a}$$

$$u_k^{0+}(x) = \begin{cases} 1-x, & z_k \leq z \leq z_{k+1} \\ 0, & \text{all other } z \end{cases} \tag{1.10b}$$

and for m = 2 (p = 0 and 1), cubic Hermite basic functions:

$$u_k^{0-}(x) = \begin{cases} 3x^2 - 2x^3, & z_{k-1} \leq z \leq z_k \\ 0 & \text{all other } z \end{cases} \tag{1.11a}$$

$$u_k^{0+}(x)=\begin{cases} 1-3x^2+2x^3, & z_k \le z \le z_{k+1} \\ 0 & \text{all other } z \end{cases} \tag{1.11b}$$

$$u_k^{1+}(x)=\begin{cases} -x^2+x^3, & z_{k-1} \le z \le z_k \\ 0 & \text{all other } z \end{cases} \tag{1.11c}$$

$$u_k^{1+}(x)=\begin{cases} x-2x^2+x^3, & z_k \le z \le z_{k+1} \\ 0 & \text{all other } z \end{cases} \tag{1.11d}$$

The forms of these linear and cubic basis functions are illustrated in Figure 1.1.

The Hermite interpolating polynomial of order m within a region $z_k \le z \le z_{k+1}$ is just a linear combination of the basis functions of the corresponding order:

$$H_k^m(x) = \sum_{p=0}^{m-1} [a_k^{p+} u_k^{p+}(x) + a_{k+1}^{p-} u_{k+1}^{p-}(x)] \tag{1.12}$$

where a_k^{p+}'s and a_{k+1}^{p-}'s are constants which can be easily related to the values and derivatives at (+) side of z_k and (-) side of z_{k+1}, respectively, of whatever the function is being approximated.

For two dimensional problems, the Hermite basis functions can be found by combining all the possible products from two sets of univariate basis functions, each representing the basis functions in one direction.

Linear Hermite Basis Functions (m = 1)

p = 0

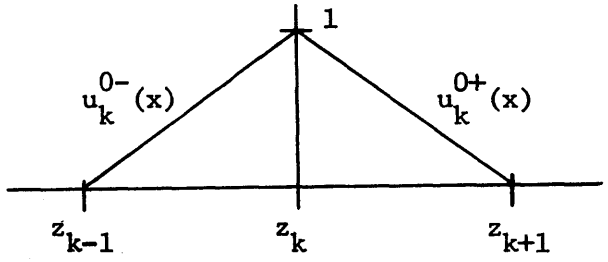

Cubic Hermite Basis Functions (m = 2)

p = 0

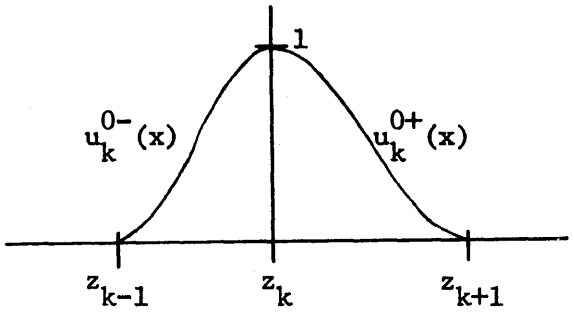

p = 1

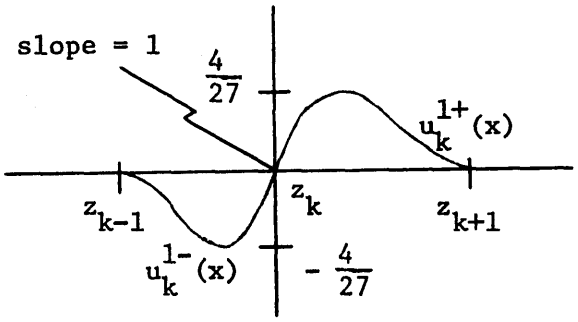

Figure 1.1 Linear and Cubic Hermite Basis Functions of Equations 1.10 and 1.11

1.4 Organization of the Thesis

The rest of the thesis is organized as follows. Chapter 2 describes the use of a variational principle in time-independent neutron diffusion theory. The difference equations of some low order finite element methods applied in one-dimension are derived from this principle to illustrate the use of this technique. Chapter 3 is devoted to some consequences of using simple finite element trial functions as approximations and to an attempt to solve the discontinuity problem at singular points. The forms of the finite element synthesis approximation in two-dimensions and the derivation of difference equations are given in Chapter 4 along with the results of some sample problems. The numerical techniques used are also discussed. Finally, Chapter 5 presents conclusions derived from this study and the possibilities of extending the method to more general cases.

CHAPTER 2

VARIATIONAL PRINCIPLES IN NEUTRON DIFFUSION PROBLEMS

Applications of the calculus of variation are concerned chiefly with the determination of maxima and minima of certain expressions involving unknown functions. Many laws of physics and mechanics can be stated in terms of some kinds of minimization and thus can be formulated in certain forms of variational principles [33], [37]-[40]. An important example is well known in classical mechanics; Hamilton's (variational) principle,

$$\delta \int_{t_1}^{t_2} L \, dt = 0 \tag{2.1}$$

is equivalent to Lagrange's equation of motion,

$$\frac{\partial L}{\partial q_i} - \frac{d}{dt} \frac{\partial L}{\partial \dot{q}_i} = 0 \tag{2.2}$$

where the Lagrangian L is a function of the generalized coordinates q_i and the velocities $\dot{q}_i$ and time t. Lagrange's equations are, in turn, equivalent to Newton's.

Variational methods are particularly useful for determining the approximate solutions of problems when the true solutions are difficult to obtain. Given the space of trial functions, the variational methods will pick a "best" one from such a space automatically. In particular, if the true solution is within the

space of trial functions, the variational methods will find it as the "best" solution.

Essentially, the variational method seeks to combine known trial functions into approximate solutions through the use of a characteristic variational functional. Therefore the first step of the method is to find the characteristic functional whose first-order variation, when set to zero, yields the describing equations and their associated conditions of the system as its Euler equations. A space of trial functions, given in terms of known functions and unknown coefficients (or functions), is then chosen to approximate the solutions of the describing equations. These approximate trial functions are then substituted into the variational functional. Setting the first variation of this functional to zero and allowing arbitrary variations in all the unknowns in the trial functions results in a set of simultaneous equations among the unknowns. Solving of this set of equations yields the "best" obtainable approximate solutions within the space of trial functions given.

Variational methods can be thought of as a kind of weighted residual method since weighting functions appear in the functional and in the equations that result from setting the first variation of the functional to zero. The weighting functions are determined by the form of the variational functional itself. In the case of known adjoint equations, such as in diffusion theory, the

functional is usually chosen so that its Euler equations include both the original describing equations and adjoint equations. The inclusion of corresponding adjoint trial functions in the functional results in adjoint weighting in the variation equations and allows greater approximation flexibility for the variational method.

2.1 Variational Principles in Diffusion Theory

The time-independent multigroup diffusion equations, given by Equation 1.4, can be written as

$$\mathbb{H}\Phi = \frac{1}{\lambda}\mathbb{F}\Phi \tag{2.3a}$$

where

$$\mathbb{H} = -\underline{\nabla}\cdot\mathbb{D}\,\underline{\nabla} + \mathbb{M} - \mathbb{T} \tag{2.3b}$$

The corresponding adjoint equations are

$$\mathbb{H}^*\Phi^* = \frac{1}{\lambda}\mathbb{F}^*\Phi^* \tag{2.4a}$$

where the adjoint operators, $\mathbb{H}^*$ and $\mathbb{F}^*$ are defined as the transpose of the corresponding operators $\mathbb{H}$ and $\mathbb{F}$, respectively:

$$\mathbb{H}^* = \mathbb{H}^T = -\underline{\nabla}\cdot\mathbb{D}\underline{\nabla} + \mathbb{M} - \mathbb{T}^T \tag{2.4b}$$

$$\mathbb{F}^* = \mathbb{F}^T$$

since $\mathbb{D}$ and $\mathbb{M}$ are diagonal. Φ^* is the group adjoint flux vector, or importance vector, which must obey the same boundary conditions as Φ[41].

The exact solutions $\Phi(\underline{r})$ and $\Phi^*(\underline{r})$ of the diffusion equations and the adjoint diffusion equations can be approximated by flux and adjoint flux trial functions $U(\underline{r})$ and $U^*(\underline{r})$ using a variational functional of the form

$$F_1[U^*,U] = \int_R U^{*T}[\mathbb{H}U - \frac{1}{\lambda}\mathbb{F}U]d\underline{r} \qquad (2.5)$$

where it is assumed that the group flux trial function vectors U^* and U as well as the normal components of the group current vectors $\mathbb{D}\nabla U^*$ and $\mathbb{D}\nabla U$ across interfaces are continuous, and that U^* and U vanish at the outer surface of the reactor region R. If we denote the arbitrary trial function variations for the adjoint flux by δU^* and making F_1 stationary with respect to U^*, we have

$$\delta F_1 = \int_R \delta U^{*T}[\mathbb{H}U - \frac{1}{\lambda}\mathbb{F}U]d\underline{r} = 0 \qquad (2.6a)$$

which contains the desired Equation 2.3a as its Euler equation. Similarly, since Equation 2.5 can be written as

$$F_1 = \int_R U^T[\mathbb{H}^T U^* - \frac{1}{\lambda}\mathbb{F}^T U^*]d\underline{r}$$

$$= \int_R U^T[\mathbb{H}^* U^* - \frac{1}{\lambda}\mathbb{F}^* U^*]d\underline{r}$$

making F_1 stationary with respect to U gives

$$\delta F_1 = \int_R \delta U^T[\mathbb{H}^* U^* - \frac{1}{\lambda}\mathbb{F}^* U^*]d\underline{r} = 0 \qquad (2.6b)$$

where δU is an arbitrary variations of flux trial function U. The Euler equation of Equation 2.6b is evidently Equation 2.4a. Thus, we see that the exact solutions along with the exact eigenvalue are reproduced if the exact solutions are contained in the given space of trial functions. Generally, however, the trial function space does not contain these exact solutions and only approximate solutions and eignevalues are obtained from invoking Equations 2.6.

Thus, the accuracy of the above approximation depends solely on the forms of the flux and the adjoint flux trial functions. Each trial function can be defined in terms of known functions and unknown coefficients (or functions). Independent variations of the unknown coefficients of the adjoint trial functions in Equation 2.6a will then yield the "best" flux solution for that class of flux and adjoint trial function. The corresponding "best" adjoint flux solution is found in a similar way by using Equation 2.6b.

The variational functional F_1 is not the only functional that produces the desired variational equations 2.6 when made stationary. Anohter functional incorporating the flux and adjoint flux diffusion equations is the Rayleigh's principle [42],

$$F_2[U^*,U] = \frac{1}{\lambda} = \frac{\int_R U^{*T} \mathbb{H} U d\underline{r}}{\int_R U^{*T} \mathbb{F} U d\underline{r}} \tag{2.7}$$

Although the forms of F_2 and F_1 differ, it can be shown [43] that functional F_2 gives identical Euler equations as Equations 2.6 and is equivalent to functional F_1. However, because the form of F_1

is much simpler than that of F_2, it will be used later in this thesis.

2.2 Discontinuous Trial Functions

In the previous section we stated that the admissable trial functions for flux and adjoint flux used in functional F_1 must satisfy certain continuity conditions inside the reactor region R. This restriction greatly reduces the flexibility and generality of our methods. In this section the class of allowable trial functions will be extended to include discontinuous flux and current trial functions.

Special provisions must be made in the approximation method such that this extended class of trial functions can be properly used. In order to account for the discontinuities in the trial functions, it is necessary to include special terms specifying continuity conditions directly in the approximation method. This can be achieved through the use of a variational functional whose Euler equations include not only the original P-1 equations but also the associated continuity conditions for both flux and current. A general functional of this type which allows discontinuous flux, current and adjoint trial functions is given [18], [44]-[46] as follows:

$$F_3[U^*,U,\underline{V}^*,\underline{V}] = \int_R \{U^{*T}[\underline{\nabla}\cdot\underline{V} + \Sigma U] + \underline{V}^{*T}\cdot[\underline{\nabla}U + \mathbb{D}^{-1}\underline{V}]\}d\underline{r}$$

$$+ \frac{1}{2}\int_\Gamma \hat{\underline{n}}\cdot[(U_+^* + U_-^*)^T(\underline{V}_+ - \underline{V}_-) + (\underline{V}_+^* + \underline{V}_-^*)^T(U_+ - U_-)]d\underline{s} \quad (2.8)$$

where U^*, U, $\underline{V}^*$, and $\underline{V}$ are the group flux and group current approximations to Φ^*, Φ, $\underline{J}^*$, and $\underline{J}$, respectively, and where the first integral extends over all $\underline{r}$ inside reactor region R and the second extends over all interior surfaces where discontinuities occur. $\hat{\underline{n}}$ is the unit vector normal to interior surfaces. Quantities evaluated on sides of surfaces toward which $\hat{\underline{n}}$ is pointing are denoted with the subscript (+) and evaluated on the other sides of such surfaces are denoted with the subscript (-).

The first variation of F_3 with respect to the adjoint quantities can be found in a straightforward manner:

$$\delta F_3 = \int_R \{\delta U^{*T}[\underline{\nabla}\cdot\underline{V} + \Sigma U] + \delta\underline{V}^{*T}\cdot[\underline{\nabla}U + \mathbb{D}^{-1}\underline{V}]\}d\underline{r}$$

$$+ \frac{1}{2}\int_\Gamma \hat{\underline{n}}\cdot[(\delta U_+^* + \delta U_-^*)^T(\underline{V}_+ - \underline{V}_-) + (\delta\underline{V}_+^* + \delta\underline{V}_-^*)^T(U_+ - U_-)]d\underline{s} \quad (2.9)$$

The desired P-1 equations, Equations 1.6, and the associated continuity conditions for flux and current at the inner surfaces follow directly by setting $\delta F_3 = 0$. To show that the adjoint P-1 equations and the continuity conditions for adjoint flux and current also resulted from this variational functional if F_3 is made stationary with respect to variation in the unstarred quantities, it is

necessary to rearrange Equation 2.8. This can be done by integrating by parts terms involving spatial derivatives and replacing all terms by their transposes. The result is the alternate expression

$$F_3[U^*,U,\underline{V}^*,\underline{V}] = \int_R \{U^T[-\underline{\nabla}\cdot\underline{V}^* + \Lambda^*U^*] + \underline{V}^T\cdot[-\underline{\nabla}U^* + \mathbb{D}^{-1}\underline{V}^*]\}d\underline{r}$$

$$- \frac{1}{2}\int_\Gamma \hat{\underline{n}}\cdot[(U_+ + U_-)^T(\underline{V}_+^* - \underline{V}_-^*) + (\underline{V}_+ + \underline{V}_-)^T(U_+^* - U_-^*)]d\underline{s} \qquad (2.10)$$

It is clear by now that if the first variation of F_3 with respect to its unstarred arguments is now set equal to zero, we get adjoint P-1 equations along with their continuity conditions:

$$-\underline{\nabla}\cdot\underline{J}^* + \Lambda^*\Phi^* = 0 \qquad (2.11a)$$

$$\underline{\nabla}\Phi^* - \mathbb{D}^{-1}\underline{J}^* = 0 \qquad (2.11b)$$

$$\Phi_+^* = \Phi_-^* \qquad (2.11c)$$

$$\hat{\underline{n}}\cdot\underline{J}_+^* = \hat{\underline{n}}\cdot\underline{J}_-^* \qquad (2.11d)$$

In most applications, only approximations to the flux and current solutions are desired. In such cases variational functional F_3 in the form of Equation 2.8 is more convenient and the approximation is then based on the following:

$$\int_R \{\delta U^{*T}[\underline{\nabla}\cdot\underline{V} + \Lambda U] + \delta\underline{V}^{*T}\cdot[\underline{\nabla}U + \mathbb{D}^{-1}\underline{V}]\}d\underline{r} +$$

$$+ \frac{1}{2}\int_\Gamma \hat{\underline{n}}\cdot[(\delta U_+^* + \delta U_-^*)^T(\underline{V}_+ - \underline{V}_-) + (\delta\underline{V}_+^* + \delta\underline{V}_-^*)^T(U_+ - U_-)]d\underline{s} = 0 \qquad (2.12)$$

If the adjoint trial functions are defined as

$$U^* = U \tag{2.13a}$$

$$\underline{V}^* = \underline{V} \tag{2.13b}$$

then Equation 2.12 reduces to the Rayleigh-Ritz Galerkin method [47]-[49], a weighted residual method based upon flux weighting.

The variation equation can be further simplified for certain cases regardless of the choice of weighting. For the approximation methods which require the currents to obey explicitly Fick's laws:

$$\underline{V} = -\mathbb{D}\underline{\nabla}U \tag{2.14a}$$

$$\underline{V}^* = +\mathbb{D}\underline{\nabla}U^* \tag{2.14b}$$

Equation 2.12 reduces to

$$\int_R [\delta U^{*T}\mathbb{\Lambda}U - \delta\underline{V}^{*T}\cdot\mathbb{D}^{-1}\underline{V}]d\underline{r}$$

$$+\frac{1}{2}\int_\Gamma \underline{\hat{n}}\cdot[(\delta\underline{U}^* - \delta U_+^*)^T(\underline{V}_+ + \underline{V}_-)+(\delta\underline{V}_+^* + \delta\underline{V}_-^*)^T(U_+ - U_-)]d\underline{s} = 0 \tag{2.15}$$

If in addition the flux and adjoint flux are required to be everywhere continuous, the above equation reduces to the simple form

$$\int_R [\delta U^{*T}\mathbb{\Lambda}U - \delta\underline{V}^{*T}\cdot\mathbb{D}^{-1}\underline{V}]d\underline{r} = 0 \tag{2.16a}$$

or equivalently,

$$\int_R [\delta U^{*T}\mathbb{\Lambda}U + (\underline{\nabla}\delta U^*)^T\cdot\mathbb{D}(\underline{\nabla}U)]d\underline{r} = 0 \tag{2.16b}$$

One note about the boundary conditions: In the present discussion the allowed trial functions used in the approximation methods must satisfy the same boundary conditions as the true solutions. Though it is possible to extend the variational principle so that the permissible class of trial functions is augmented to include functions with arbitrary conditions on the boundary, we shall not pursue this point since the imposing of boundary conditions is easy with the use of Hermite interpolating functions as trial functions.

2.3 Fick's Law as a Consequence of Variational Principle

Some simple derivations of the difference equations are given here using trial functions of finite element methods in one-dimension. These derivations will show that Fick's law always surfaces as a natural consequence of the variational equation 2.12. In each case, flux and adjoint flux continuity is assumed in the approximate trial functions while current continuity is not. Various forms of current trial functions are used in different cases. In the derivation process we shall first allow the values of trial functions at boundaries to vary arbitrarily, then impose the required boundary conditions (which usually involves setting some boundary values to zero and eliminating some equations) after we get the general system of equations. This procedure is totally equivalent to that of first imposing boundary conditions and then

finding the desired system of algebraic equations, and will be used throughout this thesis. In this way we can accomodate various sets of boundary conditions at one time.

2.3.1 The Linear Basis Function Approximation

The group flux trial functions defined as nonzero within each region k can be expressed in terms of linear basis functions as

$$U_k(z) = (1-x)P_k + xP_{k+1} \qquad (2.17a)$$

$$; \quad k = 1 \text{ to } K$$

$$U_k^*(z) = (1-x)P_k^* + xP_{k+1}^* \qquad (2.17b)$$

where P_k and P_k^* are the approximate group flux and adjoint flux column vectors, respectively, at point z_k, and $0 \leq x \leq 1$ within each region k. Figure 2.1 illustrates the form of these trial functions. Different forms of current trial functions can be used. We shall start with (i) Fick's law current, followed by (ii) constant current, (iii) linear current, and (iv) quadratic current trial functions within each region k.

(i) Fick's Law Current Trial Functions:

The group current trial functions which obey Fick's law are given, according to Equations 2.14, by

$$V_k(z) = \frac{1}{h_k} \mathbb{D}_k(x)[P_k - P_{k+1}] \qquad (2.18a)$$

$$; \quad k = 1 \text{ to } K$$

$$V_k^*(z) = \frac{1}{h_k} \mathbb{D}_k(x)[P_{k+1}^* - P_k^*] \qquad (2.18b)$$

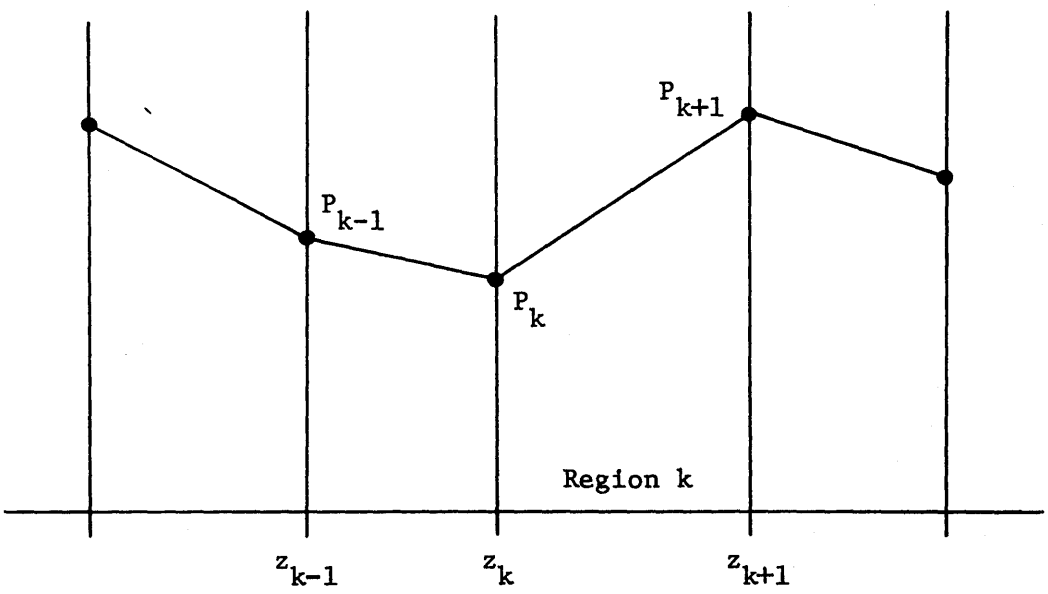

Figure 2.1 The Flux Trial Functions of Linear Finite Element Approximation

Insertion of these trial functions into variation equation 2.16a results in the equation

$$\sum_{k=1}^{K} h_k \int_0^1 \{[(1-x)\delta P_k^* + x\delta P_{k+1}^*]^T \mathbb{A}_k(x)[(1-x)P_k + xP_{k+1}]$$

$$+ [\delta P_k^* - \delta P_{k+1}^*]^T \frac{1}{h_k^2} \mathbb{D}_k(x)[P_k - P_{k+1}]\}dx = 0 \qquad (2.19)$$

Allowing arbitrary variations in all P_k^* results in a system of K+1 equations in K+1 unknowns which can be written as:

$$b_1 P_1 + c_1 P_2 = 0 \qquad (2.20a)$$

$$a_k P_{k-1} + b_k P_k + c_k P_{k+1} = 0 \; ; \quad k = 2 \text{ to } K \qquad (2.20b)$$

$$a_{K+1} P_K + b_{K+1} P_{K+1} = 0 \qquad (2.20c)$$

where the GxG matrix coefficients a_k, b_k, c_k are of the form $A - \frac{1}{\lambda} B$ and are defined in Section 1 of Appendix C assuming homogeneous regional nuclear constants. Zero flux boundary conditions can be imposed by use of only Equation 2.20b with $P_1 = P_{K+1} = 0$, while symmetry boundary conditions require the use of the other equations as well. The matrix form of these equations for the boundary conditions of zero flux on the left and symmetry on the right is given in Figure 2.2.

(ii) Constant Current Trial Functions:

The current trial functions which are constant within each region k are given by

$$\begin{bmatrix} \beta_2 & \gamma_2 & & & \\ \alpha_k & \beta_k & \gamma_k & & \\ & & \alpha_{K+1} & \beta_{K+1} \end{bmatrix} \begin{bmatrix} P_2 \\ P_k \\ P_{K+1} \end{bmatrix} = \frac{1}{\lambda} \begin{bmatrix} \varepsilon_2 & \zeta_2 & & & \\ \delta_k & \varepsilon_k & \zeta_k & & \\ & & \delta_{K+1} & \varepsilon_{K+1} \end{bmatrix} \begin{bmatrix} P_2 \\ P_k \\ P_{K+1} \end{bmatrix}$$

Figure 2.2 Matrix Form of the Linear Finite Element Method Approximation. Eqs. 2.20 for the case of zero flux on the left and symmetry boundary condition on the right.

Where:

$$\left.\begin{aligned} a_k &= \alpha_k - \frac{1}{\lambda}\delta_k \\ b_k &= \beta_k - \frac{1}{\lambda}\varepsilon_k \\ c_k &= \gamma_k - \frac{1}{\lambda}\zeta_k \end{aligned}\right\} \quad k = 2 \text{ to } K+1$$

$$V_k(z) = Q_k \quad ; \quad k = 1 \text{ to } K \tag{2.21a}$$

$$V_k^*(z) = Q_k^* \tag{2.21b}$$

where Q_k and Q_k^* are column vectors with constant elements representing the approximate values of group current and adjoint current, respectively, in the region k. Since Fick's law is not true in this case, Equation 2.12 must be used instead of Equation 2.16a. Insertion of Equations 2.17 and 2.21 into variation equation 2.12 yields the equation

$$\sum_{k=1}^{K} h_k \int_0^1 \{[(1-x)\delta P_k^* + x\delta P_{k+1}^*]^T \mathbb{A}_k(x)[(1-x)P_k + xP_{k+1}]$$

$$+ \delta Q_k^{*T}[\frac{1}{h_k}(P_{k+1}-P_k) + \mathbb{D}_k^{-1}(x)Q_k]\}dx$$

$$+ \sum_{k=2}^{K} \delta P_k^{*T}(Q_k - Q_{k-1}) = 0 \tag{2.22}$$

Allowing arbitrary variations in all Q_k^* gives

$$\int_0^1 [(P_{k+1}-P_k) + h_k \mathbb{D}_k^{-1}(x)Q_k]dx = 0; \quad k = 1 \text{ to } K$$

$$\therefore \quad [\int_0^1 \mathbb{D}_k^{-1}(x)dx]Q_k = -\frac{1}{h_k}(P_{k+1}-P_k)$$

or equivalently,

$$Q_k = V_k(z) = -\frac{1}{h_k}[\int_0^1 \mathbb{D}_k^{-1}(x)dx]^{-1}(P_{k+1}-P_k)$$

$$= -[\int_0^1 \mathbb{D}_k^{-1}(x)dx]^{-1} \frac{d}{dz} U_k(z) \quad ; \quad k = 1 \text{ to } K \tag{2.23}$$

Equation 2.23 can be thought of as Fick's law in an integrated sense. In the case of constant diffusion coefficients within each region k, Equation 2.23 reduces to the simple form of Fick's law:

$$V_k(z) = -\mathbb{D}_k \frac{d}{dz} U_k(z) \qquad (2.24)$$

in each region k.

Allowing arbitrary variations in all P_k^* results in a system of equations of the same form as Equations 2.20, if we substitute P_k's for Q_k's by using Equation 2.23. The matrix coefficients are different in general. However, for the case of homogeneous regional nuclear constants, they are identical to those given in Section 1 of Appencix C.

(iii) Linear Current Trial Functions:

The linear current trial functions which are not necessarily continuous across the inner interfaces between regions can be expressed in terms of linear basis functions as

$$V_k(z) = (1-x)Q_{k,+} + xQ_{k+1,-} \qquad (2.25a)$$

$$V_k^*(z) = (1-x)Q_{k,+}^* + xQ_{k+1,-}^* \qquad (2.25b)$$

: k = 1 to K

where $Q_{k,+}$ and $Q_{k+1,-}$ are the approximate group current column vectors at positive side of node z_k and negative side of node z_{k+1}, respectively. The form of these trial functions is illustrated in Figure 2.3.

Substitution of Equations 2.17 and 2.25 into variation equation

2.12 results in the equation

$$\sum_{k=1}^{K} h_k \int_0^1 <[(1-x)\delta P_k^* + x\delta P_{k+1}^*]^T \{ \frac{1}{h_k}(Q_{k+1,-} - Q_{k,+}) + \Lambda_k(x)[(1-x)P_k + xP_{k+1}]\}>dx$$

$$+ \sum_{k=1}^{K} h_k \int_0^1 <[(1-x)\delta Q_{k,+}^* + x\delta Q_{k+1,-}^*]^T \{\frac{1}{h_k}(P_{k+1} - P_k) + \mathbb{D}_k^{-1}(x)[(1-x)Q_{k,+} + xQ_{k+1,-}]\}>dx$$

$$+ \sum_{k=2}^{K} \delta P_k^{*T} (Q_{k,+} - Q_{k,-}) = 0 \qquad (2.26)$$

Allowing arbitrary variations in all $Q_{k,+}^*$, we have

$$\frac{1}{2h_k}(P_{k+1} - P_k) + [\int_0^1 (1-x)^2 \mathbb{D}_k^{-1}(x)dx]Q_{k,+} + [\int_0^1 (1-x)x\, \mathbb{D}_k^{-1}(x)dx]Q_{k+1,-} = 0; \quad k = 1 \text{ to } K \qquad (2.27a)$$

Similarly, arbitrary variations in all $Q_{k+1,-}^*$ gives

$$\frac{1}{2h_k}(P_{k+1} - P_k) + [\int_0^1 x(1-x)\, \mathbb{D}_k^{-1}(x)dx]Q_{k,+} + [\int_0^1 x^2\, \mathbb{D}_k^{-1}(x)dx]Q_{k+1,-} = 0; \quad k = 1 \text{ to } K \qquad (2.27b)$$

Solving simultaneous Equations 2.27 results in

$$Q_{k,+} = -\frac{1}{2h_k} \mathbb{B}_{k,+}^{-1} \{ [\int_0^1 x^2 \, \mathbb{D}_k^{-1}(x)\,dx]^{-1} - [\int_0^1 (1-x)x \, \mathbb{D}_k^{-1}(x)\,dx]^{-1} \} (P_{k+1} - P_k) \tag{2.28a}$$

$$Q_{k+1,-} = -\frac{1}{2h_k} \mathbb{B}_{k+1,-}^{-1} \{ [\int_0^1 (1-x)^2 \, \mathbb{D}_k^{-1}(x)\,dx]^{-1} - [\int_0^1 (1-x)x \, \mathbb{D}_k^{-1}(x)\,dx]^{-1} \} (P_{k+1} - P_k) \tag{2.28b}$$

where $\mathbb{B}_{k,+}$ and $\mathbb{B}_{k+1,-}$ are GxG diagonal matrices defined by

$$\mathbb{B}_{k,+} = [\int_0^1 x^2 \, \mathbb{D}_k^{-1}(x)\,dx]^{-1} [\int_0^1 x(1-x) \, \mathbb{D}_k^{-1}(x)\,dx] - [\int_0^1 x(1-x) \, \mathbb{D}_k^{-1}(x)\,dx]^{-1} [\int_0^1 (1-x)^2 \, \mathbb{D}_k^{-1}(x)\,dx] \tag{2.29a}$$

$$\mathbb{B}_{k+1,-} = [\int_0^1 (1-x)^2 \, \mathbb{D}_k^{-1}(x)\,dx]^{-1} [\int_0^1 x(1-x) \, \mathbb{D}_k^{-1}(x)\,dx] - [\int_0^1 x(1-x) \, \mathbb{D}_k^{-1}(x)\,dx]^{-1} [\int_0^1 x^2 \, \mathbb{D}_k^{-1}(x)\,dx] \tag{2.29b}$$

If $\mathbb{D}_k(x)$ is constant within each region k, then Equations 2.29 and 2.28 can be reduced to

$$\mathbb{B}_{k+1,-} = \mathbb{B}_{k,+} = (\tfrac{1}{3} \mathbb{D}_k^{-1})^{-1} (\tfrac{1}{6} \mathbb{D}_k^{-1}) - (\tfrac{1}{6} \mathbb{D}_k^{-1})^{-1} (\tfrac{1}{3} \mathbb{D}_k^{-1}) = -\frac{3}{2} \mathbb{I}$$

and

$$Q_{k+1,-} = Q_{k,+} = \frac{1}{3h_k} [(\tfrac{1}{3} \mathbb{D}_k^{-1})^{-1} - (\tfrac{1}{6} \mathbb{D}_k^{-1})^{-1}] (P_{k+1} - P_k) = -\frac{1}{h_k} \mathbb{D}_k (P_{k+1} - P_k)$$

so that the current trial functions become constant and are given by

$$V_k(z) = Q_{k,+} = -\frac{1}{h_k}\mathbb{D}_k(P_{k+1}-P_k) = -\mathbb{D}_k\frac{d}{dz}U_k(z);\ k = 1 \text{ to } K \tag{2.30}$$

i.e., the current trial functions are related to flux trial functions via Fick's law.

The system of equations relating all P_k's can be found by allowing arbitrary variations in all P_k^*'s in Equation 2.26 and substituting for all $Q_{k,+}$'s and $Q_{k+1,-}$'s with P_k's. Under the circumstance that all regional nuclear constants are homogeneous, Equation 2.20 with matrix coefficients defined in Appendix C.1 results.

One interesting situation arises when some regions are symmetric. For example, if region k is symmetric, then $\mathbb{D}_k(x) = \mathbb{D}_k(1-x)$ for $0 \leq x \leq 1$. Substract Equation 2.27b from Eq. 2.27a gives $Q_{k+1,-} = Q_{k,+}$ since

$$\int_0^1 (1-x)^2\,\mathbb{D}_k^{-1}(x)dx = \int_0^1 (1-x)^2\,\mathbb{D}_k^{-1}(1-x)dx = \int_0^1 x^2\,\mathbb{D}_k^{-1}(x)dx$$

by simple change of variables. Therefore, the current trial functions become a constant in this region and is given by

$$V_k(z)=Q_{k,+} = -\frac{1}{2h_k}\left[\int_0^1 x\,\mathbb{D}_k^{-1}(x)dx\right]^{-1}(P_{k+1}-P_k) = -\frac{1}{2}\left[\int_0^1 x\,\mathbb{D}_k^{-1}(x)dx\right]^{-1}$$

$$\frac{d}{dz}U_k(z)$$

which, as it must, reduces to Fick's law if $\mathbb{D}_k(x)$ is constant.

(iv) Quadratic Current Trial Functions:

The current trial functions which are quadratic in general are given by

$$V_k(z) = x^2 L_k + xM_k + N_k \quad ; \quad k = 1 \text{ to } K \tag{2.31a}$$

$$V_k^*(z) = x^2 L_k^* + xM_k^* + N_k^* \tag{2.31b}$$

where L_k, M_k, N_k and their corresponding adjoint quantities are all Gx1 column vectors with constant elements. They are not continuous across the region interfaces in general and are illustrated in Figure 2.4.

Insertion of Equations 2.17 and 2.31 into variation equation 2.12 results in the equation

$$\sum_{k=1}^{K} h_k \int_0^1 <[(1-x)\delta P_k^* + x\delta P_{k+1}^*]^T \{\frac{1}{h_k}(2xL_k + M_k) + \Lambda_k(x)[(1-x)P_k + xP_{k+1}]\}> dx$$

$$+ \sum_{k=1}^{K} h_k \int_0^1 <[x^2\delta L_k^* + x\delta M_k^* + \delta N_k^*]^T \{\frac{1}{h_k}(P_{k+1} - P_k) + D_k^{-1}(x)[x^2 L_k + xM_k + N_k]\}> dx$$

$$+ \sum_{k=2}^{K} \delta P_k^{*T}[N_k - (L_{k-1} + M_{k-1} + N_{k-1})] = 0 \tag{2.32}$$

Allowing arbitrary variations in L_k^*, M_k^*, and N_k^* yields a set of equations

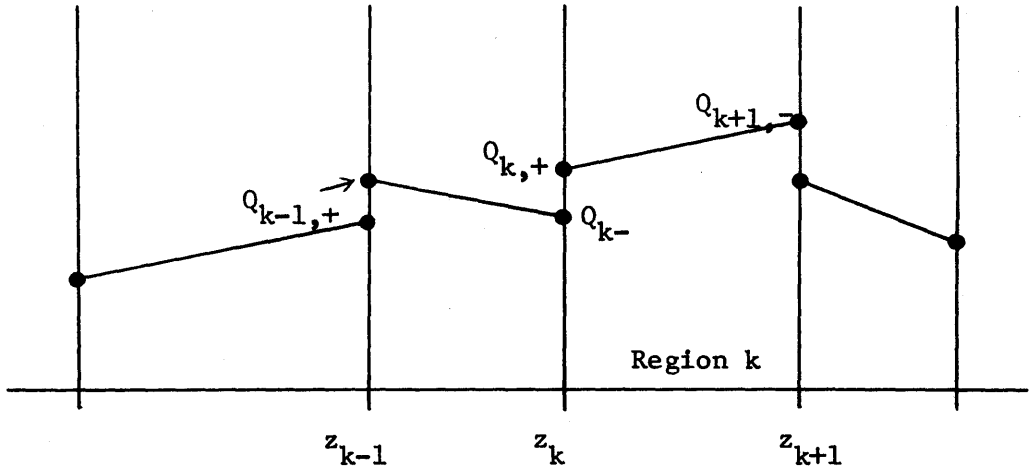

Figure 2.3 The Linear Current Trial Functions (as defined by Equation 2.25a)

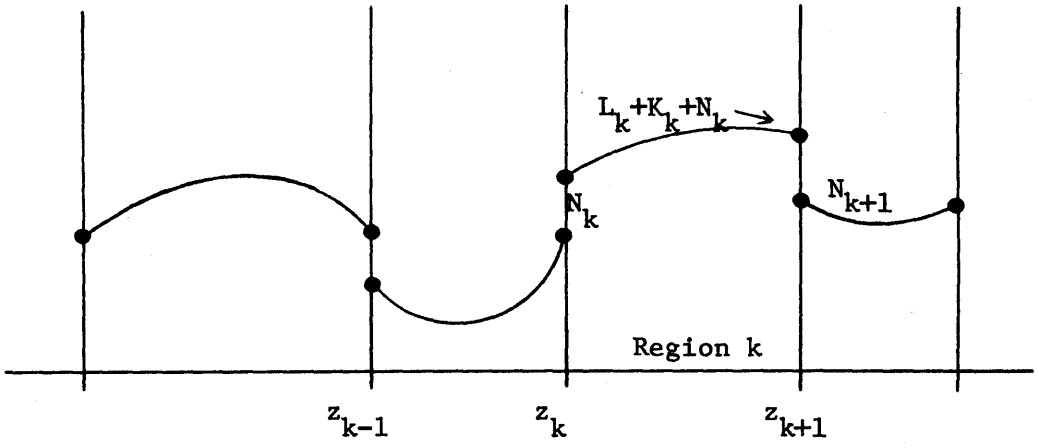

Figure 2.4 The Quadratic Current Trial Functions (as defined by Equation 2.31a)

$$h_k\int_0^1 x^2\{\frac{1}{h_k}(P_{k+1}-P_k) + \mathbb{D}_k^{-1}(x)[x^2L_k + xM_k + N_k]\}dx = 0 \quad (2.33a)$$

$$h_k\int_0^1 x\{\frac{1}{h_k}(P_{k+1}-P_k) + \mathbb{D}_k^{-1}(x)[x^2L_k + xM_k + N_k]\}dx = 0 \quad (2.33b)$$

$$h_k\int_0^1 \{\frac{1}{h_k}(P_{k+1}-P_k) + \mathbb{D}_k^{-1}(x)[x^2L_k + xM_k + N_k]\}dx = 0 \quad (2.33c)$$

$$k = 1 \text{ to } K$$

which can be solved for L_k, M_k, and N_k in terms of P_k and P_{k+1}. For the case of constant $\mathbb{D}_k$ in each region k, Equations 2.33 have the solution

$$L_k = M_k = 0$$
$$N_k = -\frac{1}{h_k}\mathbb{D}_k(P_{k+1}-P_k) \qquad ; k = 1 \text{ to } K$$

so that the current trial functions again become constant and obey Fick's law.

Again, the system of equations for all P_k's is given by Equations 2.20 under the assumption that all nuclear constants are homogeneous within each region.

2.3.2 The Cubic Hermite Basis Function Approximation [50]-[51]

The group flux trial functions within each region k can be expressed as a linear combination of cubic Hermite basis functions as

$$U_k(z) = (1-3x^2+2x^3)P_k + (3x^2-2x^3)P_{k+1}$$

$$-(x-2x^2+x^3)h_k \mathbb{D}_k^{-1}(x)Q_k - (-x^2+x^3)h_k \mathbb{D}_k^{-1}(x)Q_{k+1} \qquad (2.34a)$$

$$U_k^*(z) = (1-3x^2+2x^3)P_k^* + (3x^2-2x^3)P_{k+1}^*$$

$$-(x-2x^2+x^3)h_k \mathbb{D}_k^{-1}(x)Q_k^* - (-x^2+x^3)h_k \mathbb{D}_k^{-1}(x)Q_{k+1}^* \qquad (2.34b)$$

where k = 1 to K. P_k is the approximate group flux solution vector at node z_k and the meaning of Q_k will become apparent later. Because of the properties of basis functions, continuity of flux is automatically met since

$$U_k(z_k) = U_k(x=0)=P_k=U_{k-1}(x=1)=U_{k-1}(z_k)$$

$$U_k^*(z_k) = U_k^*(x=0)=P_k^*=U_{k-1}^*(x=1)=U_{k-1}^*(z_k)$$

Figure 2.5 illustrates the forms of these trial functions.

For the current trial functions we shall again assume various forms starting with (i) Fick's law current and followed by (ii) Quadratic current and (iii) Linear current approximations in each region k.

(i) Fick's Law Current Trial Functions:

Application of Fick's law defines the current trial functions for each k as

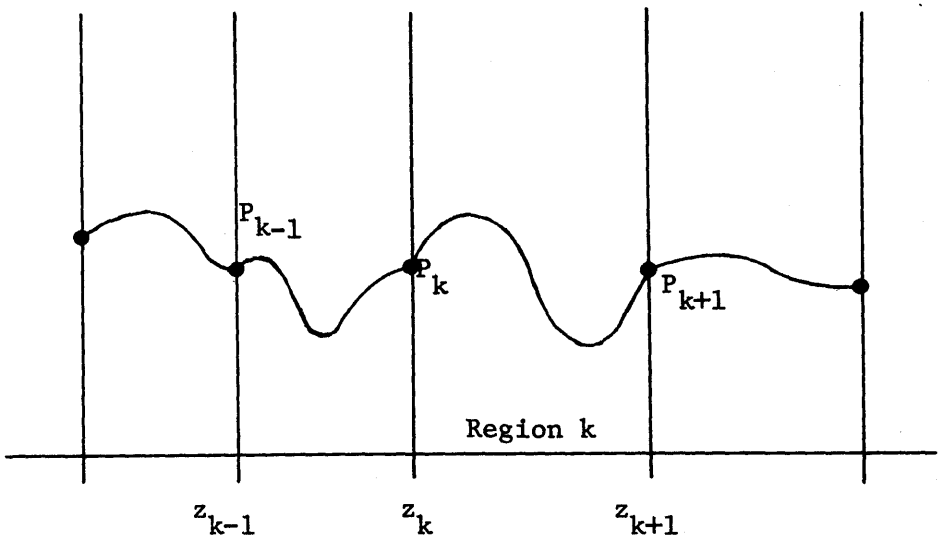

Figure 2.5 The Cubic Hermite Basis Functions

Approximation (as defined by Equation 2.34a)

$$V_k(z) = \frac{1}{h_k} \mathbb{D}_k(x)(6x-6x^2)(P_k-P_{k+1})+(1-4x+3x^2)Q_k+(-2x+3x^2)Q_{k+1} \tag{2.35a}$$

$$V_k^*(z) = \frac{1}{h_k} \mathbb{D}_k(x)(6x-6x^2)(P_{k+1}^*-P_k^*)+(-1+4x-3x^2)Q_k^*+(2x-3x^2)Q_{k+1}^* \tag{2.35b}$$

where the assumption that $\mathbb{D}_k(x)$ varies very little with x inside each region k has been made. From Equations 2.35 it is clear that Q_k is the approximate group current solution vector at node z_k and that current is continuous across the region interfaces:

$$V_k(z_k) = V_k(x=0) = Q_k = V_{k-1}(x=1) = V_{k-1}(z_k)$$

$$V_k^*(z_k) = V_k^*(x=0) = -Q_k^* = V_{k-1}^*(x=1) = V_{k-1}^*(z_k)$$

Equations 2.34 and 2.35 are now substituted into variation equation 2.16a and the resultant lengthy equation can be written as follows:

$$\delta P_1^{*T}\{b1_1P_1 + b2_1Q_1 + c1_1P_2 + c2_1Q_2\}$$

$$+ \delta Q_1^{*T}\{b3_1P_1 + b4_1Q_1 + c3_1P_2 + c4_1Q_2\}$$

$$+ \sum_{k=2}^{K} \delta P_k^{*T}\{a1_kP_{k-1} + a2_kQ_{k-1} + b1_kP_k + b2_kQ_k + c1_kP_{k+1} + c2_kQ_{k+1}\}$$

$$+ \sum_{k=2}^{K} \delta Q_k^{*T}\{a3_kP_{k-1} + a4_kQ_{k-1} + b3_kP_k + b4_kQ_k + c3_kP_{k+1} + c4_kQ_{k+1}\}$$

$$+ \delta P^*_{K+1} \{a1_{K+1} P_K + a2_{K+1} Q_K + b1_{K+1} P_{K+1} + b2_{K+1} Q_{K+1}\}$$

$$+ \delta Q^*_{K+1} \{a3_{K+1} P_K + a4_{K+1} Q_K + b3_{K+1} P_{K+1} + b4_{K+1} Q_{K+1}\} = 0 \qquad (2.36)$$

where GxG matrix coefficients {a1,---,c4} are of the form $A - \frac{1}{\lambda} B$ and are defined in Section 2 of Appendix C assuming homogeneous regional nuclear constants.

Allowing arbitrary variations in all P^*_k and Q^*_k results in a system of 2(K+1) equations in 2(K+1) unknowns. The choice of either zero flux, $P_k = 0$ as well as $\delta P^*_k = 0$, or zero current, $Q_k = 0$ as well as $\delta Q^*_k = 0$, boundary conditions for k = 1 or k = K+1 reduces the system to a set of 2K equations in 2K unknowns. Figure 2.6 illustrates the matrix form of such a system for the case of zero flux on the left and zero current on the right boundary conditions.

(ii) Quadratic Current Trial Functions:

As in Section 2.3.1(iv), the current trial functions which are quadratic are given by Equations 2.31. The insertion of Equations 2.34 and 2.31 into variation equation 2.12 yields

$$\sum_{k=1}^{K} h_k \int_0^1 < [(1-3x^2+2x^3)\delta P^*_k + (3x^2-2x^3)\delta P^*_{k+1} + (-x+2x^2-x^3) h_k \mathbb{D}_k^{-1}(x) \delta Q^*_k$$

$$+ (x^2-x^3) h_k \mathbb{D}_k^{-1}(x) \delta Q^*_{k+1}]^T \{\frac{1}{h_k}(2xL_k + M_k) + \Lambda_k(x)[(1-3x^2+2x^3)P_k$$

$$+ (3x^2-2x^3)P_{k+1} + (-x+2x^2-x^3) h_k \mathbb{D}_k^{-1}(x) Q_k + (x^2-x^3) h_k \mathbb{D}_k^{-1}(x) Q_{K+1}]\} >$$

dx

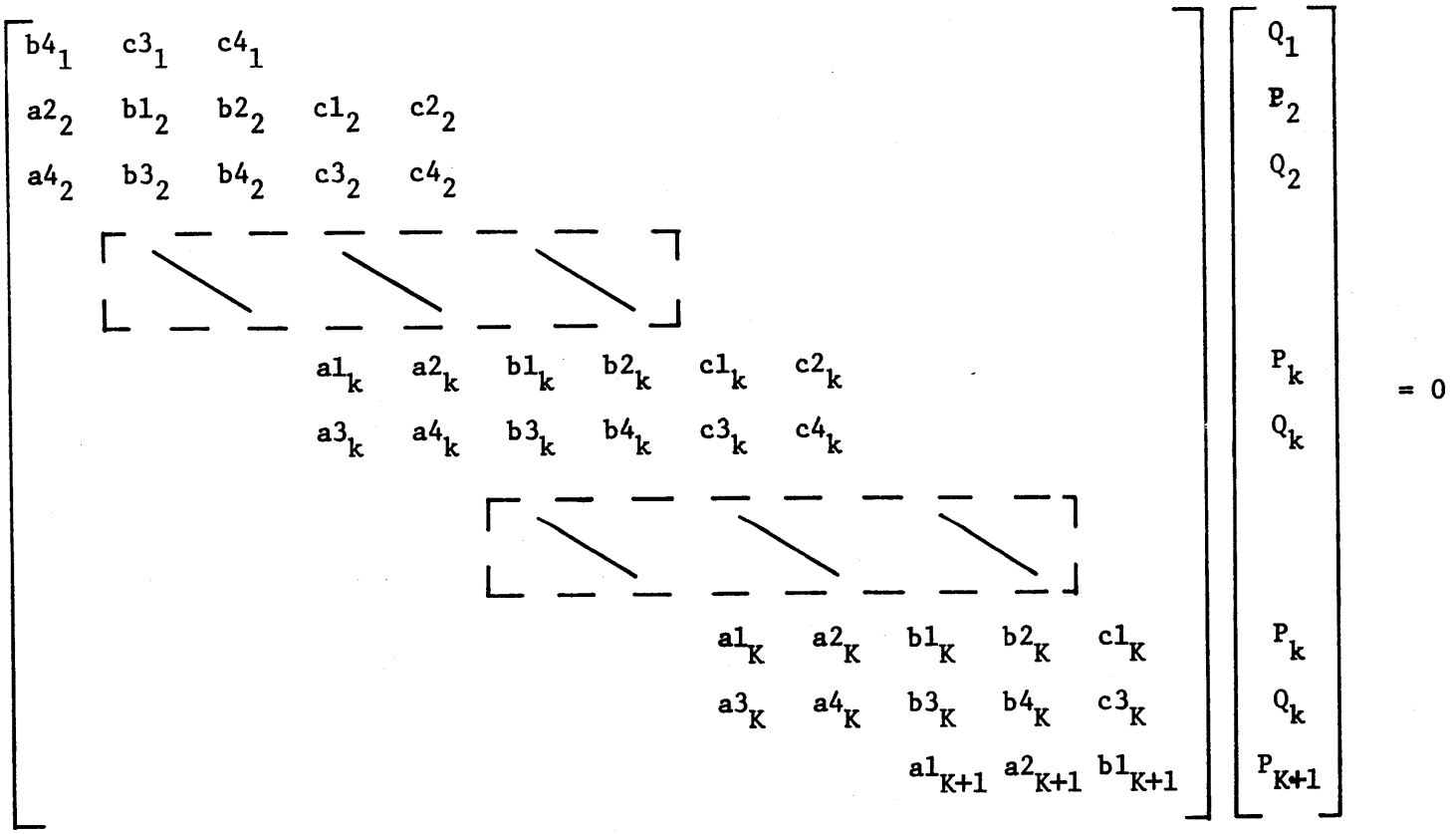

Figure 2.6 Matrix Form of the Cubic Hermite Finite Element Method Approximation Equation 2.36 for the case of zero flux on the left and symmetry boundary conditions on the right

where
$$an_k = \alpha n_k - \frac{1}{\lambda}\,\delta n_k$$
$$bn_k = \beta n_k - \frac{1}{\lambda}\,\varepsilon n_k$$
$$cn_k = \gamma n_k - \frac{1}{\lambda}\,\zeta n_k$$

$n = 1$ to 4 and $k = 1$ to $K + 1$

$$+ \sum_{k=1}^{K} h_k \int_0^1 <[x^2\delta L_k^* + x\delta M_k^* + \delta N_K^*]^T \{\frac{1}{h_k}[(6x-6x^2)(P_{k+1}-P_k)$$

$$+ (-1+4x-3x^2)h_k \mathbb{D}_k^{-1}(x)Q_k + (2x-3x^2)h_k \mathbb{D}_k^{-1}(x)Q_{k+1}]$$

$$+ \mathbb{D}_k^{-1}(x)[x^2L_k + xM_k + N_k]\}>dx$$

$$+ \sum_{k=2}^{K} \delta P_k^{*T}[N_k-(L_{k-1} + M_{k-1} + N_{k-1}] = 0 \qquad (2.37)$$

Assuming that $\mathbb{D}_k(x)$ is constant within each region k and allowing arbitrary variations in all L_k^*, M_k^*, and N_k^* results in the following equations:

$$\frac{1}{h_k}[\frac{3}{10}(P_{k+1}-P_k) + \frac{1}{15}h_k \mathbb{D}_k^{-1}Q_k - \frac{1}{10} h_k \mathbb{D}_k^{-1}Q_{k+1}]$$
$$+ \mathbb{D}_k^{-1}(\frac{1}{5} L_k + \frac{1}{4} M_k + \frac{1}{3} N_k) = 0$$

$$\frac{1}{h_k}[\frac{1}{2}(P_{k+1}-P_k) + \frac{1}{12} h_k \mathbb{D}_k^{-1}Q_k - \frac{1}{12} h_k \mathbb{D}_k^{-1} Q_{k+1}]$$
$$+ \mathbb{D}_k^{-1}(\frac{1}{4} L_k + \frac{1}{3} M_k + \frac{1}{2} N_k) = 0$$

$$\frac{1}{h_k} (P_{k+1}-P_k) + \mathbb{D}_k^{-1}(\frac{1}{3} L_k + \frac{1}{2} M_k + N_k) = 0$$

which can be readily solved to give

$$L_k = \frac{6}{h_k} \mathbb{D}_k (P_{k+1}-P_k) + 3(Q_k + Q_{k+1})$$

$$M_k = \frac{6}{h_k} \mathbb{D}_k (P_k - P_{k+1}) - 2(2Q_k + Q_{k+1})$$

$$N_k = Q_k \qquad (2.38)$$

so that the group current trial functions in this case becomes

$$V_k(z) = \frac{1}{k} D_k(6x-6x^2)(P_k-P_{k+1})+(1-4x+3x^2)Q_k+(-2x+3x^2)Q_{k+1}$$

i.e., the Fick's law current.

It can be shown that Equation 2.36 with identical matrix coefficients, as defined in Appendix C.2, is the result of taking arbitrary variations in all P_k^* and Q_k^* in Equation 2.37 and substituting for L_k, M_k and N_k using Equations 2.38.

(iii) Linear Current Trial Functions:

To make the notation more clear, the linear current trial functions given in Equations 2.25 may be rewritten in the form

$$V_k(z) = xM_k + N_k \qquad (2.39a)$$

; k = 1 to K

$$V_k^*(z) = xM_k^* + N_k^* \qquad (2.39b)$$

where N_k is the approximate group current column vector at positive side of node z_k and $(M_k + N_k)$ is the approximate group current vector at negative side of node z_{k+1}.

Substitution of Equations 2.39 and 2.34 into variation equation 2.12 results in the equation

$$\sum_{k=1}^{K} h_k \int_0^1 < [(1-3x^2+2x^3)\delta P_k^* + (3x^2-2x^3)\delta P_{k+1}^* + (-x+2x^2-x^3) h_k \mathbb{D}_k^{-1}(x)\delta Q_k^*$$

$$+ (x^2-x^3) h_k \mathbb{D}_k^{-1}(x)\delta Q_{k+1}^*]^T \{\frac{1}{h_k} M_k + \Lambda_k(x)[(1-3x^2+2x^3)P_k + (3x^2-2x^3)P_{k+1}$$

$$+ (-x+2x^2-x^3) h_k \mathbb{D}_k^{-1}(x) Q_k + (x^2-x^3) h_k \mathbb{D}_k^{-1}(x) Q_{k+1}]\} > dx$$

$$+ \sum_{k=1}^{K} h_k \int_0^1 < [x\delta M_k^* + \delta N_k^*]^T \{\frac{1}{h_k}[(6x-6x^2)(P_{k+1}-P_k) + (-1+4x-3x^2) h_k \mathbb{D}_k^{-1}(x) Q_k$$

$$+ (2x-3x^2) h_k \mathbb{D}_k^{-1}(x) Q_{k+1}] + \mathbb{D}_k^{-1}(x)(xM_k + N_k)\} > dx$$

$$+ \sum_{k=2}^{K} \delta P_k^{*T} [N_k - (M_{k-1} + N_{k-1})] = 0 \qquad (2.40)$$

Assuming that $\mathbb{D}_k(x)$ is constant within each region k and taking arbitrary variations in M_k^* and N_k^* yields the following equations:

$$\frac{1}{h_k}[\frac{1}{2}(P_{k+1}-P_k) + \frac{1}{12} h_k \mathbb{D}_k^{-1}(Q_k - Q_{k+1})] + \mathbb{D}_k^{-1}(\frac{1}{3} M_k + \frac{1}{2} N_k) = 0$$

$$\frac{1}{h_k}(P_{k+1}-P_k) + \mathbb{D}_k^{-1}(\frac{1}{2} M_k + N_k) = 0$$

which have the solution

$$M_k = Q_{k+1} - Q_k$$

$$N_k = -\frac{1}{h_k}\mathbb{D}_k(P_{k+1}-P_k) + \frac{1}{2}(Q_k - Q_{k+1})$$

The current trial functions then take the form of

$$V_k(z) = \frac{1}{h_k}\mathbb{D}_k(P_k - P_{k+1}) + (x - \frac{1}{2})(Q_{k+1} - Q_k)$$

which is not Fick's law. This result is expected since the degree of the assumed current trial functions is not high enough.

2.3.3 Summary of Section 2.3

From the study of the previous two subsections, we see that the use of variational equation 2.12, which is derived from setting the first variation with respect to adjoint quantities in the variational functional F_3 to zero, has the ability to force the current trial functions to obey Fick's law in one-dimension provided the following conditions are imposed:

1) The flux (and adjoint flux) trial functions are continuous across the region interfaces,
2) The diffusion coefficient matrix $\mathbb{D}_k$ is constant within each region k, and
3) The degree of current trial functions is higher than or equal to the degree of flux trial functions minus 1.

It can be shown (through more lengthy algebra) that the above conditions also apply to two-dimensional problems. In this case, however, we must change the third condition to say that the degree of X-direction current trial functions in x must be higher than or equal to the degree of flux trial functions in x minus 1 and the degree of flux trial functions in the y must be higher than or equal to the degree of flux trial functions in y. An analogous condition must be satisfied by Y-direction current trial functions.

In the next two chapters, we shall assume that the approximate current (and adjoint current) trial functions are always related to the approximate flux (and adjoint flux) trial functions via Fick's law, whether the latter are continuous acorss the region interfaces or not. However, when it is possible to make the flux trial functions continuous throughout the reactor (as in Chapter 3), we shall assume that too, so that the simpler variation equation, Equation 2.16a, can be used instead of Equation 2.12 in the derivation of the difference equations.

CHAPTER 3

INVESTIGATION OF FINITE ELEMENT METHOD USING DISCONTINUOUS CURRENT TRIAL FUNCTIONS

For a one-dimensional problem, the use of linear Hermite interpolation polynomials as approximate flux trial functions in the form of Equations 2.17 limits the number of unknowns to one for each node. Since these unknowns are tied up with the approximate values of the flux at nodal points $z = z_k$, this leaves us with no choice for imposing the current continuity conditions if Fick's law current trial functions are used. The same situation also exists in two-dimensional problems if we use bi-linear Hermite interpolation polynomials as flux trial functions and demand that they be continuous across all region interfaces.

The approximation employing cubic Hermite basis functions in one-dimension, as described in Section 3.2 of Chapter 2, has the ability to match both flux and current at interfaces between adjoining regions if Fick's law is assumed. Extension to using bi-cubic Hermite polynomials as flux approximations in two-dimensions, however, encounters the problem of current discontinuity in that no matter what forms of approximate trial functions are used for the flux, there is no way to force the Fick's law current trial functions to be continuous at those points which are formed by intersections of two or more material interfaces [52]. These points are called singular points.

In order to make the approximate solution to the diffusion problem more complete, it would be necessary to include the singular solutions [47], [53]-[54]. However, this is an impractical task for computation and the approach to be taken in this thesis is to ignore the singular part of the solution. The effect of singular solution on reaction rates and integral properties in reactor problems is generally negligible.

It is the aim of this chapter to investigate the consequences of not imposing <u>any</u> condition on those "current" coefficients in the cubic (or bi-cubic) flux trial functions, thus completely relaxing the requirement of current continuity. Use of the variational functional F_3, which permits the discontinuous trial functions in its solution space, whould enable us to find the "best" relation between these floating parameters. For simplicity, and without loss of generality, we shall assume that the nuclear constants are homogeneous within each individual subregions.

3.1 Derivation of Difference Equations in 1-D

The approximate cubic flux trial and weight functions, which are continuous throughout the 1-D problem domain, can be expressed in the following forms:

$$U_k(z) = u^{0+}(x)P_k + u^{0-}(x)P_{k+1} + u^{1+}(x)Q_{k,+} + u^{1-}(x)Q_{k+1,-} \quad (3.1a)$$

$$U_k^*(z) = u^{0+}(x)P_k^* + u^{0-}(x)P_{k+1}^* + u^{1+}(x)Q_{k,+}^* + u^{1-}(x)Q_{k+1,-}^* \quad (3.1b)$$

$$; \; k = 1 \text{ to } K$$

where the $U_k(z)$, P_k, $Q_{k,+}$, $Q_{k,-}$ and corresponding adjoint quantities are G-element vectors, and $u^{0\pm}(x)$ and $u^{1\pm}(x)$ are cubic Hermite basis functions defined by Equations 1.11. With the understanding that they are defined only over subregion k for each k = 1 to K, we can suppress the subscripts associated with them. The current trial functions defined by Fick's law in each region are given by

$$V_k(z) = -\frac{1}{h_k}\mathbb{D}_k\left[\frac{du^{0+}}{dx}P_k + \frac{du^{0-}}{dx}P_{k+1} + \frac{du^{1+}}{dx}Q_{k,+} + \frac{du^{1-}}{dx}Q_{k+1,-}\right] \tag{3.2a}$$

$$V_k^*(z) = \frac{1}{h_k}\mathbb{D}_k\left[\frac{du^{0+}}{dx}P_k^* + \frac{du^{0-}}{dx}P_{k+1}^* + \frac{du^{1+}}{dx}Q_{k,+}^* + \frac{du^{1-}}{dx}Q_{k+1,-}^*\right]$$

$$k = 1 \text{ to } K \tag{3.2b}$$

Insertion of these trial function forms into variation equation 2.16a results in the equation

$$\sum_{k=1}^{K} h_k \int_0^1 \{[\delta P_k^* u^{0+}(x) + \delta P_{k+1}^* u^{0-}(x) + \delta Q_{k,+}^* u^{1+}(x) + \delta Q_{k+1,-}^* u^{1-}(x)]^T$$

$$\mathbb{A}_k[u^{0+}(x)P_k + u^{0-}(x)P_{k+1} + u^{1+}(x)Q_{k,+} + u^{1-}(x)Q_{k+1,-}]\}dx$$

$$\sum_{k=1}^{K} \frac{1}{h_k}\int_0^1 \{[\delta P_k^* \frac{du^{0+}}{dx} + \delta P_{k+1}^* \frac{du^{0-}}{dx} + \delta Q_{k,+}^* \frac{du^{1+}}{dx} + \delta Q_{k+1,-}^* \frac{du^{1-}}{dx}]^T$$

$$\mathbb{D}_k\left[\frac{du^{0+}}{dx}P_k + \frac{du^{0-}}{dx}P_{k+1} + \frac{du^{1+}}{dx}Q_{k,+} + \frac{du^{1-}}{dx}Q_{k+1,-}\right]\}dx = 0 \tag{3.3}$$

Allowing arbitrary variations in all P^*_k, $Q^*_{k,+}$, and $Q^*_{k+1,-}$ results in a system of 3K+1 equations in 3K+1 unknowns (P_k, k = 1 to K + 1; $Q_{k,+}$, k = 1 to K; and $Q_{k,-}$, k = 2 to K + 1). These equations are given in Section 1 of Appendix D. The GxG matrix coefficients in these equations are of the form $A - \frac{1}{\lambda} B$ where A includes diffusion, absorption and scattering of neutrons and B includes fission neutron production of certain regions.

The choice of either zero flux, $P_k=0$ as well as $\delta P^*_k=0$ for k=1 or K+1, or zero current, $Q_{1,+}=\delta Q^*_{1,+}= 0$ or $Q_{K+1,-} = \delta Q^*_{K+1,-} = 0$, boundary conditions reduces the system to 3K-1 equations in 3K-1 unknowns. If we arrange the unknowns in order of $Q_{k,-}$, P_k, $Q_{k,+}$, then the resultant coefficients matrix of this system of equations is a symmetric, 7-stripe matrix.

3.2 Derivation of Differentc Equations in 2-D

For two-dimensional rectangular geometry problem domain shown in Figure 3.1, we subdivide the continuous variable X in the horizontal direction into I adjoining intervals and variable Y in the vertical direction into J adjoining intervals so that each region (i,j) is bounded by the lines $X=X_i$, $X=X_{i+1}$, $Y=Y_j$, and $Y=Y_{j+1}$. Similar to the one-dimensional case, we define $h_{xi}=X_{i+1}-X_i$ and $h_{yj}=Y_{j+1}-Y_j$ as the widths of region (i,j) in X and Y directions, respectively. We also define the dimensionless variables x and y within each region (i,j) as

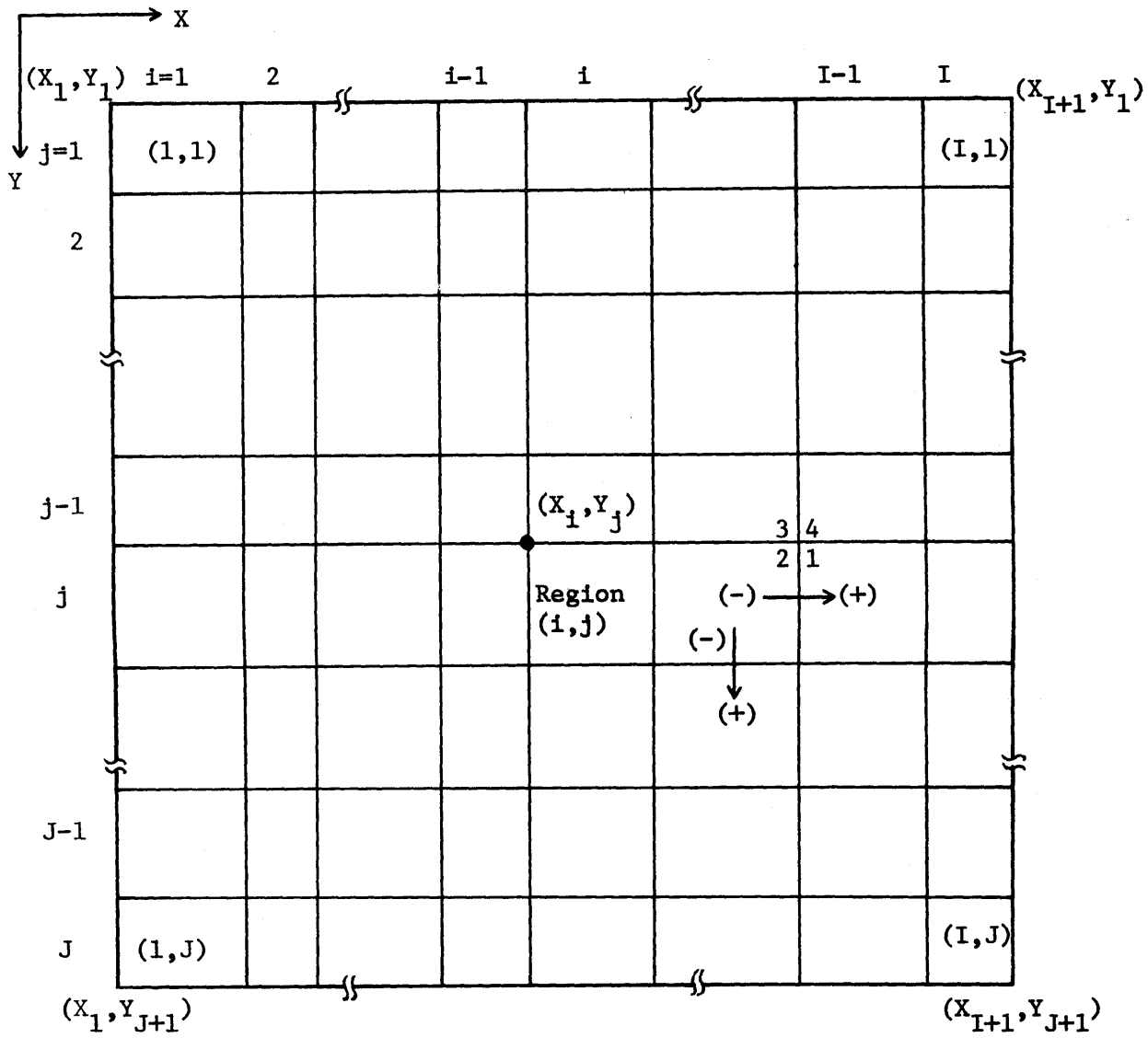

$$h_{xi} = X_{i+1} - X_i$$

$$h_{yj} = Y_{j+1} - Y_j$$

$$x = \frac{X - X_i}{h_{xi}} \; ; \quad X_i \leq X \leq X_{i+1}$$

$$y = \frac{Y - Y_j}{h_{yj}} \; ; \quad Y_j \leq Y \leq Y_{j+1}$$

} in each of the region (i,j)

Figure 3.1 The Subdivisions of Rectantular Problem Domain

$$x = \frac{X - X_i}{h_{xi}} \tag{3.4a}$$

$$y = \frac{Y - Y_j}{h_{yj}} \tag{3.4b}$$

so that region (i,j) can be described in terms of x and y as

$$0 \leq x \leq 1 \; ; \quad 0 \leq y \leq 1$$

for each region (i,j), i = 1 to I, j = 1 to J.

Because there are four cubic Hermite basis functions in each direction, 16 bi-cubic basis functions can be formed for a two-dimensional problem within a region. The most general form of flux trial function in any region (i,j) is thus a linear combination of these sixteen basis functions. Careful examination to satisfy the requirement of flux continuity reduces the general form of flux trial function in region (i,j) to

$$\begin{aligned} U_{i,j}(x,y) = [&P^{(0,0)}_{i,j} u^{0+}(x)u^{0+}(y) + P^{(0,0)}_{i+1,j} u^{0-}(x)u^{0+}(y) + P^{(0,0)}_{i+1,j+1} u^{0-}(x)u^{0-}(y) \\ &+ P^{(0,0)}_{i,j+1} u^{0+}(x)u^{0-}(y) + P^{(1,0)}_{i,j}(+)u^{1+}(x)u^{0+}(y) + P^{(1,0)}_{i+1,j}(-)u^{1-}(x)u^{0+}(y) \\ &+ P^{(1,0)}_{i+1,j+1}(-)u^{1-}(x)u^{0-}(y) + P^{(1,0)}_{i,j+1}(+)u^{1+}(x)u^{0-}(y) \\ &+ P^{(0,1)}_{i,j}(+)u^{0+}(x)u^{1+}(y) + P^{(0,1)}_{i+1,j}(+)u^{0-}(x)u^{1+}(y) \\ &+ P^{(0,1)}_{i+1,j+1}(-)u^{0-}(x)u^{1-}(y) + P^{(0,1)}_{i,j+1}(-)u^{0+}(x)u^{1-}(y) \end{aligned}$$

$$+ P_{i,j}^{(1,1)}(1)u^{1+}(x)u^{1+}(y)+P_{i+1,j}^{(1,1)}(2)u^{1-}(x)u^{1+}(y)$$

$$+ P_{i+1,j+1}^{(1,1)}(3)u^{1-}(x)u^{1-}(y) + P_{i,j+1}^{(1,1)}(4)u^{1+}(x)u^{1-}(y)] \qquad (3.5)$$

where $P_{i,j}^{(0,0)}$ is the approximate value of flux column vector at node (X_i, X_j), $P_{i,j}^{(1,0)}(\mp)$ and $P_{i,j}^{(0,1)}$ $(\pm)$ are related to X-direction current column vector at node $(X_{i\pm}, Y_j)$ and Y-direction column vector at node $(X_i, Y_{j\pm})$, respectively, and $P_{i,j}^{(1,1)}$ (k=1 to 4) are related to the approximate values of $\frac{\partial^2 \Phi}{\partial X \partial Y}$ at (X_{i+}, Y_{j+}), (X_{i-}, Y_{j+}), (X_{i-}, Y_{j-}), and (X_{i+}, Y_{j-}), respectively. Similar expression for adjoint flux trial functions in region (i,j), $U_{i,j}^{*}(x,y)$ is formed by replacing all P's with their corresponding adjoint quantities (P*'s).

The current trial function in region (i,j) can be written as

$$\underline{V}_{i,j}(x,y) = \underline{i}\, Q_{i,j}(x,y) + \underline{j}\, R_{i,j}(x,y) \qquad (3.6)$$

where $Q_{i,j}(x,y)$ is the approximate X-direction current trial function and $R_{i,j}(x,y)$ is the approximate Y-direction current trial function, both in region (i,j). $\underline{i}$ and $\underline{j}$ are unit vectors in the X- and Y-directions, respectively. According to Fick's law,

$$Q_{i,j}(x,y) = -\frac{\mathbb{D}_{ij}}{h_{xi}} \frac{\partial}{\partial x} U_{i,j}(x,y)$$

$$= -\frac{\mathbb{D}_{ij}}{h_{xi}} [P_{i,j}^{(0,0)} \frac{du^{0+}}{dx} u^{0+}(y) + P_{i+1,j}^{(0,0)} \frac{du^{0-}}{dx} u^{0+}(y)$$

$$+ P_{i+1,j+1}^{(0,0)} \frac{du^{0-}}{dx} u^{0-}(y) + P_{i,j+1}^{(0,0)} \frac{du^{0+}}{dx} u^{0-}(y)$$

$$+ P_{i,j}^{(1,0)} (+) \frac{du^{1+}}{dx} u^{0+}(y) + P_{i+1,j}^{(1,0)} (-) \frac{du^{1-}}{dx} u^{0+}(y)$$

$$+ P_{i+1,j+1}^{(1,0)} (-) \frac{du^{1-}}{dx} u^{0-}(y) + P_{i,j+1}^{(1,0)} (+) \frac{du^{1+}}{dx} u^{0-}(y)$$

$$+ P_{i,j}^{(0,1)} (+) \frac{du^{0+}}{dx} u^{1+}(y) + P_{i+1,j}^{(0,1)} (+) \frac{du^{0-}}{dx} u^{1+}(y)$$

$$+ P_{i+1,j+1}^{(0,1)} (-) \frac{du^{0-}}{dx} u^{1-}(y) + P_{i,j+1}^{(0,1)} (-) \frac{du^{0+}}{dx} u^{1-}(y)$$

$$+ P_{i,j}^{(1,1)} (1) \frac{du^{1+}}{dx} u^{1+}(y) + P_{i+1,j}^{(1,1)} (2) \frac{du^{1-}}{dx} u^{1+}(y)$$

$$+ P_{i+1,j+1}^{(1,1)} (3) \frac{du^{1-}}{dx} u^{1-}(y) + P_{i,j+1}^{(1,1)} (4) \frac{du^{1+}}{dx} u^{1-}(y)] \qquad (3.7a)$$

and

$$R_{i,j}(x,y) = - \frac{\mathbb{D}_{i,j}}{h_{yj}} \frac{\partial}{\partial y} U_{i,j}(x,y)$$

$$= - \frac{\mathbb{D}_{i,j}}{h_{yj}} [P_{i,j}^{(0,0)} u^{0+}(x) \frac{du^{0+}}{dy} + P_{i+1,j}^{(0,0)} u^{0-}(x) \frac{du^{0+}}{dy}$$

$$+ P_{i+1,j+1}^{(0,0)} u^{0-}(x) \frac{du^{0-}}{dy} + P_{i,j+1}^{(0,0)} u^{0+}(x) \frac{du^{0-}}{dy}$$

$$+ P_{i,j}^{(1,0)} (+) u^{1+}(x) \frac{du^{0+}}{dy} + P_{i+1,j}^{(1,0)} (-) u^{1-}(x) \frac{du^{0+}}{dy}$$

$$+ P_{i+1,j+1}^{(1,0)} (-) u^{1-}(x) \frac{du^{0-}}{dy} + P_{i,j+1}^{(0,0)} (+) u^{1+} \frac{du^{0-}}{dy}$$

$$+ P^{(0,1)}_{i,j} (+)\ u^{0+}(x)\ \frac{du^{1+}}{dy} + P^{(0,1)}_{i+1,j} (+)\ u^{0-}(x)\ \frac{du^{1+}}{dy}$$

$$+ P^{(0,1)}_{i+1,j+1} (-)\ u^{0-}(x)\ \frac{du^{1-}}{dy} + P^{(0,1)}_{i,j+1} (-)\ u^{0+}(x)\ \frac{du^{1-}}{dy}$$

$$+ P^{(1,1)}_{i,j} (1)\ u^{1+}(x)\ \frac{du^{1+}}{dy} + P^{(1,1)}_{i+1,j} (2)\ u^{1-}(x)\ \frac{du^{1+}}{dy}$$

$$+ P^{(1,1)}_{i+1,j+1}(3)\ u^{1-}(x)\ \frac{du^{1-}}{dy} + P^{(1,1)}_{i,j+1} (4)\ u^{1+}(x)\ \frac{du^{1-}}{dy}] \qquad (3.7b)$$

Similar expressions can be written for adjoint current trial functions in each region (i,j).

The variation equation 2.16a can now be written as

$$\sum_{i=1}^{I} \sum_{j=1}^{J} h_{xi} h_{yj} \int_0^1 dx \int_0^1 dy\ [\delta U^{*T}_{i,j}\ \mathbb{A}_{i,j}\ U_{i,j} -$$

$$(\delta Q^{*T}_{i,j}\ \mathbb{D}^{-1}_{i,j} Q_{i,j} + R^{*T}_{i,j}\ \mathbb{D}^{-1}_{i,j}\ R_{i,j})] = 0 \qquad (3.8)$$

Substitution of Equations 3.5 and 3.7 into this equation, then allowing arbitrary variations in all starred adjoint quantities results in a system of equations involving (3I+1)(3J+1) equations in same number of unknowns. These equations are given in Section 2 of Appendix D. The GxG matrix coefficients in these equations are of the form $A - \frac{1}{\lambda} B$. The ordering of unknowns follows the rule that: (i) j=1 to J + 1, (ii) for each j, i=1 to I+1, and (iii) for each (i,j), the nine unknowns (less than nine at boundary points) are in the order $P^{(0,0)}_{i,j}$, $P^{(1,0)}_{i,j}(+)$, $P^{(1,0)}_{i,j}(-)$, $P^{(0,1)}_{i,j}(+)$, $P^{(0,1)}_{i,j}(-)$, $P^{(1,1)}_{i,j}(1)$,

$P_{i,j}^{(1,1)}(2)$, $P_{i,j}^{(1,1)}(3)$, and $P_{i,j}^{(1,1)}(4)$.

Imposing the boundary conditions reduces slightly the number of equations as well as number of unknowns. However, regardless of the types of boundary conditions imposed, the system of equations is an NxN matrix problem of the form

$$\mathbb{A}\,\underline{P} + \frac{1}{\lambda}\mathbb{B}\,\underline{P} \tag{3.9}$$

where $\mathbb{A}$ and $\mathbb{B}$ are independent of λ and $\underline{P}$ is a column vector consisted of N unknown elements. The order N of the matrix equation is dependent on the chosen boundary conditions and is given for various choices in Table 3.1.

3.3 Numerical Method

The matrix equations which results from the approximations given in this chapter are of the form of Equation 3.9. The source iterative scheme and the Cholesky method which are used in solving these equations are discussed in this section.

In this Chapter, Equation 3.9 has been defined as ordered first by spatial indexing followed by group indexing within each spatial index. For convenience, it is a general practice to reorder these equations so that they are ordered first by group indexing followed by spatial indexing within each group. After reordering, Equation 3.9 can be written as

$$(\mathbb{L} + \mathbb{M})\,\underline{P} = \mathbb{T}\underline{P} + \frac{1}{\lambda}\,\mathbb{B}\,\underline{P} \tag{3.10a}$$

Table 3.1 Matrix Order N of the Bi-cubic Hermite Basis Functions Approximations with Discontinuous Current Trial Functions

1 - Zero flux boundary condition

2 - Symmetry (zero current) boundary condition

Boundary Condition Type				Matrix Order
Left	Right	Top	Bottom	N
1	1	1	1	G(9IJ+I+J+1)
1	1	1	2	G(9IJ+I+J-1)
1	1	2	1	
1	2	1	1	
2	1	1	1	
1	1	2	2	G(9IJ+I+J-3)
2	2	1	1	
1	2	2	2	
2	1	2	2	
2	2	1	2	
2	2	2	1	
2	2	2	2	
1	2	1	2	G(9IJ+I+J-2)
1	2	2	1	
2	1	1	2	
2	1	2	1	

where

$$\mathbb{A} = \mathbb{L} + \mathbb{M} - \mathbb{T} \tag{3.10b}$$

and: $\mathbb{L}$, the stiffness matrix, results from leakage; $\mathbb{M}$, the mass matrix, results from absorption; $\mathbb{T}$ is the group-to-group scattering transfer matrix; and $\mathbb{B}$ is the fission source production matrix. If N is the number of unknowns in each of the G groups, $\mathbb{L}$ and $\mathbb{M}$ are GxN block diagonal matrices composed of G NxN symmetric matrices $\mathbb{L}_g$ and $\mathbb{M}_g$ of the form

$$\mathbb{L} = \text{Diag}[\mathbb{L}_1, ---, \mathbb{L}_G]$$

$$\mathbb{M} = \text{Diag}[\mathbb{M}_1, ---, \mathbb{M}_G]$$

and $\mathbb{T}$ and $\mathbb{B}$ are in general full block matrices composed of G^2 NxN symmetric matrices $\mathbb{T}_{gg'}$ and $\mathbb{B}_{gg'}$, respectively. If only down-scattering is permitted, T becomes lower block triangular; $\mathbb{T}_{gg'} = 0$ whenever $g' \geq g$.

A direct method such as the Gauss elimination method [42],[55] is inefficient compared to iterative schemes for solving large systems of linear equations, such as Equation 3.10a. One very commonly used method in reactor physics calculation is the source iterative scheme [5], [56]-[57]. In this method, the equation for the j-th iterative solution of Equation 3.10a is set in the following form

$$(\mathbb{L}_g + \mathbb{M}_g)\, \underline{P}_G^{(j)} = \sum_{g'=1}^{G} [\, \mathbb{T}_{gg'} + \frac{1}{\lambda} \mathbb{B}_{gg'}] \, \underline{P}_{g'}^{(i)} \tag{3.11}$$

where $g = 1, 2, ---, G$

$$i = \begin{cases} j & ; \quad g' < g \\ j-1; & \quad g' \geq g, \end{cases}$$

$$j = 1,2,\ldots,$$

and $\underline{P}^{(0)} = \text{Col}\,[\underline{P}_1^{(0)}, \underline{P}_2^{(0)}, \ldots, \underline{P}_G^{(0)}]$ is an initial guess. In our case, $\mathbb{K}_g \equiv \mathbb{L}_g + \mathbb{M}_g$ is positive definite and we can use the Cholesky scheme [58]-[59], which always gives a unique factorization of $\mathbb{K}_g$ in the form

$$\mathbf{K}_g = \mathbf{E}\,\mathbf{E}^T \tag{3.12}$$

where $\mathbb{E}$ is a lower triangular matrix. Let $\mathbb{K}_g = (k_{ij})$, $\mathbb{E} = (e_{ij})$. Then we note that according to Equation 3.12 we have

$$k_{jj} = e_{ji}^2 + e_{j2}^2 + \cdots + e_{jj}^2$$

$$k_{ij} = e_{i1}e_{j1} + e_{12}e_{j2} + \cdots + e_{ij}e_{jj}, \qquad j \leq i$$

Therefore, e_{ij} can be determined using the algorithm,

$$e_{jj} = \left[k_{jj} - \sum_{n=1}^{j-1} e_{jn}^2\right]^{1/2}$$

$$e_{ij} = \left[k_{ij} - \sum_{n=1}^{j-1} e_{in}e_{jn}\right]/e_{jj} \tag{3.13}$$

The matrices $\mathbb{E}$ and $\mathbb{E}^T$ possess the same band structure as $\mathbb{K}_g$. By using the Cholesky scheme, the numerical inversion of $\mathbb{K}_g$ is simplified, and it requires only a forward and a backward sweep to invert $\mathbb{E}$ and $\mathbb{E}^T$, respectively.

In the eigenvalue problem defined by Equation 3.9, only the largest

eigenvalue λ is of interest because it corresponds to the neutron multiplication constant in the reactor physics. The largest eigenvalue of Equaion 3.9 can be determined by the power method [5], [56], [60] which is determined briefly below. Suppose $\underline{P}_g^{'(j+1)}$ is the (j+1)-th iterative solution to Equation 3.11 for group g before renormalization and $\underline{P}_g^{(j)}$ is the j-th iterative solution for group g after normalization, then the largest eigenvalue and its eigenfunction are defined by

$$\lambda^{(j+1)} = \frac{\sum_g (\underline{P}_g^{'(j+1)}, \underline{P}_g^{'(j+1)})}{\sum_g (\underline{P}_g^{'(j+1)}, \underline{P}_g^{(j)})} \tag{3.14a}$$

$$\underline{P}_g^{(j+1)} = \frac{\underline{P}_g^{'(j+1)}}{\lambda^{(j+1)}} \; ; \; g = 1,2,---,G \tag{3.14b}$$

Steps defined by Equations 3.11 and 3.14 are repeated until the following convergence criteria are satisfied:

$$\left| \frac{\lambda^{(j+1)} - \lambda^{(j)}}{\lambda^{(j)}} \right| \leq \varepsilon_\lambda \tag{3.15a}$$

$$\max_{n,g} \left| \frac{P_{ng}^{(j+1)} - P_{ng}^{(j)}}{P_{ng}^{(j)}} \right| \leq \varepsilon_p \tag{3.15b}$$

The whole procedure described in this section can be best illustrated in Figure 3.2.

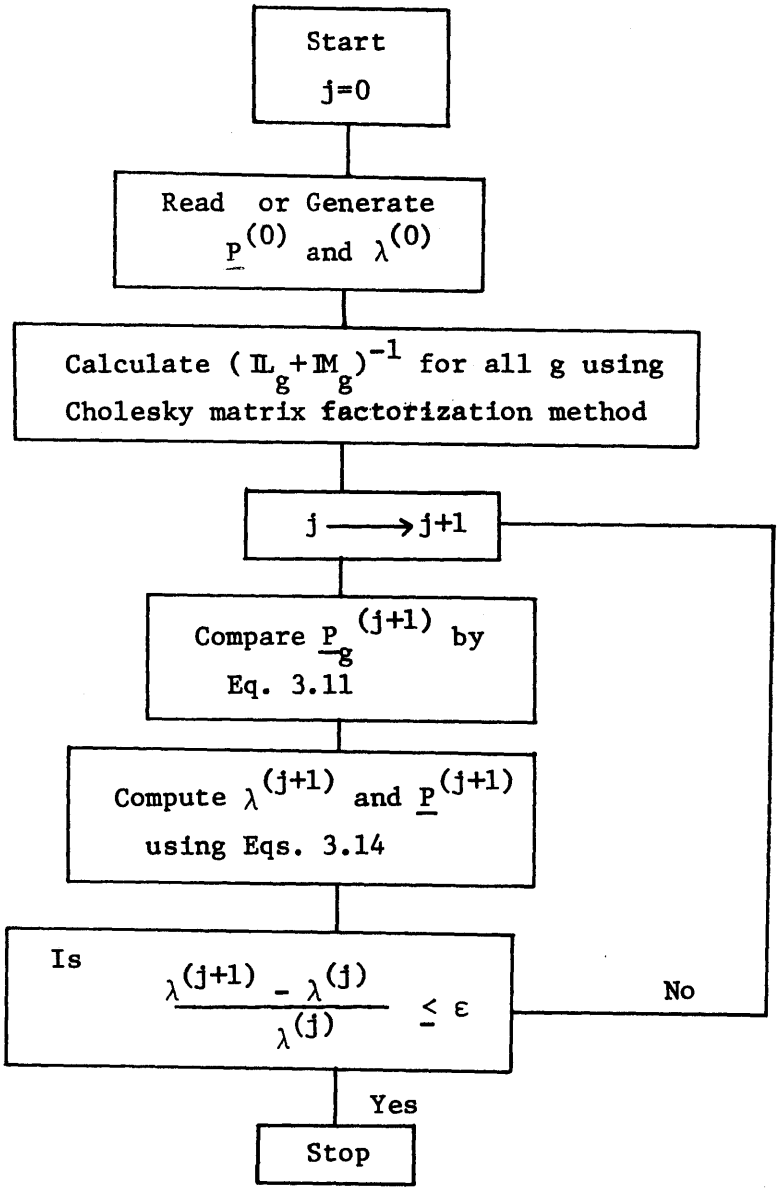

Figure 3.2 Solution Scheme for $\mathbb{A}\,\underline{P} = \frac{1}{\lambda}\mathbb{B}\,\underline{P}$ Using Source Iterative Method.

3.4 Numerical Results

In this section, some of the numerical results for stationary eigenvalue problems are presented in order to demonstrate the accuracy of the variational method using cubic Hermite basis functions as flux approximations with discontinuous Fick's law current trial functions. No special computer programs were written for the calculations and each individual case was treated as a single computer problem. The two-group parameters used in the following examples are given in Table 3.2.

Example 3.1 One-dimensional, Two-group, Single Region Problem

We consider an eigenvalue problem for a one-dimensional two-group, one region simple diffusion problem. The reactor configuration is depcited in Figure 3.3.

The analytical solution for this simple problem can be found easily and is given by

$$\phi_1(z) = C \sin(\frac{\pi}{2L} z)$$

$$\phi_2(z) = \sin(\frac{\pi}{2L} z) \qquad (3.16)$$

where L = 60 cm is the width of the reactor and C is the fast to thermal flux ratio which is a constand independent of position z given by

$$C = \frac{D_2(\frac{\pi}{2L})^2 + \Sigma_2}{\Sigma_{21}} = 3.337902595$$

The largest eigenvalue λ for the problem can be shown to be

Table 3.2 Two-group Nuclear Constants

(a) Thermal Group

	Fuel	Water Reflectors
D_2	0.4	0.15
Σ_2	0.2	0.02
$\nu\Sigma_{f2}$	0.218	0.0
χ_2	0.0	———

(b) Fast Group

	Fuel	Water Reflectors
D_1	1.5	1.2
Σ_1	0.0623	0.101
Σ_{21}	0.06	0.1
$\nu\Sigma_{f1}$	0.0	0.0
χ_1	1.0	———

$$\lambda = \frac{(\nu\Sigma_{f2})(\Sigma_{21})}{[D_1(\frac{\pi}{2L})^2 + \Sigma_1][D_2(\frac{\pi}{2L})^2 + \Sigma_2]} = 1.031303490$$

In Table 3.3(a), comparisons are made for eigenvalues and average fast to thermal flux ratios obtained by various mesh spacings. It is seen that both the eigenvalues and flux ratios converge to the true analytical values with decreasing mesh spacings. The average fast to thermal flux ratio is defined as the average value obtained by dividing the fast group result by the corresponding thermal group result for each space unknowns. In Table 3.3(b), the thermal fluxes at various points of the reactor are compared and it is seen that the flux shape converges rapidly to the analytical shape as the mesh sizes are refined. The relative error is defined as

$$\text{Average Error} = \frac{\text{Approximate Value} - \text{True Value}}{\text{True Value}} \tag{3.17}$$

In Table 3.3(c), the thermal currents at various points of the reactor are compared with the analytical results. It is seen that the "best" results for current obtained using a variational method that permits discontinuities in current are <u>not</u> continuous at mesh points. As the mesh size shrinks, more and more current discontinuities are introduced, although the magnitude of discontinuities seems to become smaller and smaller.

Since the problem is a homogeneous one, the converges to the true eigenvalue and true flux and current shapes are quite fast. Accuracies of 10^{-9} in eigenvalue, 10^{-5} in flux shape and 10^{-3} in current shape can

Table 3.3 Results of One-dimensional, Two-group, One-region Problem: Example 3.1

(a) Eigenvalues and Average Fast to Thermal Flux Ratios

Δz	Eigenvalue, λ	Flux Ratio, C
Analytical	1.031303490	3.337902595
L/2	1.031303421	3.337902612
L/3	1.031303485	3.337902596
L/6	1.031303490	3.337902595
L/12	1.031303490	3.337902595

Figure 3.3 Reactor Configuration for Example 3.1

Table 3.3 (Continued)

(b) Thermal Fluxes with Relative Error

z	Analytical	$\Delta z = L/2$ (error x 10^4)	$\Delta z = L/3$ (error x 10^5)	$\Delta z = L/6$ (error x 10^6)
0.0	0.0	0.0	0.0	0.0
5.0	0.13052619	0.13053365 (+0.572)	0.13051992 (-4.80)	0.13052531 (-6.74)
10.0	0.25881905	0.25871065 (-4.19)	0.25879147 (-10.7)	0.25881793 (-4.33)
15.0	0.38268343	0.38248222 (-5.26)	0.38265889 (-6.41)	0.38268085 (-6.74)
20.0	0.5	0.49979957 (-4.01)	0.49996639 (-6.72)	0.49999785 (-4.30)
25.0	0.60876143	0.60861390 (-3.98)	0.60872601 (-5.82)	0.60875732 (-6.75)
30.0	0.70710678	0.70687644 (-3.26)	0.70703144 (-10.7)	0.70710374 (-4.30)
35.0	0.79335334	0.79328492 (-0.862)	0.79330454 (-6.15)	0.79334798 (-6.76)
40.0	0.86602540	0.86568184 (-3.97)	0.86596717 (-6.72)	0.86602167 (-4.31)
45.0	0.92387953	0.92330950 (-6.17)	0.92383484 (-4.84)	0.92387329 (-6.75)
50.0	0.96592583	0.96541020 (-5.34)	0.96580584 (-12.4)	0.96592166 (-4.32)
55.0	0.99144486	0.99122627 (-2.20)	0.99136572 (-7.98)	0.99143708 (-7.85)
60.0	1.0	1.0	1.0	1.0

Table 3.3 (Concluded)

(c) Thermal Currents and Relative Errors

* Currents are in the unit of D_2 and since D_2 is a constant in this example, it is just a scaling factor

** Wherever a double-value appears, the upper one corresponds to the value at the left-hand side and the lower one corresponds to the value at the right-hand side of z_k.

z	Analytical	$\Delta z = L/2$ (error x 10^3)	$\Delta z = L/3$(error x 10^3)	$\Delta z = L/6$(error x 10^4)
0.0	1.0	1.00098816(+0.988)	1.00019725(+0.197)	1.00001242 (+0.124)
5.0	0.99144486	0.99081050(-0.640)	0.99125542(-0.191)	0.99143956(-0.0535)
10.0	0.96592583	0.96498125(-0.978)	0.96584471(-0.0840)	0.96589942(-0.273) 0.96597621(+0.522)
15.0	0.92387953	0.92350042(-0.410)	0.92396515(+0.0927)	0.92387459(-0.0535)
20.0	0.86602540	0.86636800(+0.396)	0.86561671(-0.472) 0.86677571(+0.866)	0.86596197(-0.732) 0.86611033(+0.981)
25.0	0.79335334	0.79358399(+0.291)	0.79293956(-0.522)	0.79334909(-0.0536)
30.0	0.70710678	0.70514840(-2.77) 0.71170298(+6.50)	0.70704737(-0.0840)	0.70701064(-1.36) 0.70722045(+1.61)
35.0	0.60876143	0.60755666(-1.98)	0.60909913(+0.555)	0.60875816(-0.0537)
40.0	0.5	0.49762201(-4.76)	0.49909484(-1.81) 0.50148711(+2.97)	0.49987771(-2.45) 0.50013468(+2.69)
45.0	0.38268343	0.38189902(-2.05)	0.38201065(-1.76)	0.38268138(-0.0536)
50.0	0.25881905	0.26038768(+6.06)	0.25860398(-0.831)	0.25867894(-5.41) 0.25901496(+7.57)
55.0	0.13052619	0.13308801(+19.6)	0.13126710(+5.68)	0.13050076 (-1.95)
60.0	0.0	0.0	0.0	0.0

be obtained even when a mesh size of $\Delta z = L/6 = 10$ cm is used. This is not the case when the reactor becomes more heterogeneous, as can be seen from the next example.

Example 3.2 One-dimensional, Two-group, Two-region Problem

The reactor configuration is shown in Figure 3.4. It consists of a water reflector region and a fuel region. The analytical solution of this problem is also possible [61], though not easy. The largest eigenvalue is $\lambda = 1.020902463$ and the flux and current shapes are combinations of hyperbolic functions as well as trigonometric functions.

Table 3.4(a) gives the eigenvalues obtained by various methods. It is seen that all eigenvalues converge to the true value and that the rate of convergence of the present method is comparable to that of cubic Hermite method ($m = 2$). This result should be expected since the only difference between these two methods is in the initial assumption about current coefficients in the flux trial functions. In Table 3.4(b), the thermal fluxes at 5 cm intervals using different mesh spacings are compared with the analytical solution. The neutron fluxes are seen to converge to the true solution, though not as fast as in the homogeneous case. And when $\Delta z = L/12$ spacing is used, the result is quite good. Table 3.4(c) compares thermal neutron currents predicted by the present method against analytical results. It is observed that the most severe discontinuity usually occurs at the material interface and that the magnitudes of discontinuities decrease as Δz decreases and as the distances from the interface become larger.

Table 3.4 One-dimensional, Two-group, Two-region Eigenvalue Problem: Example 3.2

(a) Eigenvalue, λ

Δz	Hermite Method*		Present Method (m = 2)	Finite Difference
	m = 1	m = 2		
L/3	1.02483992	1.02145224	1.021534466	1.02397928
L/6	1.02257106	1.02096418	1.020964354	1.02410016
L/12	1.02147201	1.02090512	1.020904977	1.02139257

*From C.M. Kang [24].

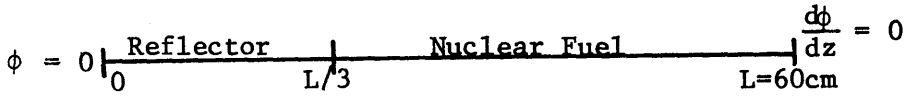

Figure 3.4 Reactor Configuration for Example 3.2

Table 3.4 (Continued)

(b) Thermal Fluxes with Relative Errors

z (cm)	Analytical	$\Delta z = L/3$ (error x 10^2)	$\Delta z = L/6$ (error x 10^3)	$\Delta z = L/12$ (error x 10^4)
0.0	0.0	0.0	0.0	0.0
5.0	0.08486903	-0.02365409 (-128.0)	0.08575762 (+10.5)	0.08492856 (+7.01)
10.0	0.30882356	0.046933375 (+52.0)	0.32170626 (+41.7)	0.30907204 (+8.05)
15.0	0.83938228	0.87290130 (+3.99)	0.90204065 (+74.6)	0.84008346 (+8.35)
20.0	0.57723662	0.58098635 (+0.650)	0.57136244 (-10.2)	0.57652361 (-12.4)
25.0	0.41559201	0.42719308 (+2.79)	0.39992663 (-37.7)	0.41503756 (-13.3)
30.0	0.55164109	0.53331112 (-3.32)	0.54655308 (-9.22)	0.55164881 (+0.140)
35.0	0.68057223	0.71250788 (+4.69)	0.68137634 (+1.18)	0.68059766 (+0.374)
40.0	0.79133441	0.77795075 (-1.69)	0.79187389 (+0.682)	0.79135182 (+0.220)
45.0	0.88074847	0.88394510 (+0.363)	0.88098813 (+0.272)	0.88075832 (+0.112)
50.0	0.94639693	0.95235240 (+0.629)	0.94650201 (+0.111)	0.94640103 (+0.0433)
55.0	0.98650822	0.98907119 (+0.260)	0.98651891 (+0.0108)	0.98650875 (+0.00537)
60.0	1.0	1.0	1.0	1.0

Normalized to $\phi_2(L) = 1.0$

Table 3.4 (Concluded)
(c) Thermal Currents with Relative Errors

z	Analytical	$\Delta z = L/3$(error x 10)	$\Delta z = L/6$(error x 10^2)	$\Delta z = L/12$(error x 10^2)
0.0	-0.001968220	+0.014519873(-83.8)	-0.002226754(+13.1)	-0.001983346(+0.769)
5.0	-0.003766414	-0.010070317(+16.7)	-0.003872149(+2.81)	-0.003751260(-0.402) -0.003787034(+0.547)
10.0	-0.010764179	-0.016478641(+5.31)	-0.011238215(+4.40) +0.003528296(-133)	-0.010768653(+0.0416) -0.010350732(-3.84)
15.0	-0.019144018	-0.004705100(-7.54)	-0.021046600(+9.94)	-0.019788388(+3.37) -0.014183722(-25.9)
17.5	-0.033976720	+0.007999870(+13.5)	+0.005594907(-265)	-0.003683987(+8.43)
20.0	+0.082977003	+0.025250308(-6.96) +0.027682116(-6.66)	+0.058189052(-29.9) +0.052060765(-37.3)	+0.076360442(-7.97) +0.072401290(-12.7)
22.5	+0.002761894	+0.011680686(+32.3)	+0.010511939(+281)	+0.002087998(-24.4)
25.0	-0.009608219	-0.000584092(-9.39)	-0.011819330(+23.0)	-0.003239979(-66.3) -0.010026411(+4.35)
30.0	-0.010914588	-0.013903693(+2.74)	+0.000585402(-105) -0.012137192(+11.2)	-0.010769183(-1.33) -0.010928165(+0.124)
35.0	-0.009637810	-0.012276687(+2.74)	-0.009623681(-0.147)	-0.009633476(-0.0450) -0.009637838(+0.000291)
40.0	-0.008043424	+0.004296928(-15.3) -0.010140324(+2.61)	-0.008245078(+2.51) -0.008008875(-0.430)	-0.008042316(-0.0138) -0.008043171(-0.00315)
45.0	-0.006230551	-0.006897419(+1.07)	-0.006217263(-0.213)	-0.006229599(-0.0153) -0.006230457(-0.00151)
50.0	-0.004249518	-0.004126398(-0.290)	-0.004232819(-0.393) -0.00424573(-0.0891)	-0.004248694(-0.0194) -0.004249614(+0.00226)
55.0	-0.002153818	-0.001827257(-1.52)	-0.002148447(-0.249)	-0.002153151(-0.0310) -0.002154272(+0.0211)
60.0	0.0	0.0	0.0	0.0

Example 3.3 Two-dimensional, One-group, One-region Model Problem

An eigenvalue problem for a two-dimensional neutron diffusion equation is considered in this example. The configuration consists of uniform nuclear fuel and is shown in Figure 3.5. For the one-group D, $\sum$, and $\nu\sum_f$, we use the thermal group constants given in Table 3.2.

For the present method, we only calculate the eigenvalue and flux shape using a mesh size of L/2 = 20 cm in both directions because of large number of unknowns (In fact, the number of unknowns is 38 per group for a 2x2 problem, from Table 3.1). This eigenvalue is listed in Table 3.5 with eigenvalues for different meshes obtained by the cubic finite element method and the finite difference scheme. Note that the present method yields a worse eigenvalue than the finite difference scheme using the same mesh size. The flux shapes at y = 0 cm and y = 20 cm obtained from present method are compared with the true cosine shapes in Figure 3.6. The currents are not continuous across all mesh interfaces.

Example 3.4 Two-dimensional, Two-group, Two-region Problem

In this example, we consider an eigenvalue problem of the two-group neutron diffusion equations. The system consists of a fuel region inside and a reflector region outside (Figure 3.7).

In Table 3.6, comparisons are made for eigenvalues obtained by various methods. For cubic (m = 2) Hermite method, the results given correspond to using Equation 3.5 as flux trial functions and setting

Table 3.5 Eigenvalue $1/\lambda$ of a Two-dimensional, One-group, One-region Problem: Example 3.3

Analytical, $1/\lambda = 0.9230903697$

Δr	Cubic Hermite*	Finite Difference	Present Method
L/2	0.9230904055	0.92280573	0.9212300089
L/4	0.9230903703	0.92301801	————
L/6	0.9230903697	0.92305812	————

* From C.M.Kang [24].

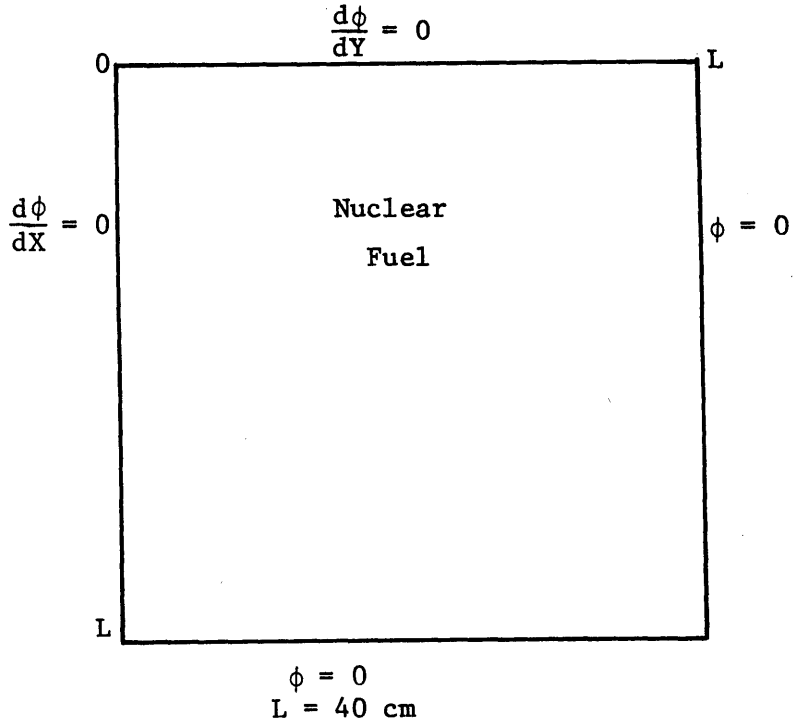

Figure 3.5 Reactor Configuration for Example 3.3

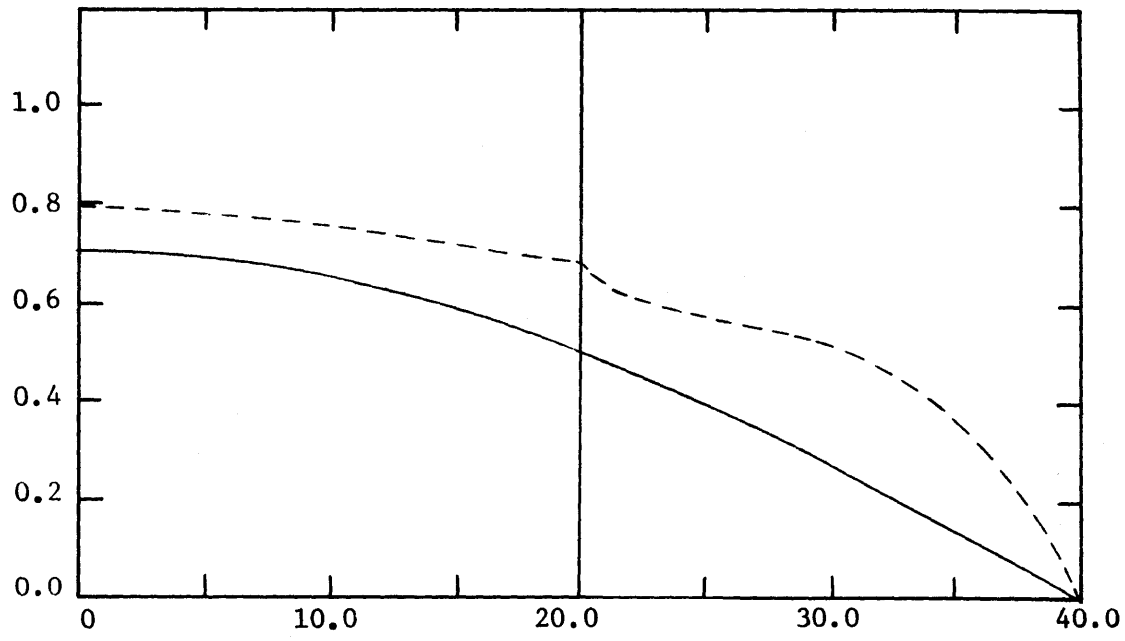

Analytic 0.9230903697

2x2 0.92122300089 (-0.2023%)

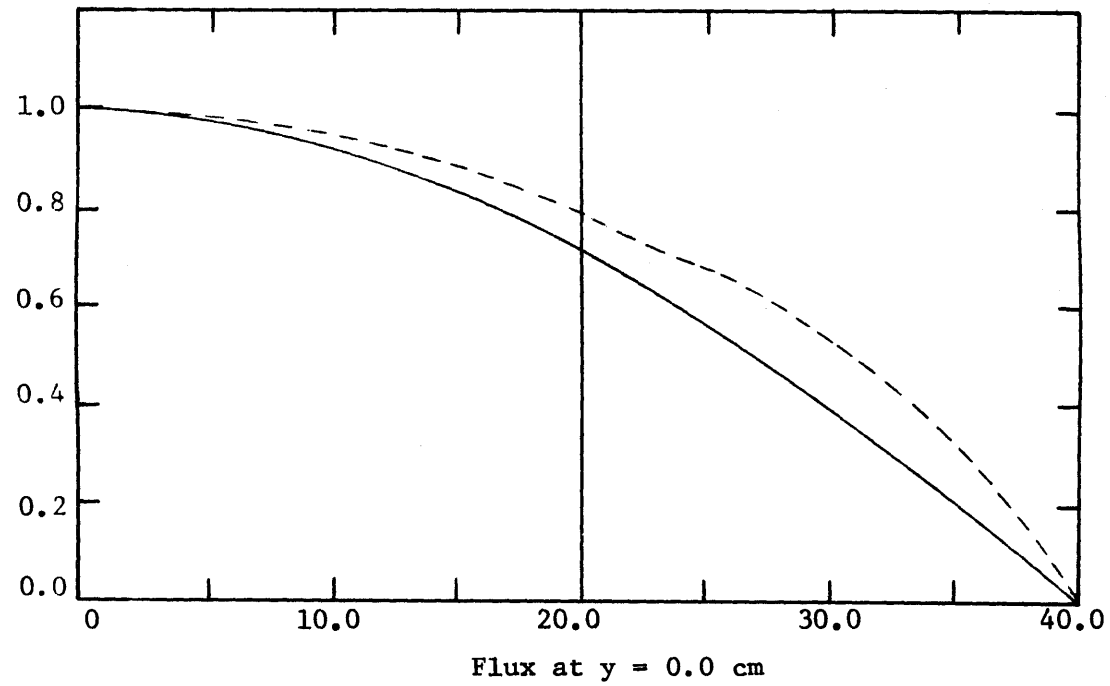

Figure 3.6 Flux Shapes: Example 3.3

1) $\mathbb{D}_1 P^{(1,1)}_{i,j}(1) = \mathbb{D}_2 P^{(1,1)}_{i,j}(2) = \mathbb{D}_3 P^{(1,1)}_{i,j}(3) = \mathbb{D}_4 P^{(1,1)}_{i,j}(4)$ (3.18)

where $\mathbb{D}_k$ is the diffusion constant matrix at k-th corner of point (X_i, X_j), at singular points ($\mathbb{D}_1 \mathbb{D}_3 \neq \mathbb{D}_2 \mathbb{D}_4$), and

2) Eq. 3.18, $\mathbb{D}_1 P^{(1,0)}_{i,j}(+) = \mathbb{D}_2 P^{(1,0)}_{i,j}(-)$, and $\mathbb{D}_2 P^{(0,1)}_{i,j}(+) = \mathbb{D}_3 P^{(0,1)}_{i,j}(-)$ at all regular points ($\mathbb{D}_1 \mathbb{D}_3 = \mathbb{D}_2 \mathbb{D}_4$), before applying the weighted residual process in Ritz-Galerkin method. It is seen that both the cubic Hermite method and the present method for $\Delta r = L/2$ yield accuracy comparable to that of the finite difference scheme for $\Delta r = L/20$.

In Figure 3.8, thermal fluxes at y = 0 cm and y = 20 cm for (i) Cubic Hermite method, $\Delta r = L/2$, (ii) Present variational method, $\Delta r = L/2$, and (iii) Finite difference method, $\Delta r = L/20$ are compared. Note that present method gives slightly better flux shapes than the cubic Hermite method.

From the results of these numerical examples, it is observed that the present variational method using discontinuous Fick's law current trial functions yields eigenvalues and flux shapes comparable to those obtained from the cubic Hermite method and is generally better than the linear Hermite method and finite difference method. However, since the number of unknowns in present method is considerably larger than that of the cubic Hermite method if the same mesh spacing is used, we conclude that the cubic Hermite method is better than our present method.

Table 3.6 Eigenvalues $1/\lambda$ of Two-dimensional, Two-group, Two-region Problem: Example 3.4

Δr	Hermite Method*		Present Method	Finite Difference
	m = 1	m = 2		
L/2	1.0802150	1.1082321	1.1075521	1.0783013
L/4	1.0962251	1.1134916	———	1.0797120
L/6	1.1040456	1.1140943	———	1.1105031

*From C.M. Kang [24].

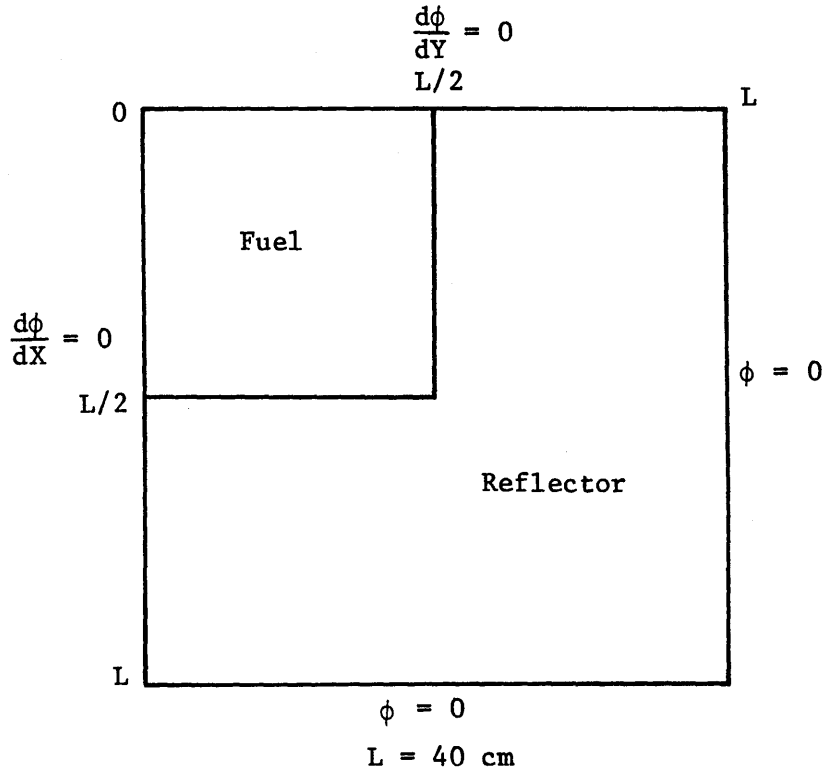

Figure 3.7 Reactor Configuration for Example 3.4

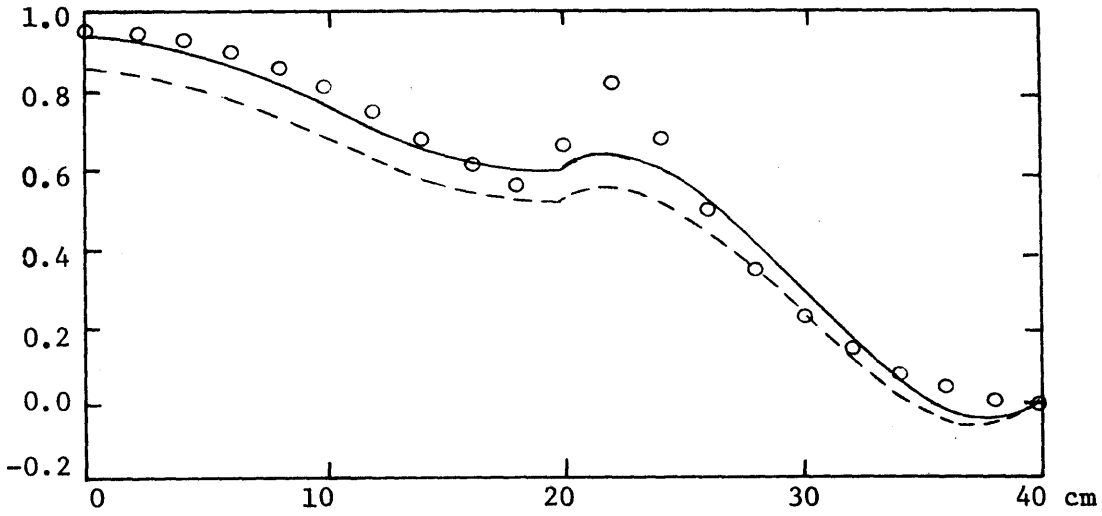

Thermal Flux at y = 20.0 cm

——— Kang's, L/2 1.1082321

– – – – Variational, L/2 1.1075521

o o o o Finite Difference, L/20 1.1105031

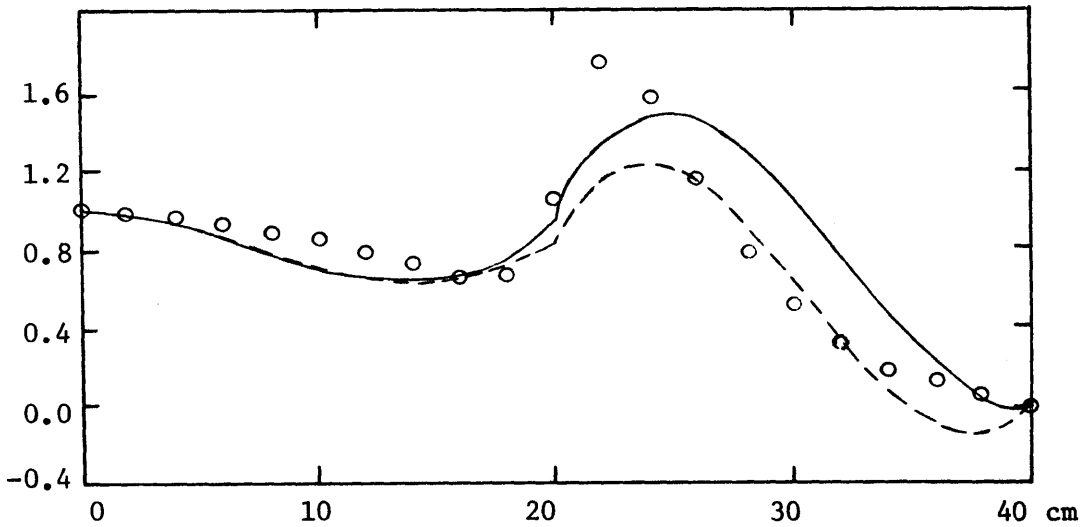

Thermal Flux at y = 0.0 cm

Figure 3.8 Thermal Flux Shapes: Example 3.4

CHAPTER 4

FINITE ELEMENT SYNTHESIS APPROXIMATION METHOD IN NEUTRON DIFFUSION PROBLEMS

As described in the beginning of this thesis, the finite element methods have been shown [24], [62] to approximate accurately flux solutions and eigenvalues of multigroup diffusion theory when applied to problems having homogeneous material within the mesh regions. However, when this method is applied to a reactor system having very complex geometrical details, the region mesh sizes must be limited unless some types of homogenization procedures are used. If the mesh spacing is chosen such that some mesh regions are heterogeneous, then application of the variational principle given in Chapter 2 results in weight averaging of the nuclear constants with products of the basis functions and their derivatives, as given by the approximate trial functions.

A useful homogenization procedure which is commonly used in reactor physics analysis is to homogenized the nuclear material within each mesh region by flux weighting with an assumed flux shape determined a priori within that region in order to preserve reaction rates,

$$\langle \Sigma_n \rangle = \frac{\int_n \psi_n(r) \Sigma_n(r) dr}{\int_n \psi_n(r) dr} \tag{4.1}$$

where $\psi_n(r)$ is the assumed flux shape in region n.

In large reactors the core is usually composed of a lattice of heterogeneous fuel subassemblies containing fuel, clad, coolant channels, and possibly control rods or coolant-filled control rod channels. Each subassembly can be divided into several distinct homogeneous regions whose microcell macroscopic group constants are found by multigroup energy-dependent calculations [63]. Detailed subassembly solutions are then found for each subassembly by assuming that the current on the outside boundary of the subassembly is zero. Flux weighting the nuclear material in each subassembly with the corresponding detailed subassembly solution for each subassembly region (according to Equation 4.1) then results in regional homogeneous nuclear constants which may better approximate the physics of the region.

Proper use of detailed flux weighted constants can lead to accurate criticality measurements, but the detailed fine flux structure within each region is lost since it appears only in crosssections homogenization and not in the approximation. The present finite element synthesis method is intended to solve this difficulty by combining the detailed subassembly solutions with finite element basis functions in the flux approximation, so that the fine structure can be retained in the flux solution. The application of this method to 1-D problems has been shown to be successful [30]. The purpose of this chapter is to extend the finite element synthesis method to 2-D diffusion problems using bl-linear basis functions.

4.1 Derivation of the Difference Equations

4.1.1 Linear Basis Function Approximation in 1-D

The proposed finite element synthesis method, utilizing linear basis functions and defined as nonzero within each mesh region k, k = 1 to K in one-dimension, is given by

$$U_k(z) = \psi_k(x)[\psi_k^{-1}(0)(1-x)P_k + \psi_k^{-1}(1)\ x\ P_{k+1}] \tag{4.2a}$$

$$U_k^*(z) = \psi_k^*(x)[\psi_k^{*-1}(0)(1-x)P_k^* + \psi_k^{-1}(1)\ x\ P_{k+1}^*] \tag{4.2b}$$

$$V_k(z) = \eta_k(x)[\psi_k^{-1}(0)(1-x)P_k + \psi_k^{-1}(1)xP_{k+1}]$$

$$+ \frac{1}{h_k}\ \mathbb{D}_k(x)\,\psi_k(x)\,[\psi_k^{-1}(0)P_k - \psi_k^{-1}(1)P_{k+1}] \tag{4.2c}$$

$$V_k^*(z) = \eta_k^*(x)[\psi_k^{*-1}(0)(1-x)P_k^* + \psi_k^{*-1}(1)\ xP_{k+1}^*]$$

$$+ \frac{1}{h_k}\ \mathbb{D}_k(x)\,\psi_k^*(x)[\psi^{*-1}_k(1)P_{k+1}^* - \psi_k^{*-1}(0)P_k^*] \tag{4.2d}$$

where: P_k is the unknown approximate group flux column vector at point z_k, and ψ_k, ψ_k^*, η_k, and η_k^* are GxG diagonal matrices composed of detailed group flux $\psi_{g,k}(z)$ and group current $\eta_{g,k}(z)$ solutions, and their adjoints, defined as nonzero only within region k. Because of the variable transformation between z and x, $\psi_k(0)$ represents $\psi_k(z_k)$, and $\psi_k(1)$ represents $\psi_k(z_{k+1})$; neither of which for the moment is allowed to be zero for any region. The detailed current solutions are given from

the detailed flux solutions by Fick's law as

$$\eta_k(z) = -\mathbb{D}_k(z) \frac{d\psi_k(z)}{dz} \tag{4.3a}$$

$$\eta^*_k(z) = +\mathbb{D}_k(z) \frac{d\psi^*_k(z)}{dz} \tag{4.3b}$$

As a result, the current trial functions are related to the flux trial functions by analogous expressions. Also, be definition of the detailed flux solutions,

$$\eta_k(0) = \eta_k(1) = \eta^*_k(0) = \eta^*_k(1) = 0$$

From the forms of the trial functions, we see that the flux continuity conditions are obeyed since

$$U_k(0) = U_{k-1}(1) = P_k \tag{4.4a}$$

$$U^*_k(0) = U^*_{k-1}(1) = P^*_k \tag{4.4b}$$

The current trial functions, however, are discontinuous. It is evident that this approximation reduces to the simple linear basis function finite element method if detailed flux solutions for each group are taken to be constant. The detailed derivation and the resulting difference equations using approximation Equations 4.2 are given in Chapter 3 and Appendix C of Bailey's thesis [30].

4.1.2 Bi-linear Basis Function Approximation in 2-D

The flux trial functions for the finite element synthesis method

using bi-linear basis functions and defined as nonzero within each mesh region (i,j), i = 1 to I, j = 1 to J in two-dimension, is given by

$$U_{i,j}(x,y) = \psi_{i,j}(x,y)[\psi^{-1}_{i,j}(0,0)P_1(x)P_1(y)P_{i,j}$$

$$+ \psi^{-1}_{i,j}(1,0)P_2(x)P_1(y)P_{i+1,j} + \psi^{-1}_{i,j}(1,1)P_2(x)P_2(y)P_{i+1,j+1}$$

$$+ \psi^{-1}_{i,j}(0,1)P_1(x)P_2(y)P_{i,j+1}] \qquad (4.5a)$$

$$U^*_{i,j}(x,y) = \psi^*_{i,j}(x,y)[\psi^{*-1}_{i,j}(0,0)P_1(x)P_1(y)P^*_{i,j}$$

$$+ \psi^{*-1}_{i,j}(1,0)P_2(x)P_1(y)P^*_{i+1,j} + \psi^{*-1}_{i,j}(1,1)P_2(x)P_2(y)P^*_{i+1,j+1}$$

$$+ \psi^{*-1}_{i,j}(0,1)P_1(x)P_2(y)P^*_{i,j+1}] \qquad (4.5b)$$

where

$$P_1(x) = 1 - x$$

$$P_2(x) = x$$

are the univariate linear basis functions. $P_{i,j}$ is the unknown approximation group flux column vector at point (X_i,Y_j), and $\psi_{i,j}$, $\psi^*_{i,j}$ are GxG diagonal matrices composed of the detailed group flux solutions $\psi_{g,i,j}(X,Y)$ and their adjoints, respectively, defined as nonzero only within region (i,j). For the moment, we assume that $\psi_{i,j}$ is nonzero at the region boundary.

The detailed current solutions are given from the detailed flux

solutions by Fick's law as

$$\xi_{i,j}(x,y) = -\frac{1}{h_{xi}} D_{i,j}(x,y) \frac{\partial}{\partial x} \psi_{i,j}(x,y)$$

$$\xi^*_{i,j}(x,y) = \frac{1}{h_{xi}} D_{i,j}(x,y) \frac{\partial}{\partial x} \psi^*_{i,j}(x,y)$$

$$\eta_{i,j}(x,y) = -\frac{1}{h_{yj}} D_{i,j}(x,y) \frac{\partial}{\partial y} \psi_{i,j}(x,y)$$

$$\eta^*_{i,j}(x,y) = \frac{1}{h_{yj}} D_{i,j}(x,y) \frac{\partial}{\partial y} \psi^*_{i,j}(x,y)$$

where $\xi_{i,j}$ and $\xi^*_{i,j}$ are X-direction detailed current and adjoint current solutions and $\eta_{i,j}$ and $\eta^*_{i,j}$ are Y-direction current and adjoint current solutions. Then the X-direction and Y-direction current trial functions which obey Fick's law are given by

$$\begin{aligned} Q_{i,j}(x,y) = \xi_{i,j}(x,y)[&\psi^{-1}_{i,j}(0,0)P_1(x)P_1(y)P_{i,j} \\ &+\psi^{-1}_{i,j}(1,0)P_2(x)P_1(y)P_{i+1,j} + \psi^{-1}_{i,j}(1,1)P_2(x)P_2(y)P_{i+1,j+1} \\ &+ \psi^{-1}_{i,j}(0,1)P_1(x)P_2(y)P_{i,j+1}] \\ + \frac{1}{h_{xi}} D_{i,j}(x,y)\psi_{i,j}(x,y)[&\psi^{-1}_{i,j}(0,0)q_1(x)P_1(y)P_{i,j} \\ &+ \psi^{-1}_{i,j}(1,0)q_2(x)P_1(y)P_{i+1,j} + \psi^{-1}_{i,j}(1,1)q_2(x)P_2(y)P_{i+1,j+1} \\ &+ \psi^{-1}_{i,j}(0,1)q_1(x)P_2(y)P_{i,j+1}] \end{aligned} \qquad (4.6a)$$

$$R_{i,j}(x,y) = \eta_{i,j}(x,y)[\psi^{-1}_{i,j}(0,0)P_1(x)P_1(y)P_{i,j}$$

$$+ \psi^{-1}_{i,j}(1,0)P_2(x)P_1(y)P_{i+1,j} + \psi^{-1}_{i,j}(1,1)P_2(x)P_2(y)P_{i+1,j+1}$$

$$+ \psi^{-1}_{i,j}(0,1)P_1(x)P_2(y)P_{i,j+1}]$$

$$+ \frac{1}{h_{yj}} \mathbb{D}_{i,j}(x,y)\ \psi_{i,j}(x,y)\ [\psi^{-1}_{i,j}(0,0)P_1(x)q_1(y)P_{i,j}$$

$$+ \psi^{-1}_{i,j}(1,0)P_2(x)q_1(y)P_{i+1,j} + \psi^{-1}_{i,j}(1,1)P_2(x)q_2(y)P_{i+1,j+1}$$

$$+ \psi^{-1}_{i,j}(0,1)P_1(x)q_2(y)P_{i,j+1}] \qquad (4.6b)$$

$$Q^*_{i,j}(x,y) = \xi^*_{i,j}(x,y)[\psi^{*-1}_{i,j}\ (0,0)P_1(x)P_1(y)P^*_{i,j}$$

$$+ \psi^{*-1}_{i,j}(1,0)P_2(x)P_1(y)P^*_{i+1,j} + \psi^{*-1}_{i,j}(1,1)P_2(x)P_2(y)P^*_{i+1,j+1}$$

$$+ \psi^{*-1}_{i,j}(0,1)P_1(x)P_2(y)P^*_{i,j+1}]$$

$$- \frac{1}{h_{xi}} \mathbb{D}_{i,j}(x,y)\psi^*_{i,j}(x,y)[\psi^{*-1}_{i,j}(0,0)q_1(x)P_1(y)P^*_{i,j}$$

$$+ \psi^{*-1}_{i,j}(1,0)q_2(x)P_1(y)P^*_{i+1,j} + \psi^{*-1}_{i,j}(1,1)q_2(x)P_2(y)P^*_{i+1,j+1}$$

$$+ \psi^{*-1}_{i,j}(0,1)q_1(x)P_2(y)P^*_{i,j+1}] \qquad (4.6c)$$

$$R^*_{i,j}(x,y) = \eta^*_{i,j}(x,y)[\psi^{*-1}_{i,j}(0,0)P_1(x)P_1(y)P^*_{i,j}$$

$$+ \psi^{*-1}_{i,j}(1,0)P_2(x)P_1(y)P^*_{i+1,j} + \psi^{*-1}_{i,j}(1,1)P_2(x)P_2(y)P^*_{i+1,j+1}$$

$$+ \psi^{*-1}_{i,j}(0,1)P_1(x)P_2(y)P^*_{i,j+1}]$$

$$- \frac{1}{h_{yj}} D_{i,j}(x,y)\psi^*_{i,j}(x,y)[\psi^{*-1}_{i,j}(0,0)P_1(x)q_1(y)P^*_{i,j}$$

$$+ \psi^{*-1}_{i,j}(1,0)P_2(x)q_1(y)P^*_{i+1,j} + \psi^{*-1}_{i,j}(1,1)P_2(x)q_2(y)P^*_{i+1,j+1}$$

$$+ \psi^{*-1}_{i,j}(0,1)P_1(x)q_2(y)P^*_{i,j+1}] \qquad (4.6d)$$

where

$$q_1(x) = -\frac{d}{dx}P_1(x) = +1$$

$$q_2(x) = -\frac{d}{dx}P_2(x) = -1$$

We note that the flux trial functions are continuous only at the mesh points and are discontinuous at the interfaces of mesh regions in general. The current trial functions are discontinuous also across region interfaces. Also, be definition of the detailed subassembly solutions

$$\xi_{i,j}(0,y) = \xi_{i,j}(1,y) = \xi^*_{i,j}(0,y) = \xi^*_{i,j}(1,y) = 0$$

$$\eta_{i,j}(x,0) = \eta_{i,j}(x,1) = \eta^*_{i,j}(x,0) = \eta^*_{i,j}(x,1) = 0$$

Since the flux is not continuous across region interfaces while Fick's law is still valid within regions, the suitable variation equation to be used is Equation 2.15. For two-dimensional case, Equation 2.15 can be written in the form

$$\sum_{i=1}^{I}\sum_{j=1}^{J} h_{xi}h_{yj}\int_0^1 dx \int_0^1 dy[\delta U^{*T}_{i,j}(x,y)\, \mathbb{A}_{i,j}(x,y)U_{i,j}(x,y)$$

$$- \delta Q^{*T}_{i,j}(x,y)\, \mathbb{D}^{-1}_{i,j}(x,y)Q_{i,j}(x,y)-\delta R^{*T}_{i,j}(x,y)\, \mathbb{D}^{-1}_{i,j}(x,y)R_{i,j}(x,y]$$

$$+ \frac{1}{2}\sum_{i=1}^{I-1}\sum_{j=1}^{J} h_{yj}\int_0^1 dy[\delta U^{*}_{i,j}(1,y)-\delta U^{*}_{i+1,j}(0,y)]^T[Q_{i+1,j}(0,y)+Q_{i,j}(1,y)]$$

$$+ \frac{1}{2}\sum_{i=1}^{I}\sum_{j=1}^{J-1} h_{xi}\int_0^1 dx[\delta U^{*}_{i,j}(x,1)-\delta U^{*}_{i,j+1}(x,0)]^T[R_{i,j+1}(x,0)+R_{i,j}(x,1)]$$

$$+ \frac{1}{2}\sum_{i=1}^{I-1}\sum_{j=1}^{J} h_{yj}\int_0^1 dy[\delta Q^{*}_{i+1,j}(0,y)+ Q^{*}_{i,j}(1,y)]^T[U_{i+1,j}(0,y)-U_{i,j}(1,y)]$$

$$+ \frac{1}{2}\sum_{i=1}^{I}\sum_{j=1}^{J-1} h_{xi}\int_0^1 dx[\delta R^{*}_{i,j+1}(x,0)+\delta R^{*}_{i,j}(1,y)]^T[U_{i,j+1}(x,0)-U_{i,j}(x,1)]=0 \quad (4.7)$$

Substitution of Equations 4.5 and 4.6 results in the equation

$$\sum_{i=1}^{I+1}\sum_{j=1}^{J+1} \delta P^{*T}_{i,j}[\underline{aa}_{i,j}P_{i-1,j-1} + \underline{ab}_{i,j}P_{i-1,j} + \underline{ac}_{i,j}P_{i-1,j+1}$$

$$+ \underline{ba}_{i,j}P_{i,j-1} + \underline{bb}_{i,j}P_{i,j} + \underline{bc}_{i,j}P_{i,j+1}$$

$$+ \underline{ca}_{i,j}P_{i+1,j-1} + \underline{cb}_{i,j}P_{i+1,j} + \underline{cc}_{i,j}P_{i+1,j+1}] = 0 \quad (4.8)$$

where "undefined" quantities (corresponding to points that would lie outside the physical limits of the reactor) are always set equal to zero. The GxG matrix coefficients $\{\underline{aa}_{i,j}, \underline{ab}_{i,j}, ---, \underline{cc}_{i,j}\}$ are integral quantities having the mathematical form $A - \frac{1}{\lambda}B$ and are defined in detail in Appendix E.

Zero flux boundary conditions are easily imposed. For example, if zero flux conditions are imposed on the left boundary of the reactor, we can set $P_{1,j} = 0$, $j = 1$ to $J + 1$. This also requires that $P^*_{1,j}$, $j = 1$ to $J + 1$ be zero, which in turn requires the $\delta P_{1,j}$ coefficients in Equation 4.8 to vanish. If all four sides of the reactor have zero flux conditions, then allowing arbitrary variations in $P^*_{i,j}$, $j = 2$ to J, results in a system of $(I-1)(J-1)$ equations in $(I-1)(J-1)$ unknowns. Zero current boundary conditions are found using symmetry considerations. If, for example, zero current boundary conditions are imposed on the right boundary, then "boundary condition equations" can be derived by assuming pseudo-regions $(I+1,j)$, $j = 1$ to J of width $h_{x,I}$ and height h_{yj}'s having mirror image properties of region (I,j), $j = 1$ to J, about line $X=X_{I+1}$:

$$\mathbb{D}_{I+1,j}(x,y) = \mathbb{D}_{I,j}(1-x,y) \qquad (4.9a)$$

$$; \; j = 1 \text{ to } J$$

$$\mathbb{\Lambda}_{I+1,j}(x,y) = \mathbb{\Lambda}_{I,j}(1-x,y) \qquad (4.9b)$$

and the detailed flux and current solutions for these regions are assumed to be symmetric and anti-symmetric in the X-direction, respectively, to the corresponding detailed flux and current solutions

in the regions (I,j), j = 1 to J:

$$U_{I+1,j}(x,y) = U_{I,j}(1-x,y) \tag{4.10a}$$

$$U^*_{I+1,j}(x,y) = U^*_{I,j}(1-x,y) \tag{4.10b}$$

; j = 1 to J

$$V_{I+1,j}(x,y) = -V_{I,j}(1-x,y) \tag{4.10c}$$

$$V_{I+1,j}(x,y) = -V^*_{I,j}(1-x,y) \tag{4.10d}$$

The addition of pseudo-regions (I+1,j), j = 1 to J to the summation in Equation 4.7 results in the calculation of coefficients $\underline{aa}_{I+1,j}$ (j=2 to J+1), $\underline{ab}_{I+1,j}$(j=1 to J+1), $\underline{ac}_{I+1,j}$(j=1 to J), $\underline{ba}_{I+1,j}$(j=2 to J+1), $\underline{bb}_{I+1,j}$ (j=1 to J+1), and $\underline{bc}_{I+1,j}$(j=1 to J) in Equation 4.8. If all four sides of the reactor have symmetry conditions, then allowing arbitrary variations in $P^*_{i,j}$, i=1 to I+1, j=1 to J+1, results in a system of (I+1)(J+1) equations in the same number of unknowns.

Like the situation in one-dimensional case [30], a serious drawback of the approximation given by Equations 4.5 and 4.6 is that it does not allow the use of detailed flux solutions containing explicitly zero flux boundary conditions. However, such detailed solutions can be allowed by modifying the trial function forms in the boundary regions. For example, if a zero-flux condition is imposed on the left boundary and a detailed solutions $\psi_{1,j}(x,y)$ is given such that $\psi_{1,j}(0,y) = 0$ in the region (1,j) for a particular j, the trial functions of Equations 4.5 and 4.6 can be modified for

this region as

$$U_{1,j}(x,y) = \psi_{1,j}(x,y)[\psi^{-1}_{1,j}(1,0)P_1(y)P_{2,j}$$

$$+ \psi^{-1}_{2,j}(1,1)P_2(y)P_{2,j+1}] \qquad (4.11a)$$

$$U^*_{1,j}(x,y) = \psi^*_{1,j}(x,y)[\psi^{*-1}_{1,j}(1,0)P_1(y)P^*_{2,j}$$

$$+ \psi^{*-1}_{1,j}(1,1)P_2(y)P^*_{2,j+1}] \qquad (4.11b)$$

$$Q_{i,j}(x,y) = \xi_{1,j}(x,y)[\psi^{-1}_{1,j}(1,0)P_1(y)P_{2,j}$$

$$+ \psi^{*-1}_{1,j}(1,1)P_2(y)P_{2,j+1}] \qquad (4.11c)$$

$$Q^*_{1,j}(x,y) = \xi^*_{1,j}(x,y)[\psi^{*-1}_{i,j}(1,0)P_1(y)P^*_{2,j}$$

$$+ \psi^{*-1}_{1,j}(1,1)P_2(y)P^*_{2,j+1}] \qquad (4.11d)$$

$$R_{1,j}(x,y) = \eta_{1,j}(x,y)[\psi^{-1}_{1,j}(1,0)P_1(y)P_{2,j} + \psi^{-1}_{1,j}(1,1)P_2(y)P_{2,j+1}]$$

$$+ \frac{1}{h_{yj}} D_{1,j}(x,y)\psi_{1,j}(x,y)[\psi^{-1}_{1,j}(1,0)q_1(y)P_{2,j}$$

$$+ \psi^{-1}_{1,j}(1,1)q_2(y)P_{2,j+1}] \qquad (4.11e)$$

$$R^*_{1,j}(x,y) = \eta^*_{1,j}(x,y)[\psi^{*-1}_{1,j}(1,0)P_1(y)P^*_{2,j}+\psi^{*-1}_{1,j}(1,1)P_2(y)P^*_{2,j+1}]$$

$$- \frac{1}{h_{yj}} D_{1,j}(x,y)\psi^*_{1,j}(x,y)[\psi^{*-1}_{1,j}(1,0)q_1(y)P^*_{2,j}$$

$$+ \psi^{*-1}_{1,j}(1,1)q_2(y)P^*_{2,j+1}] \qquad (4.11f)$$

The above equations are equivalent to fixing the X-direction basis functions for this particular region (1,j) so that

$$P_1(x) = 0 \ , \ P_2(x) = 1$$
$$q_1(x) = 0 \ , \ q_2(x) = 0 \qquad (4.12)$$

in Equations 4.5 and 4.6. In this way, the imposed zero boundary condition is explicitly given by $\psi_{1,j}(x,y)$ rather than by the form of the trial functions. The use of these special trial functions in the boundary regions alters the definitions of some of the matrix coefficients, but the whole system of equations are of the same form as that of the ordinary zero-flux boundary conditions.

Regardless of the types of boundary conditions imposed, Equation 4.8 results in an NxN matrix problem of the form

$$\mathbb{A}\ \underline{P} = \frac{1}{\lambda}\mathbb{B}\ \underline{P} \qquad (4.13)$$

where $\mathbb{A}$ and $\mathbb{B}$ are independent of λ. The order N of the matrix equations, which depends on the chosen boundary conditions, is given in Table 4.1.

Careful examination of the matrix coefficients given in Appendix E shows that neither $\mathbb{A}$ nor $\mathbb{B}$ are symmetric matrices in general. Only

Table 4.1 Matrix Order N of the Bi-linear Finite Element Synthesis Approximations as a Function of the Imposed Boundary Conditions.

1 - Zero Flux

2 - Symmetry

Boundary Condition Type				Matrix Order
Left	Right	Top	Bottom	N
1	1	1	1	G(I-1)(J-1)
1	1	1	2	G(I-1)J
1	1	2	1	
1	2	1	1	GI(J-1)
2	1	1	1	
1	1	2	2	G(I-1)(J+1)
1	2	1	2	GIJ
1	2	2	1	
2	1	1	2	
2	1	2	1	
2	2	1	1	G(I+1)(J-1)
1	2	2	2	GI(J+1)
2	1	2	2	
2	2	1	2	G(I+1)J
2	2	2	1	
2	2	2	2	G(I+1)(J+1)

when the geometry of the problem is symmetric about the 45^{o} line, do $\mathbb{A}$ and $\mathbb{B}$ become symmetric.

4.2 Calculational and Programming Techniques

The matrix equations which result from the approximations given in this chapter are of the form of Equation 4.13, which is identical to Equation 3.9 in the previous chapter except that $\mathbb{A}$ and $\mathbb{B}$ are not symmetric in the present situation. The conventional group indexing followed by spatial indexing within each group in ordering the unknowns is assumed. For the double spatial indexing, we shall order the unknowns first by Y-direction indexing, j, followed by X-direction indexing, i, for each j.

Because of the complexity of the matrix coefficients $\{\underline{aa}_{i,j}, \underline{ab}_{i,j}, ---, \underline{cc}_{i,j}\}$ encountered in the approximation, it is difficult to find a systematic way for assembling the coefficients so that a single computer program can be used to find the eigenvalue λ and corresponding eigenfunction directly when the geometry and regional detailed nuclear constants are the input. Therefore, the calculations were performed in four steps as follows:

(i) Calculation of the Detailed Subassembly Solutions:

Calculation of the two-dimensional subassembly detailed fluxes and adjoint solutions were performed using the existing code PDQ-7 [64]-[66]. The PDQ-7 program solves neutron diffusion-depletion problems in one, two, or three dimensions in rectangular, cylindrical

or hexagonal geometries. Up to five energy groups, including two overlapping thermal groups, are permitted. For the present application, the non-depleting option for two dimensions, rectangular geometry, one or two energy groups was needed.

The boundary conditions imposed were zero-current conditions on all four boundaries, in accord with the definition of detailed subassembly solutions. Also, subassembly (i,j) is divided into MxN homogeneous subregions having widths of $z_{x,m}$ and $z_{y,n}$, respectively, in the X and Y directions. Omitting group subscripts, the detailed flux solutions for each group in subassembly (i,j) is represented by a set of (M+1)(N+1) points

$$\psi_{i,j}(x,y) = \{\psi_{m,n};\ m=1,M+1,\ n=1,N+1\} \tag{4.14}$$

(ii) Calculation of Double and Linear Integrals:

The matrix elements required for use in the approximation methods are combinations of various double and linear integrals of products of subassembly detailed solutions and polynomial functions. The double integrals are calculated for each subassembly (i,j) from the basic integral unit

$$DIA_{i,j} = \int_0^1 dx \int_0^1 dy\ f_{i,j}(x,y)g_{i,j}(x,y)C_{i,j}(x,y)x^k y^\ell \tag{4.15}$$

where the functions $f_{i,j}(x,y)$ and $g_{i,j}(x,y)$ represent flux and/or X- or Y-direction current solutions for the same or different groups. $C_{i,j}(x,y)$ represents a group nuclear constant which is homogeneous in each subregion (m,n) of the subassembly (i,j)

$$C_{i,j}(x,y) = \{C_{m,n};\ m=1,M,\ n=1,N\} \tag{4.16}$$

and k and ℓ are positive integers in the ranges $0 \leq k,\ell \leq 2$.

If we assume that for the detailed flux solutions of the form Equation 4.14, the average flux in subregion (m,n) is given by

$$f_{m,n} = \frac{1}{4}\left(\psi_{m,n} + \psi_{m+1,n} + \psi_{m+1,n+1} + \psi_{m,n+1}\right) \tag{4.17a}$$

the average X-direction current in subregion (m,n) is given by

$$g_{m,n} = -\frac{D_{m,n}}{2z_{x,m}}\left[(\psi_{m+1,n} - \psi_{m,n}) + (\psi_{m+1,n+1} - \psi_{m,n+1})\right] \tag{4.17b}$$

and the average Y-direction current in subregion (m,n) is given by

$$g_{m,n} = -\frac{D_{m,n}}{2z_{y,n}}\left[(\psi_{m,n+1} - \psi_{m,n}) + (\psi_{m+1,n+1} - \psi_{m+1,n})\right] \tag{4.17c}$$

then the basic integral unit can be broken into sums over each subregion (m,n)

$$DIA_{i,j} = \sum_{m=1}^{M}\sum_{n=1}^{N} f_{m,n}g_{m,n}C_{m,n}\frac{1}{(k+1)}\frac{1}{(\ell+1)}$$

$$(x_{m+1}^{k+1} - x_m^{k+1})(y_{n+1}^{\ell+1} - y_n^{\ell+1}) \tag{4.18}$$

The linear integrals are integrations along the subassembly interfaces. For a horizontal interface between subassemblies (i,j) and (i,j+1), the line integrals can be calculated from basic integral unit of the form

$$SIA = \int_0^1 dx\ f_{i,j}(x,1)g_{i,j+1}(x,0)D_{i,j}(x,1)x^k \tag{4.19}$$

where $f_{i,j}(x,1)$ is the detailed flux solution at the bottom edge of the subassembly (i,j), $g_{i,j+1}(x,0)$ is the detailed flux soltuion at the top edge of the subassembly (i,j+1), $D_{i,j}(x,1)$ is the diffusion constant at the bottom edge of the subassembly (i,j) and $0 \leq k \leq 2$.

If we assume that the average fluxes along this particular interface are given by

$$f_{m,N+1} = \frac{1}{2} (\psi_{m,N+1} + \psi_{m+1,N+1})_{sub.(i,j)} \tag{4.20a}$$

$$g_{m,1} = \frac{1}{2} (\psi_{m,1} + \psi_{m+1,1})_{sub.(i,j+1)} \tag{4.20b}$$

then Equation 4.19 can be written as

$$DIA = \sum_{m=1}^{M} f_{m,N+1} g_{m,1} D_{m,N} \frac{1}{(k+1)} (x_{m+1}^{k+1} - x_m^{k+1}) \tag{4.21}$$

Programs DOB1 and DOB2 which calculate quantities $E_{i,j}(a,b;c,d)$, defined by Equation E1 and consisting of combinations of various double integrals, in one-group and two-group, respectively, are listed in Appendix F. Programs LIN1 and LIN2 which calculate various linear integrals in one-group and two-group, respectively, are also listed in Appendix F.

(iii) Computation of Matrix Elements:

This step involves the calculation of matrix elements from the results of the previous step. Careful bookkeeping is necessary in order to insure the accuracy of the computation. However, for a reactor system consisting of a relatively small number (≤ 4) of

different subassemblies, this is not a difficult task; it usually takes several hours of work.

(iv) Calculation of Eigenvalue and Eigenfunction:

The source iterative scheme and power method discussed in Section 3.3 are used to find the largest eigenvalue λ and corresponding eigenfunction once the matrix elements for $\mathbb{L}_g$, $\mathbb{M}_g$, $\mathbb{T}_{gg'}$, and $\mathbb{B}_{gg'}$ are known. The inverting procedures for $\mathbb{K}_g \equiv \mathbb{L}_g + \mathbb{M}_g$, however, must be changed because $\mathbb{K}_g$ is not symmetric. Thus, instead of using the Cholesky scheme of matrix factorization, the Gauss-Jordan method [42], [55] was used to invert $\mathbb{K}_g$.

Programs MAN1 and MAN2 which calculate the eigenvalue λ and its corresponding eigenfunction for one-group and two-group problems, are listed in Appendix F.

4.3 Numerical Results

In this section we present the results of three cases obtained through the use of the finite element synthesis method. Each case was also analyzed by the pure linear finite element method using detailed flux weighted nuclear constants. These results are compared with reference solutions obtained from the finite difference code CITATION [67].

4.3.1 Case 1: 25 Subassembly Reactor Configuration Made up of 2 Different Types of Subassemblies - One Group.

The reactor configuration and its 2 different types of subassemblies are depicted in Figure 4.1. The one-group nuclear constants of subassemblies are given in Table 4.2. The detailed flux solutions for each subassembly were found using the finite difference code PDQ-7 with symmetry boundary conditions and a 20x20-mesh region per subassembly geometry as indicated in Figure 4.2. The resulting detailed flux solutions for Sub. 1 and Sub. 2 are shown in Figures 4.3 and 4.4, for y = 0 cm and y = 4 cm, respectively. The detailed-flux-weighted, homogenized, subassembly nuclear constants are given in Table 4.3, and are used in the linear finite element calculations.

The reference solution for this problem was found using the same mesh intervals in each subassembly as in the calculation for detailed subassembly solutions. With the symmetry about X=20 cm taken into account, this is a 50x100-mesh region problems for CITATION.

The graphical results for the one-group approximation methods for this case are shown in Figures 4.5, 4.6 and 4.7 for three elevations Y = 12 cm, 20 cm and 24 cm, respectively. The flux discontinuity across subassembly boundaries, which is inherent in the approximation, is shown in Figure 4.6, and more clearly in Figure 4.7. The magnitude of the gap along a boundary depends on those two bordering subassembly detailed flux solutions at that boundary. It is seen that the present synthesis method using a coarse mesh of 8 cm gives reasonably good results compared to the reference solutions. They are farther better than finite element method using the same

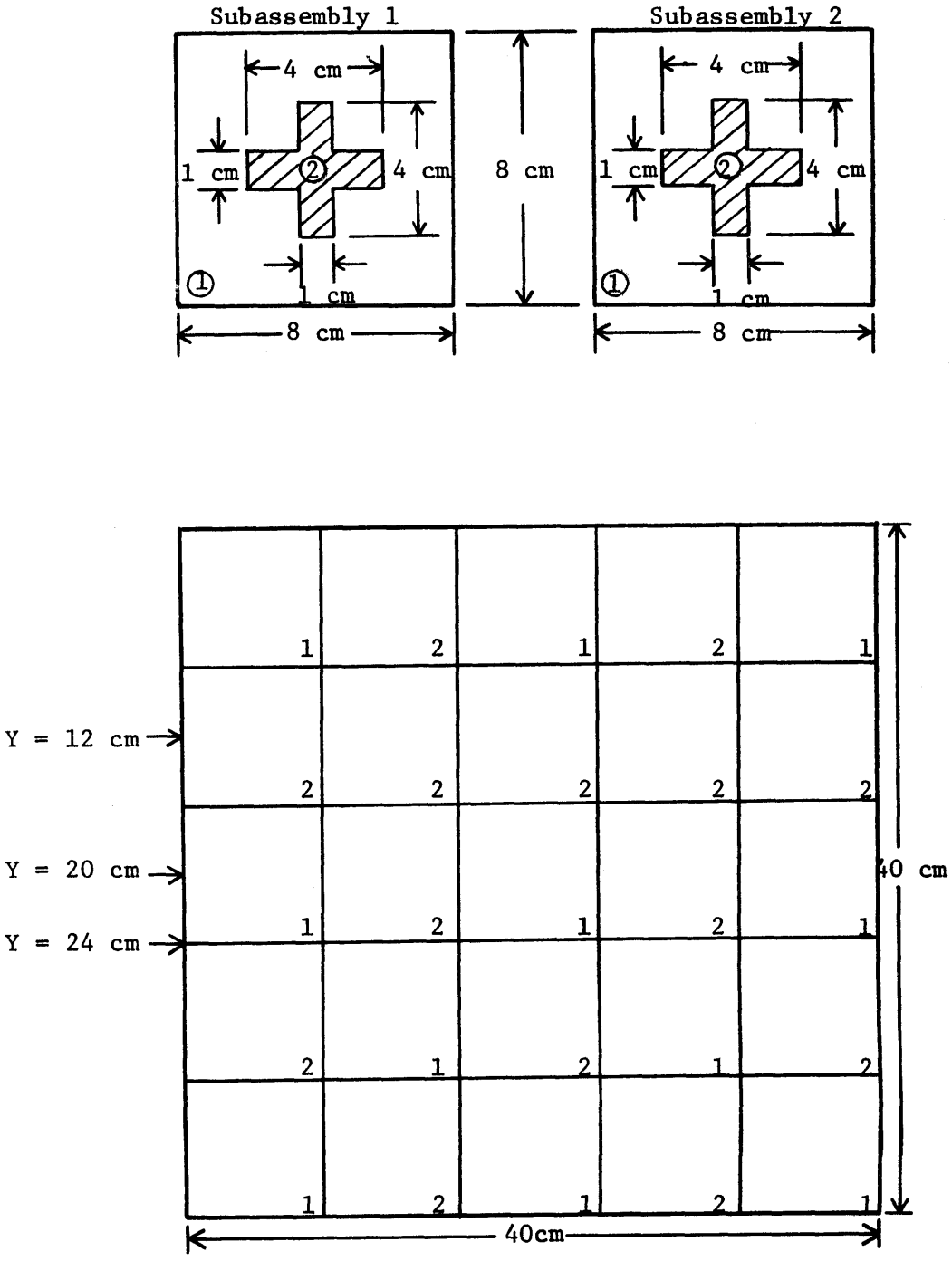

Figure 4.1 A 25 Subassembly Reactor Configuration and Its 2 Different Types of Subassemblies - Case 1

Table 4.2 One-group Nuclear Constants of Subassemblies of Figure 4.1 - Case 1

Subassembly 1

	Material 1 (fuel)	Material 2 (moderator)
$\sum_f (cm^{-1})$	0.0232927	0.0
$\sum_a (cm^{-1})$	0.04	0.015
D(cm)	0.3	0.1
ν	2.5	

Subassembly 2

	Material 1 (fuel)	Material 2(absorber)
$\sum_f (cm^{-1})$	0.0232927	0.0
$\sum_a (cm^{-1})$	0.04	0.500
D(cm)	0.3	0.5
ν	2.5	

Table 4.3 Homogenized Subassembly One-group Nuclear Constants - Case 1

	Sub. 1	Sub. 2
D(cm)	0.2790721	0.3108547
$\sum_a (cm^{-1})$	0.03738401	0.06496583
$\nu\sum_f (cm^{-1})$	0.05213841	0.05507131

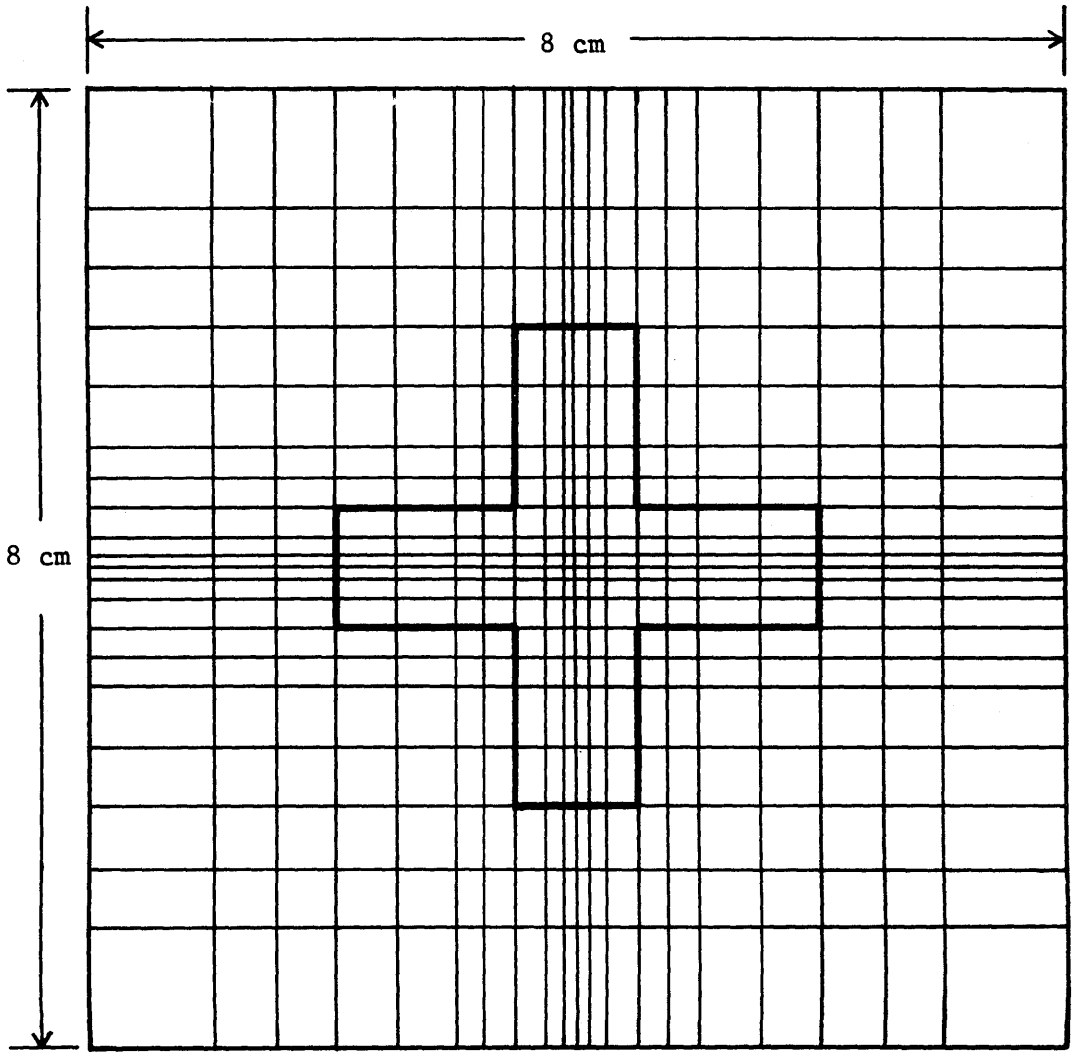

Symmetric Partitioning in Both X- and Y-directions:
1(1.0cm) + 4(0.5) + 3(0.25) + 1(0.15) + 1(0.1)

Figure 4.2 Mesh Geometry in a Subassembly -- Cases 1 and 2

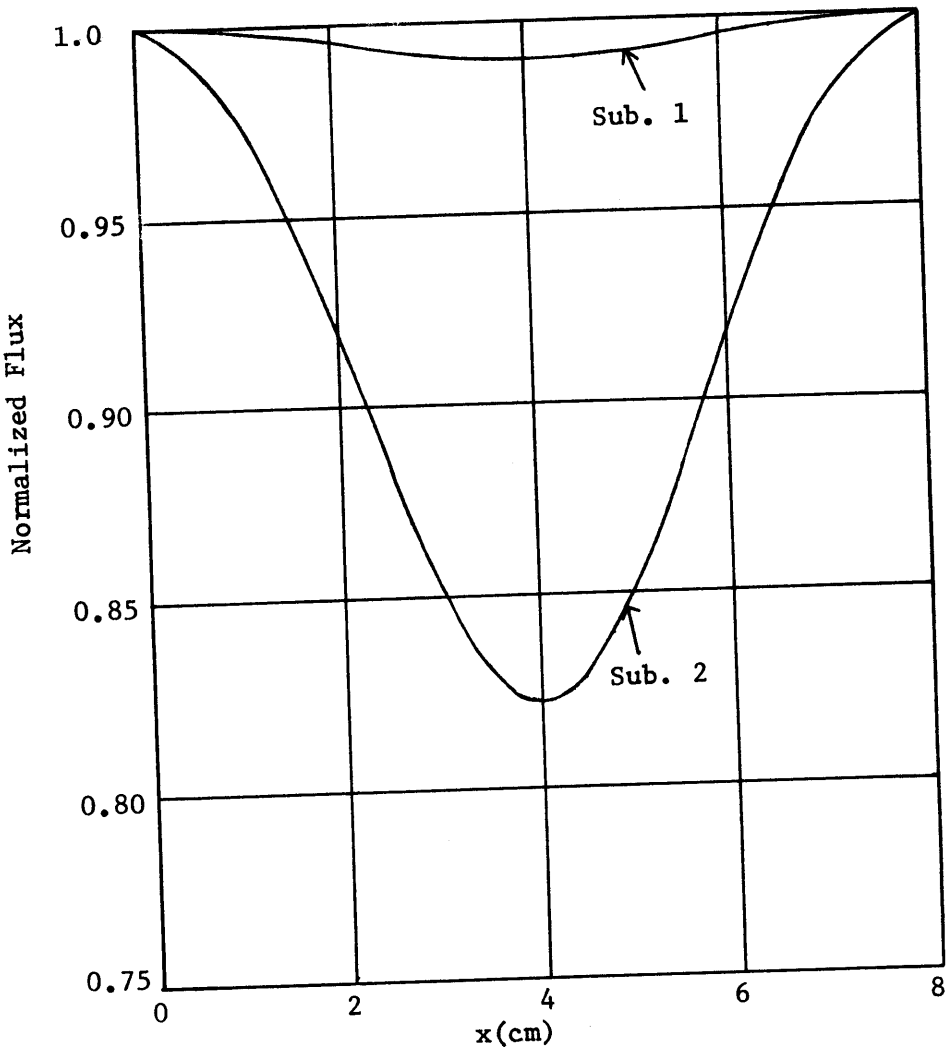

Figure 4.3 Detailed Flux Solutions at y = 0 cm - Case 1

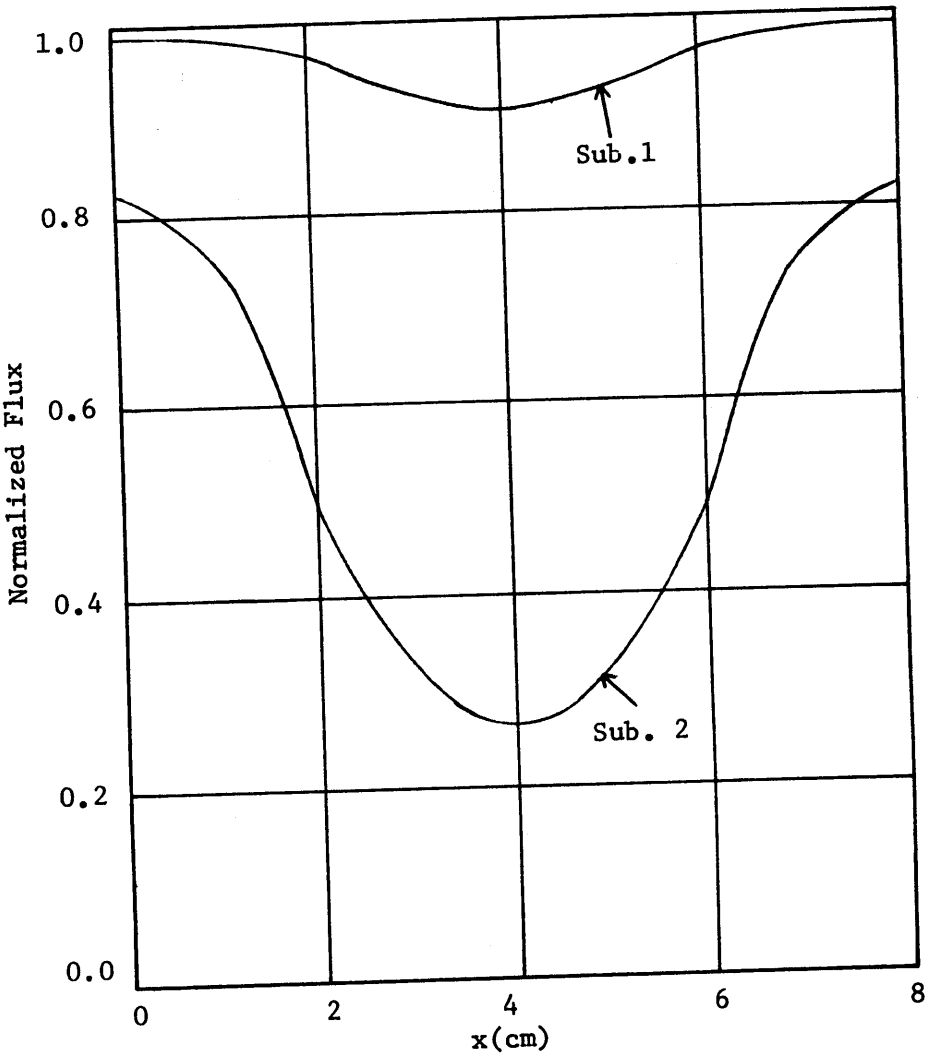

Figure 4.4 Detailed Flux Solutions at y = 4 cm - Case 1

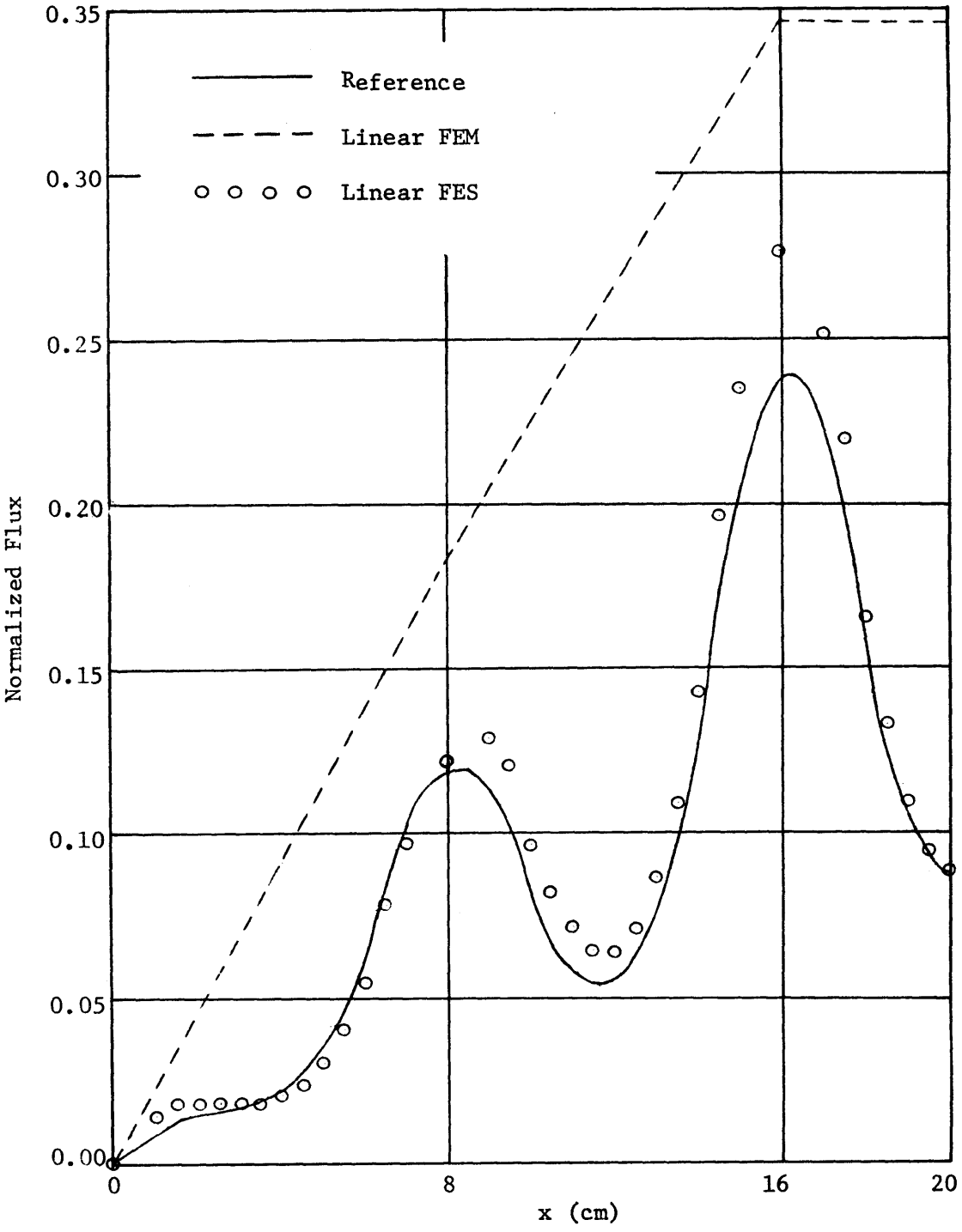

Figure 4.5 Flux at Y = 12 cm - Case 1

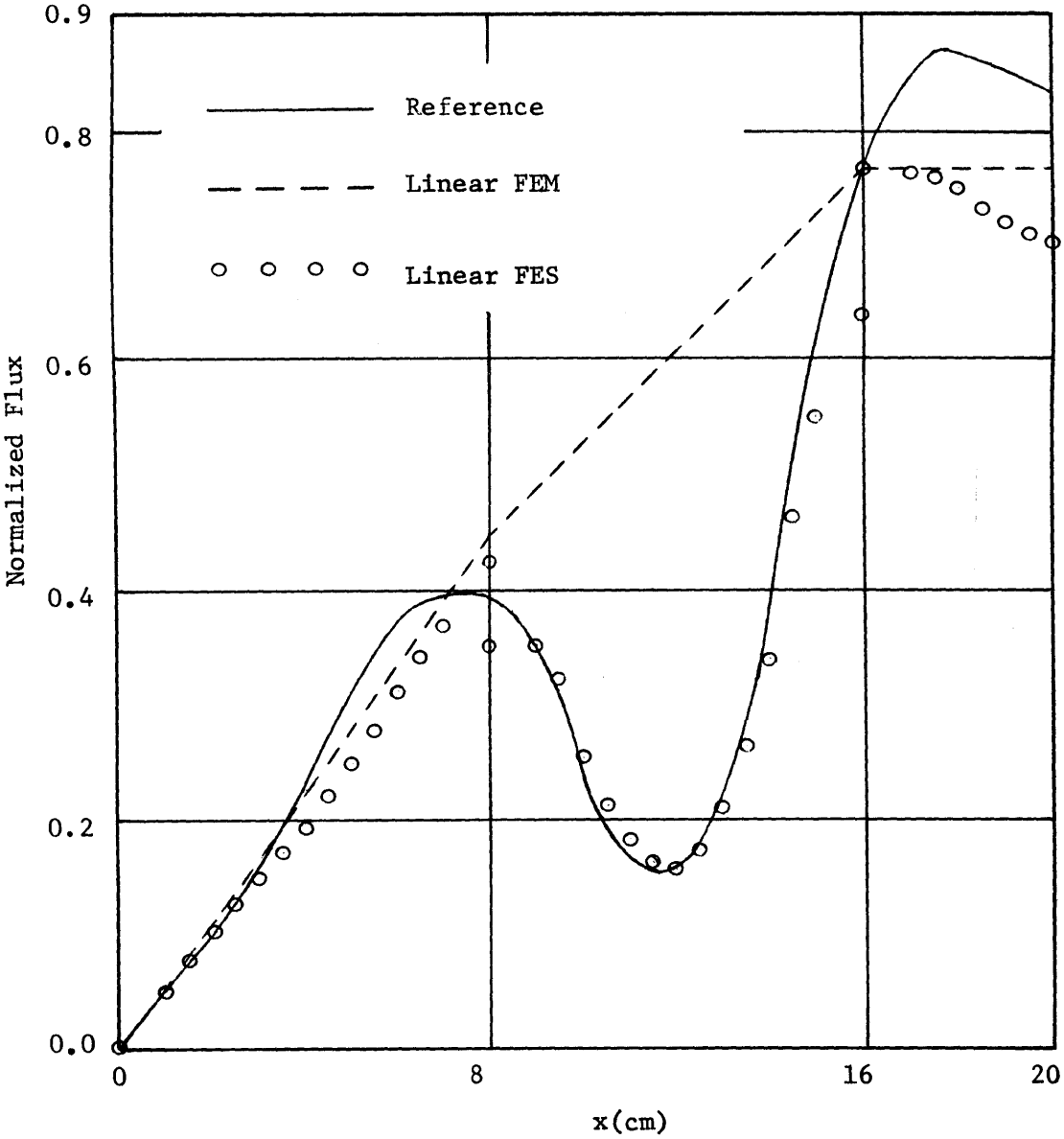

Figure 4.6 Flux at Y = 20 cm - Case 1

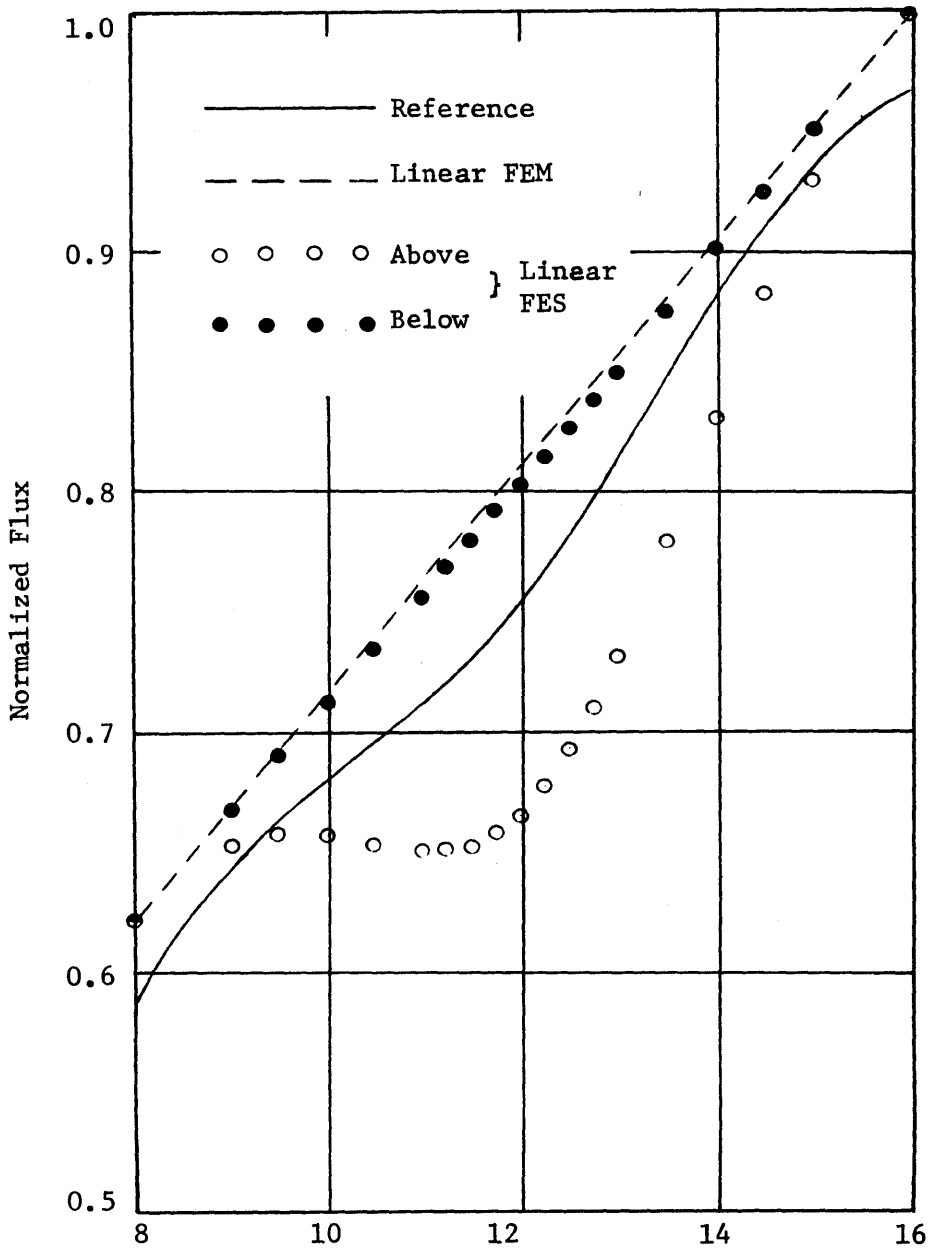

Figure 4.7 Flux at Y = 24 cm - Case 1

coarse mesh.

Comparisons of eigenvalues, λ, obtained from different methods are shown in Table 4.8 (p.146). We see that the present synthesis method gives a much better eigenvalue than the linear finite element method using identical coarse mesh.

4.3.2 Case 2: 25 Subassembly Reactor Configuration Made up of One Type of Core Subassembly and One Type of Reflector Subassembly - One Group

The difference between case (1) and case (2) is that in (1) fuel is present right up to the edge of the reactor, while in (2) there is a reflector zone of moderator subassemblies. The reactor configuration and its two different types of subassemblies for case (2) are depicted in Figure 4.8. The one-group nuclear constants of subassemblies are given in Table 4.4. The detailed flux solution for Sub. 1, obtained by using PDQ-7 with geometry indicated in Figure 4.2, is shown in Figure 4.9 for y = 0 and 4 cm. The detailed flux weighted homogenized nuclear constants, used in finite element calculation, are given in Table 4.5. Note that for reflector subassembly, we assume that the detailed flux solution is constant over the whole subassembly, because there is no fission inside. The resultant flux weighted homogenized constants are thus the same constants as for the reflector subassembly itself.

The reference solution for this case was found using the same mesh intervals in each subassembly as in the calculation for detailed

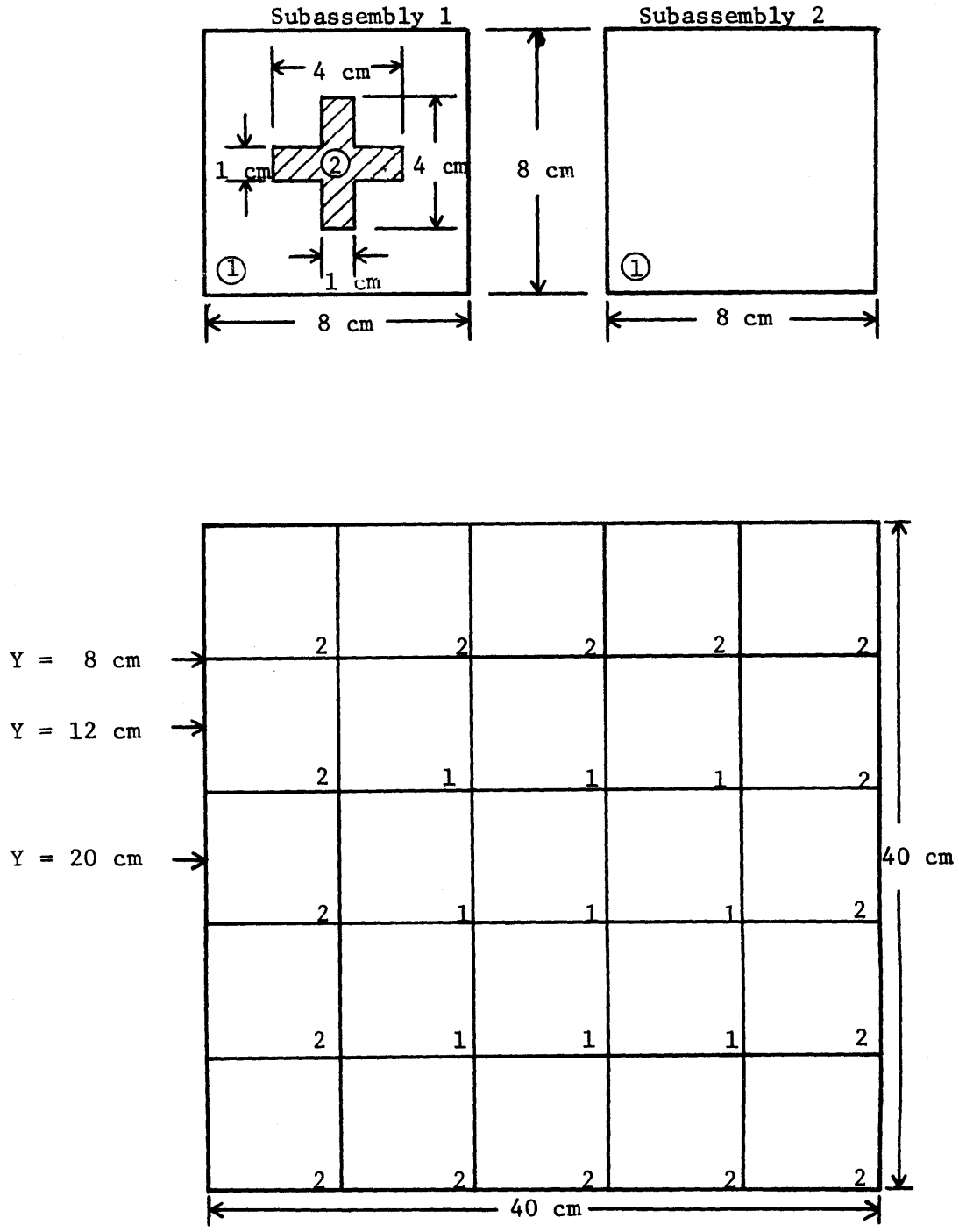

Figure 4.8 A 25 Subassembly Symmetric Reactor Configuration and Its 2 Different Types of Subassemblies - Case 2

Table 4.4 One-group Nuclear Constants of Subassemblies of Figure 4.8 - Case 2

Subassembly 1

	Material 1 (fuel)	Material 2 (moderator)
$\Sigma_f(cm^{-1})$	0.0228646	0.0
$\Sigma_a(cm^{-1})$	0.045	0.015
D(cm)	0.4	0.4
ν	2.5	

Subassembly 2 (reflector)

$\Sigma_f(cm^{-1})$	0.0
$\Sigma_a(cm^{-1})$	0.02
D(cm)	0.6
ν	

Table 4.5 Homogenized Subassembly One-group Nuclear Constants - Case 2

	Sub. 1	Sub. 2
D(cm)	0.4	0.6
$\Sigma_a(cm^{-1})$	0.04179954	0.02
$\nu\Sigma_f(cm^{-1})$	0.05106339	0.0

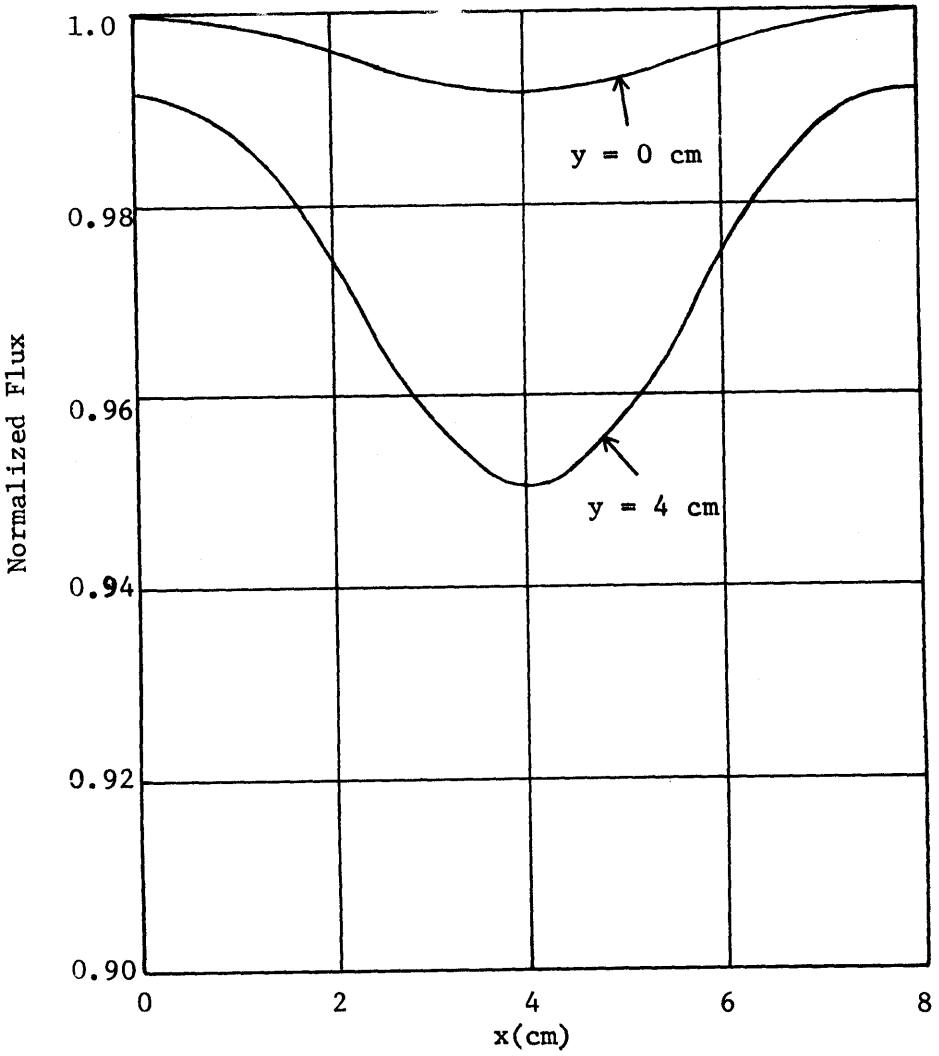

Figure 4.9 Detailed Flux Solutions for Subassembly 1 -- Case 2

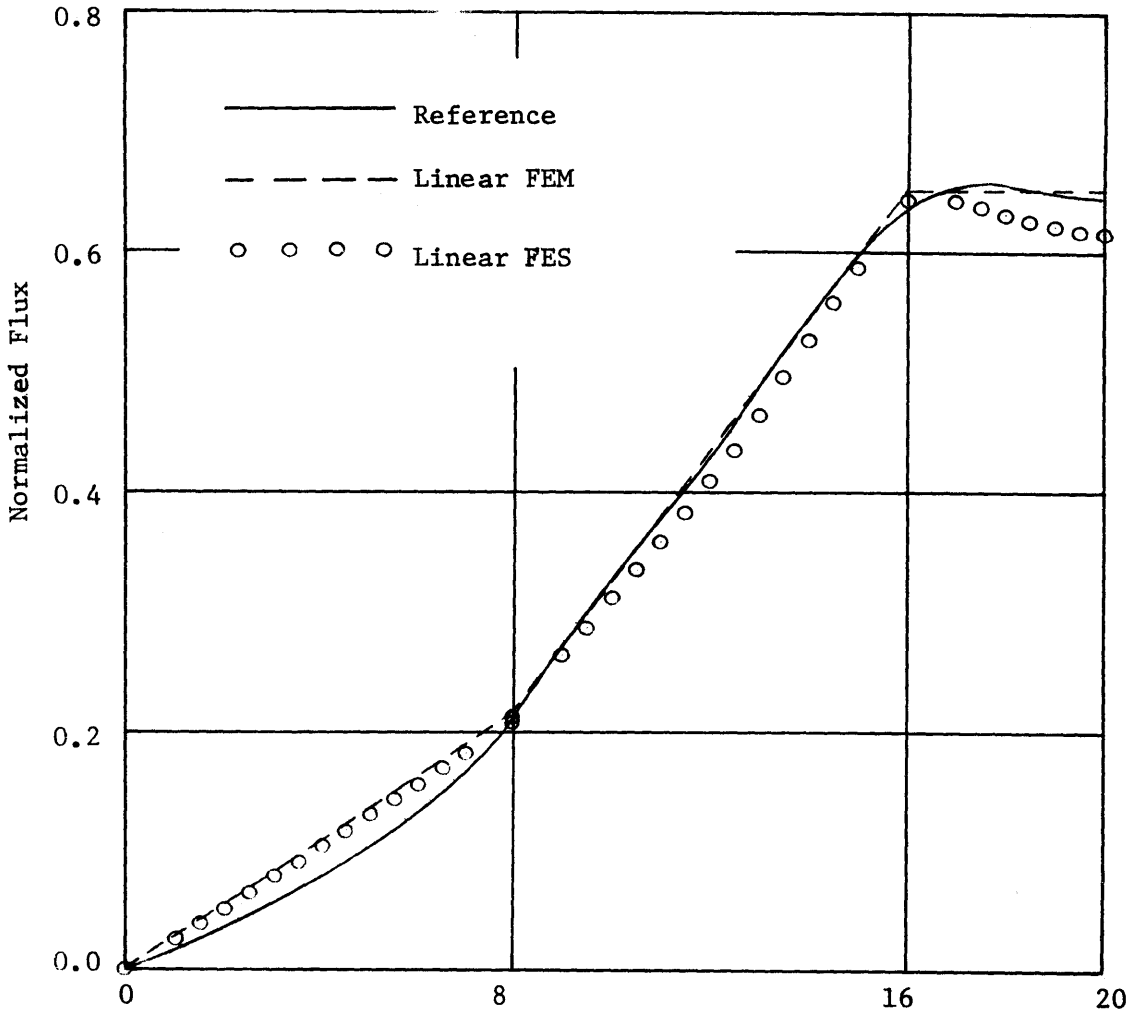

Figure 4.10 Flux at Y = 12 cm - Case 2

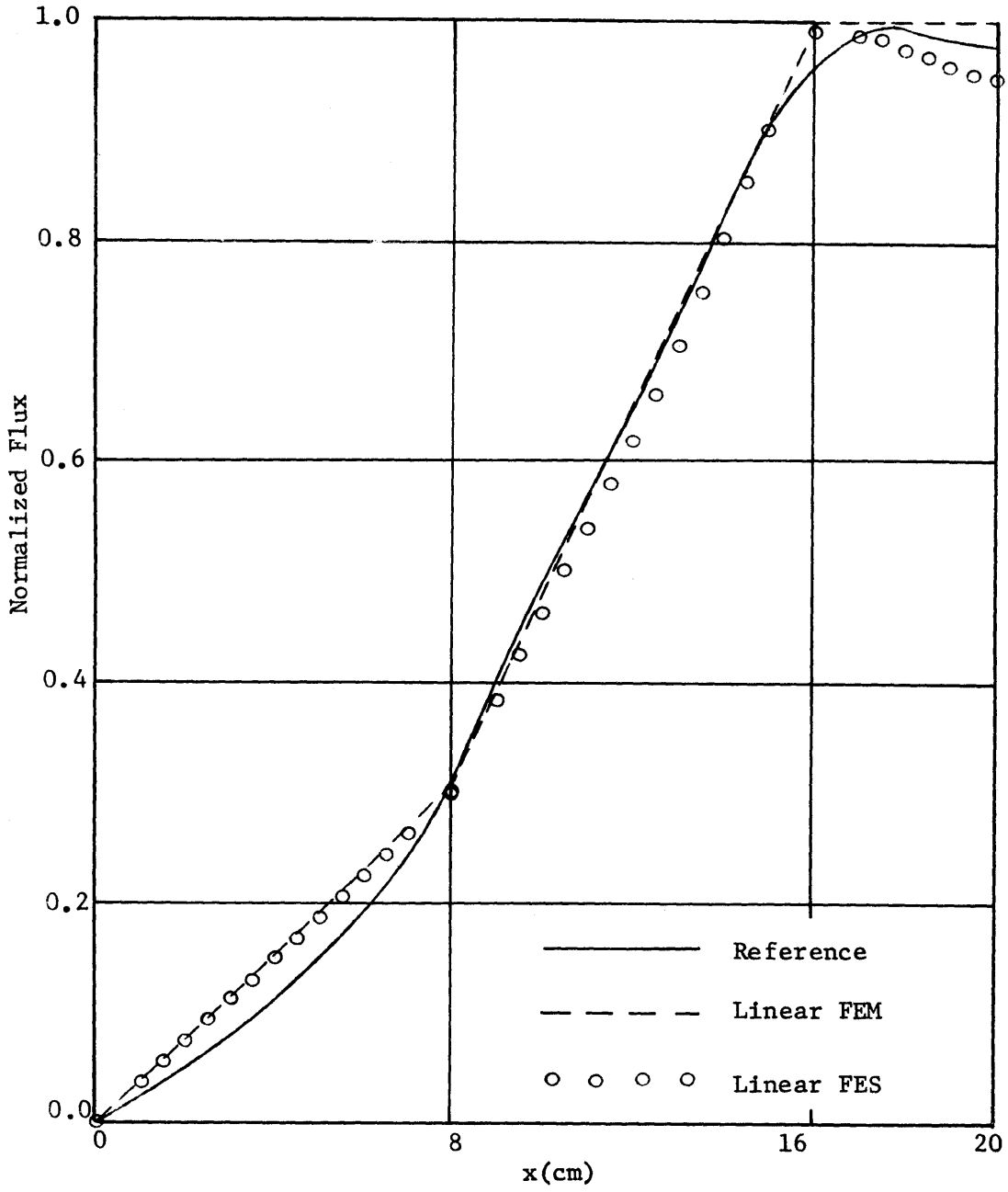

Figure 4.11 Flux at Y = 20 cm - Case 2

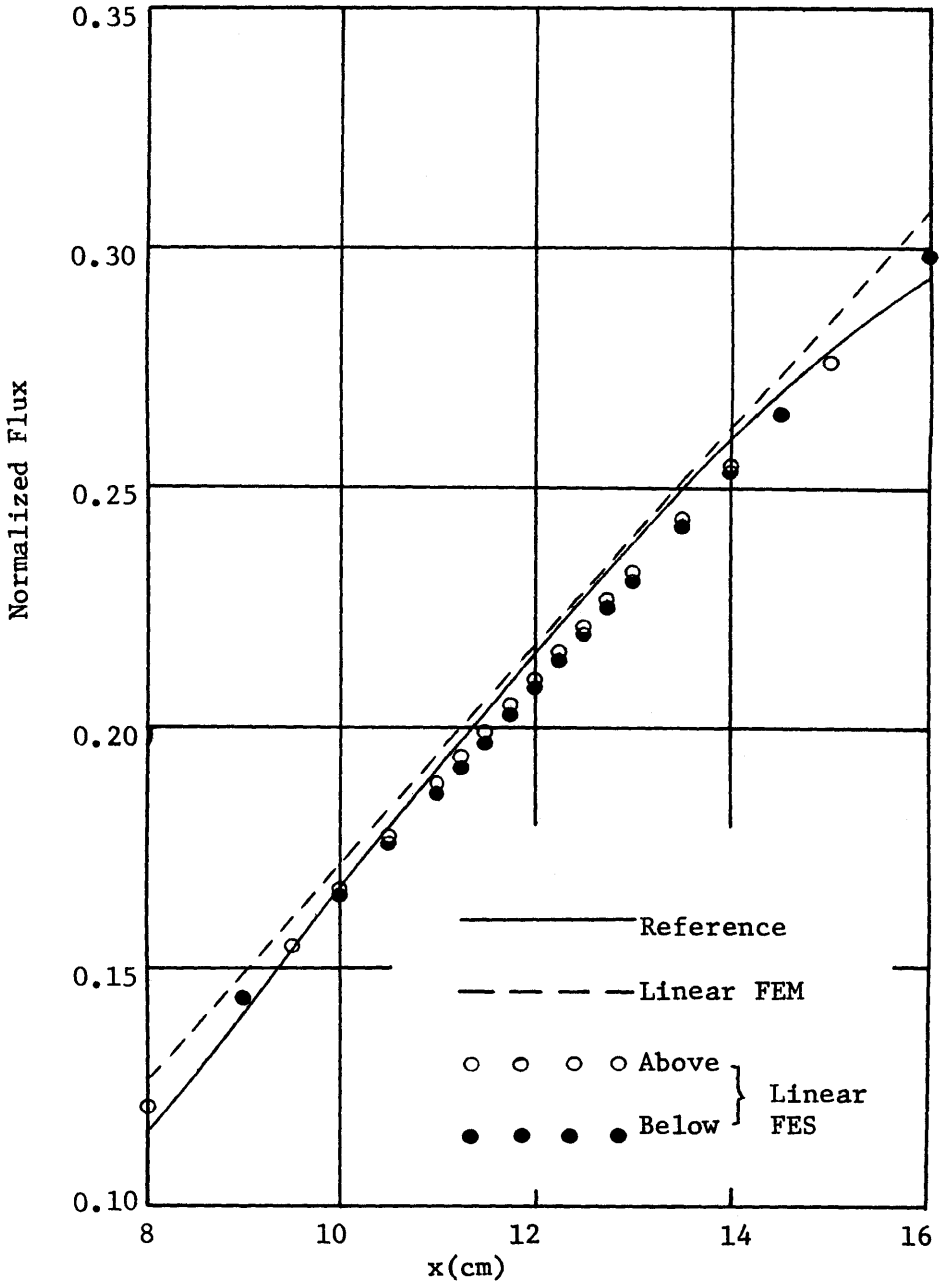

Figure 4.12 Flux at Y = 8 cm - Case 2

subassembly solutions. Because of the quarter-core symmetry, the problem size was 50x50.

The graphical results for this case are shown in Figures 4.10, 4.11 and 4.12 for elevations Y=12 cm, 20 cm, and 8 cm, respectively. The magnitude of flux discontinuities across the interfaces of two different types of subassemblies is much less than that of case 1. This is because there is no strong absorber present in the reactor core and thus the subassembly 1 detailed flux shape is relatively flat. Also, because of this fact, the results obtained from the linear finite element method and linear synthesis method are closed to each other and both predict quite good flux shapes and eigenvalues (Table 4.8) compared to the reference solutions.

4.3.3 Case 3: 49 Subassembly Reactor Configuration Made up of 2 Types of Core Subassemblies and One Type of Reflector Subassembly - Two Groups

The reactor system for this problem consists of a 25-subassembly core made up of 2 different types of subassemblies surrounded by a ring of 24 identical water reflector subassemblies. The reactor configuration and its 3 different types of subassemblies are depicted in Figure 4.13. The two-group nuclear constants for three different kinds of materials, (fuel, absorber and water moderator) which form the three types of subassemblies, are given in Table 4.6.

The detailed subassembly flux and adjoint flux solutions are found using PDQ-7 with a 14x14-mesh region per subassembly. The

partitioning of mesh intervals is 4(1.5cm) + 6(1.0) + 4(1.5) in both X and Y directions. Figures 4.14 - 4.17 illustrate these subassembly detailed solutions for Sub. 1 and Sub. 2. For water subassembly, Sub. 3, the detailed solutions are constant over the whole region. The homogenized two-group constants for each type of subassembly are given in Table 4.7.

The reference solution for this case was found using the same mesh intervals in each subassembly as in the calculation for detailed subassembly solutions. The total number of mesh regions is 49x49, because of quarter-core symmetry.

The graphical results for this two-group problem are shown in Figures 4.18 - 4.21. It is seen that the coarse-mesh linear finite element method cannot predict the thermal flux peaks and dips in the reactor. This indicates that finer meshes must be used to obtain good results. The linear synthesis method, whether calculated by adjoint weighting or flux weighting, gives reasonably good general shapes both for fast and thermal fluxes in the core region. However, the magnitudes of thermal peaks in subassemblies of type 2 can be very different compared to those of reference solutions. The cause of this phenomenon is the inability to predict the thermal flux peak in the reflector near the core-reflector interface by using flat flux shapes in the reflector subassembly and treating each subassembly as one mesh-region.

One way to overcome this difficulty is to put more mesh points in the reflector region by partitioning the reflector subassemblies further. Another way is to use some prescribed flux shapes in the

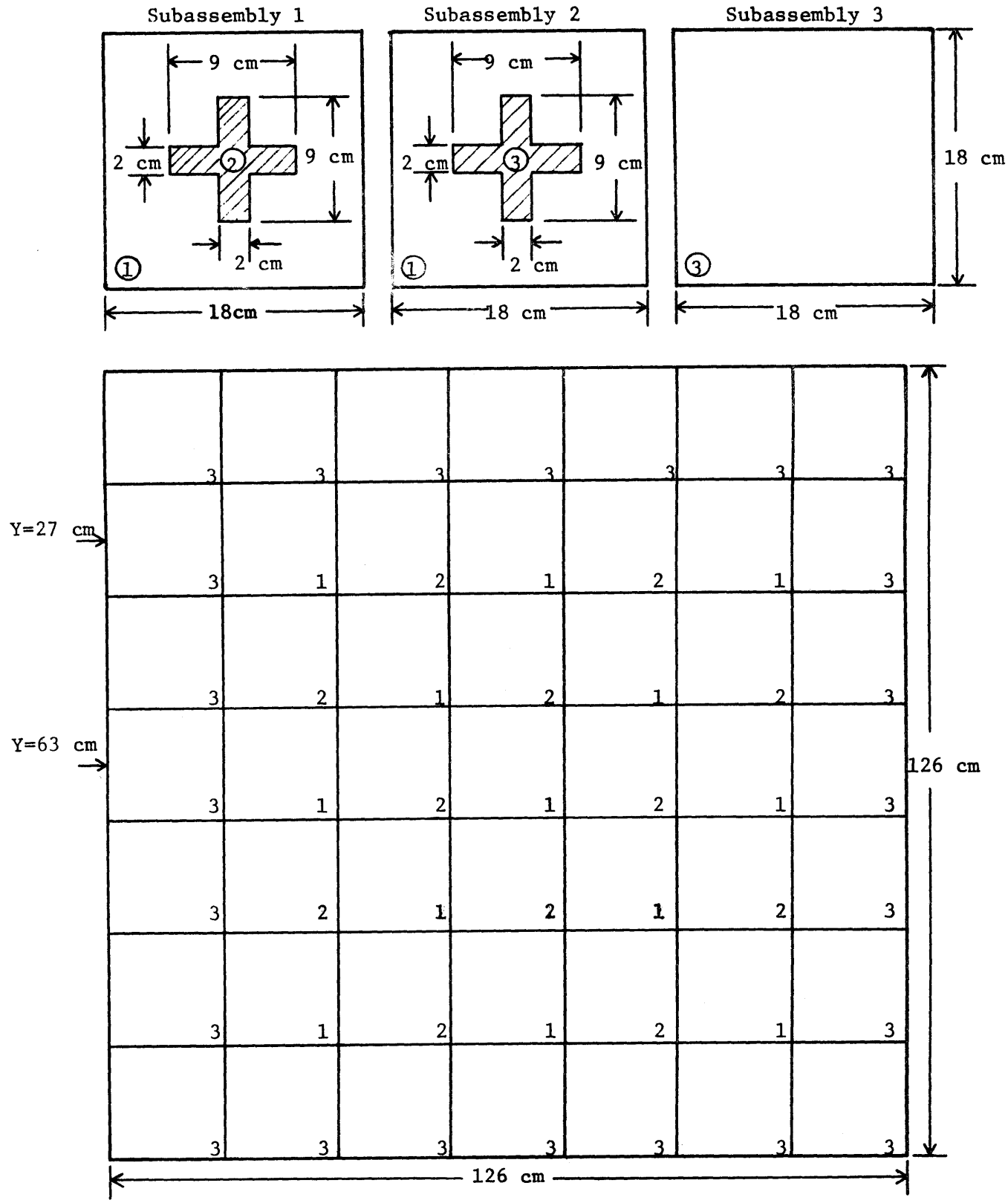

Figure 4.13 A 49 Subassembly Symmetric Reactor Configuration and Its 3 Different Types of Subassemblies - Case 3

Table 4.6 Two-group Nuclear Constants of Three Different Materials in Subassemblies of Figure 4.13 - Case 3

	fuel	absorber	moderator
	Material 1	Material 2	Material 3
D_1	1.436	1.092	1.545
Σ_1	0.02647	0.003185	0.028824
$\nu\Sigma_{f1}$	0.007293	0.0	0.0
Σ_{21}	0.01596	0.0	0.02838
χ_1	1.0	—	—
D_2	0.3868	0.3507	0.3126
Σ_2	0.1018	0.4021	0.008736
$\nu\Sigma_{f2}$	0.1531	0.0	0.0
χ_2	0.0	—	—

Table 4.7 Homogenized Subassembly Two-group Nuclear Constants - Case 3

	Sub.1	Sub. 2	Sub. 3
D_1	1.4030165	1.4464270	1.545
Σ_1	0.02423738	0.009547083	0.028824
$\nu\Sigma_{f1}$	0.006593731	0.006596349	0.0
Σ_{21}	0.01442972	0.01714810	0.02838
D_2	0.3854548	0.3749848	0.3126
Σ_2	0.1129898	0.08698106	0.008736
$\nu\Sigma_{f2}$	0.1473952	0.1287213	0.0

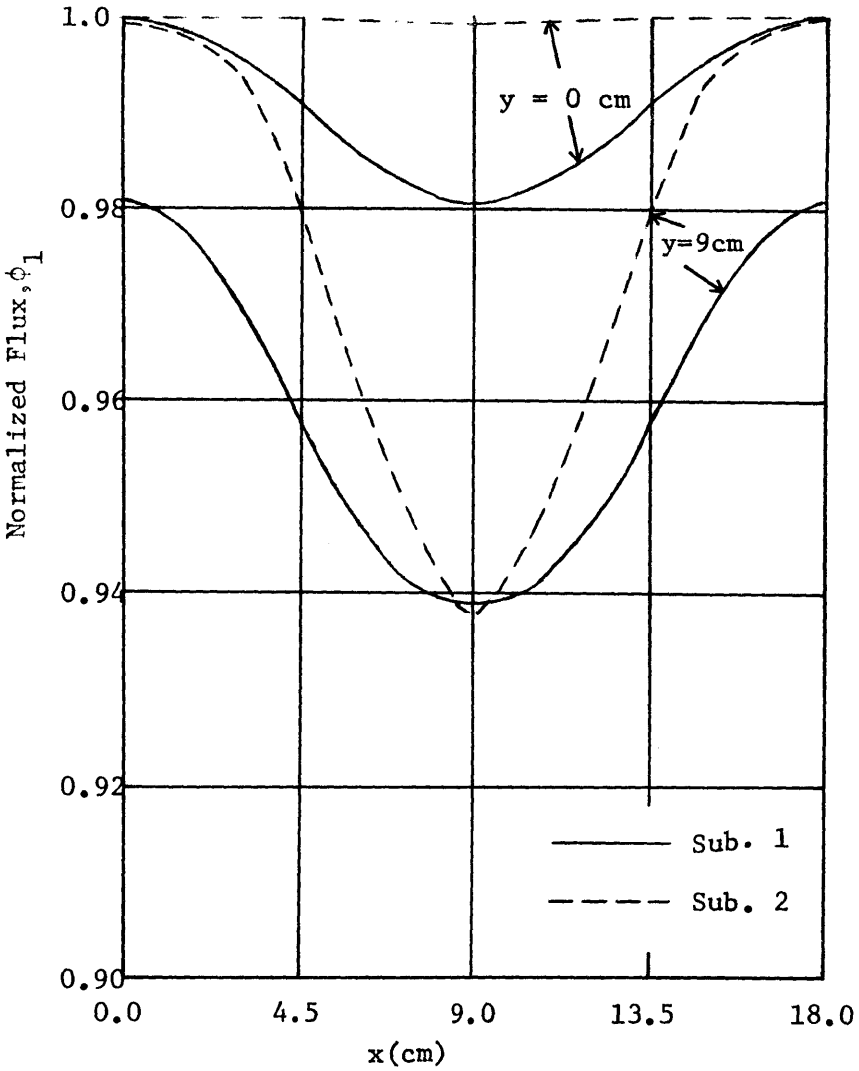

Figure 4.14 Detailed Fast Fluxes for Sub-assemblies - Case 3

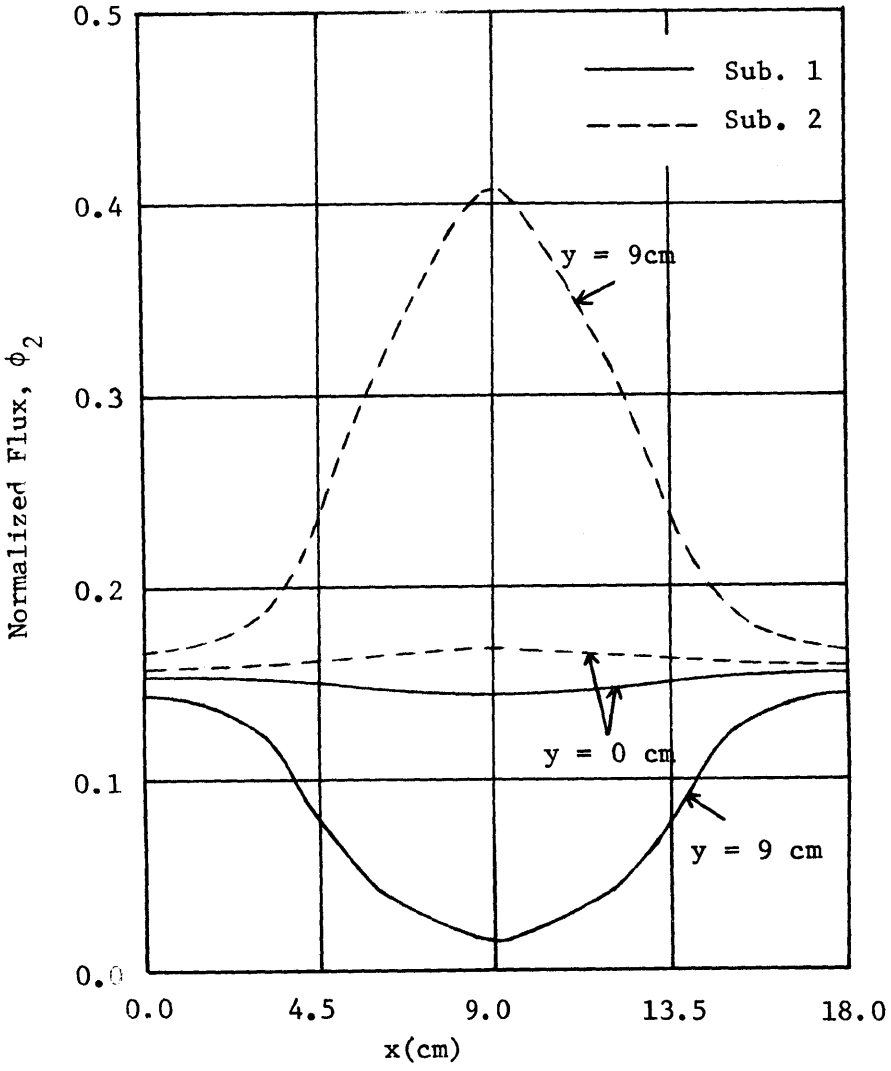

Figure 4.15 Detailed Thermal Fluxes for Subassemblies -- Case 3

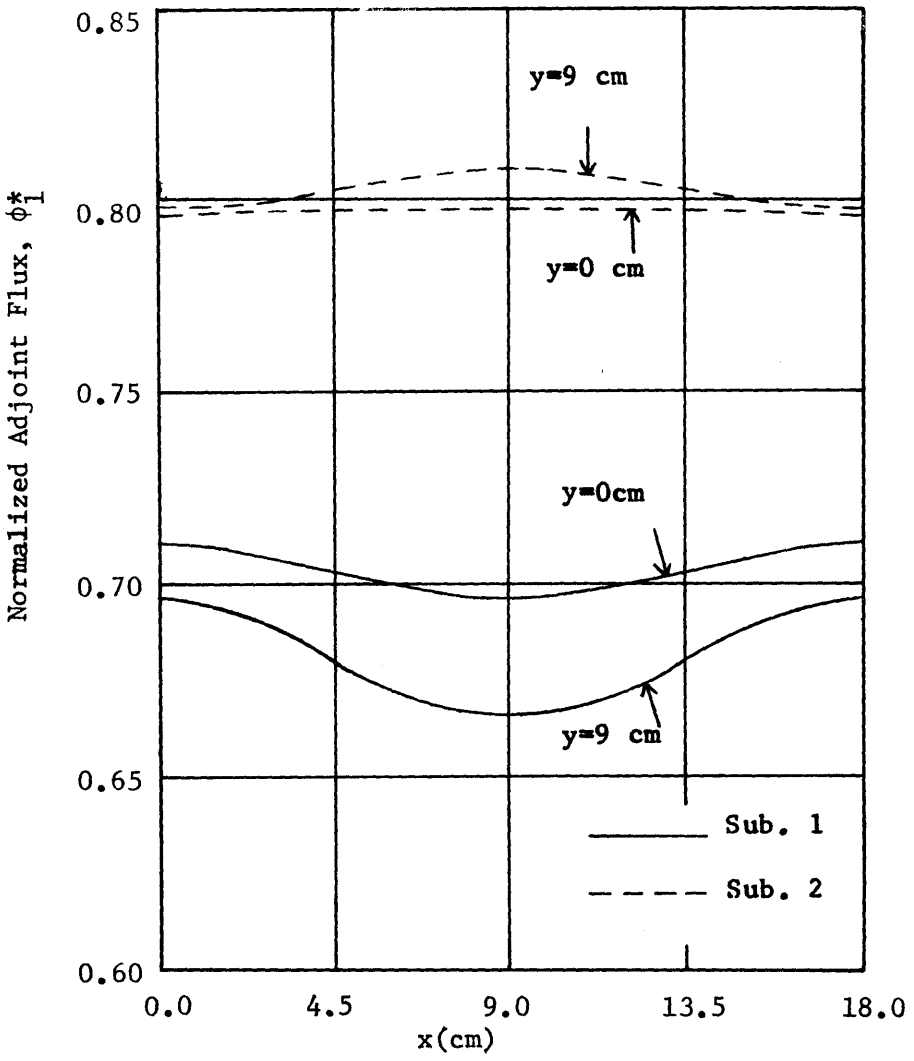

Figure 4.16 Detailed Fast Adjoint Fluxes for Sub-assemblies - Case 3

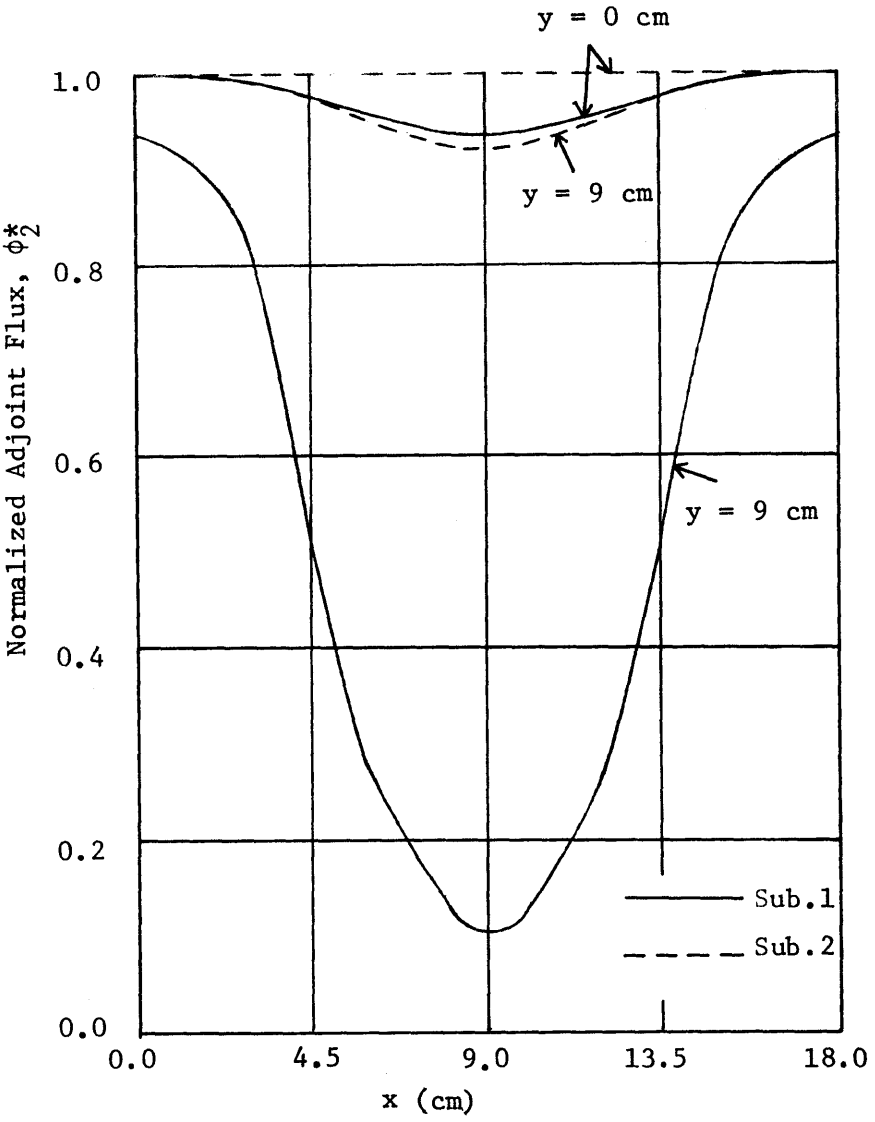

Figure 4.17 Detailed Thermal Adjoint Flux for Sub-assemblies - Case 3

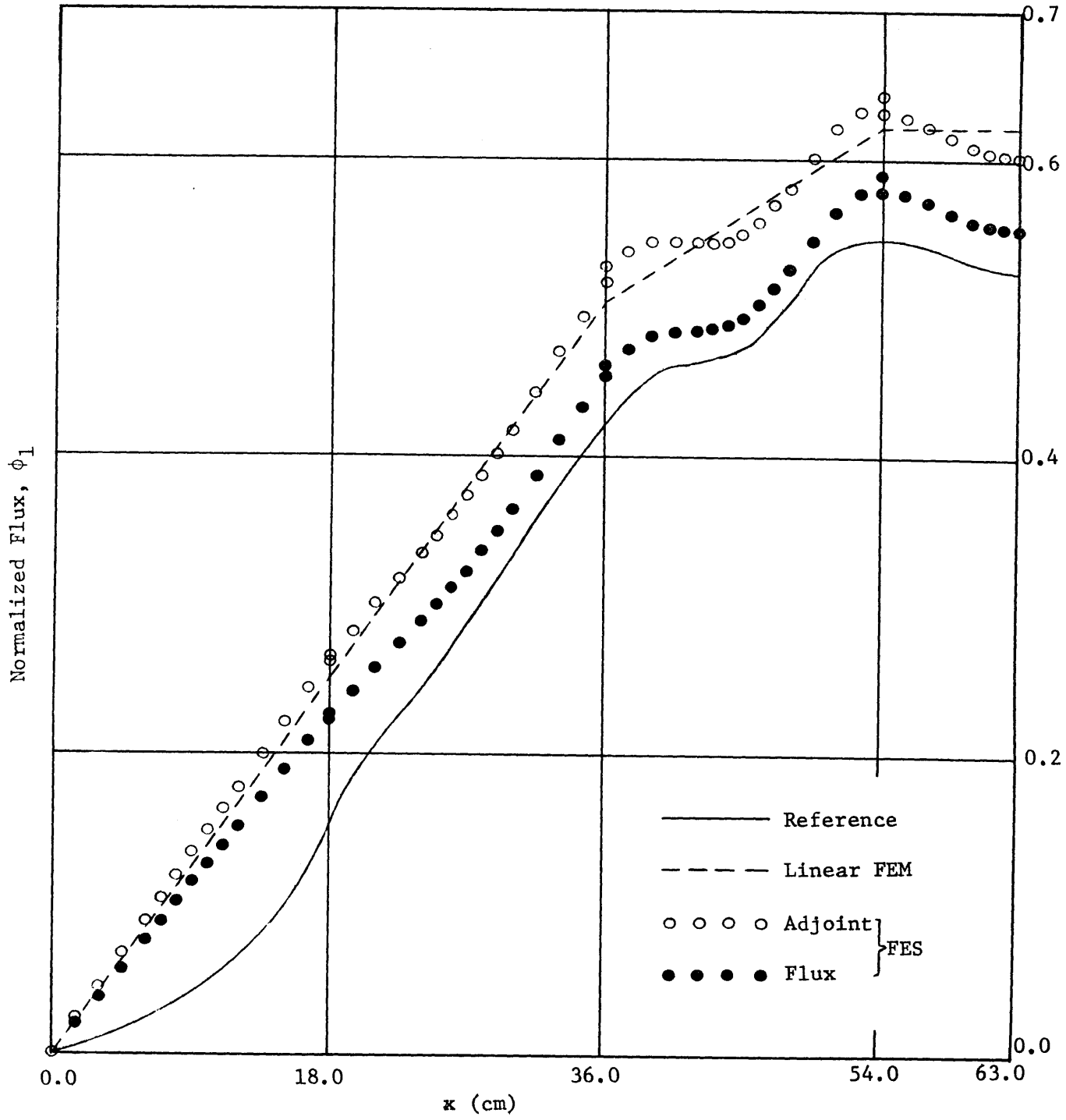

Figure 4.18 Fast Flux at Y = 27 cm - Case 3

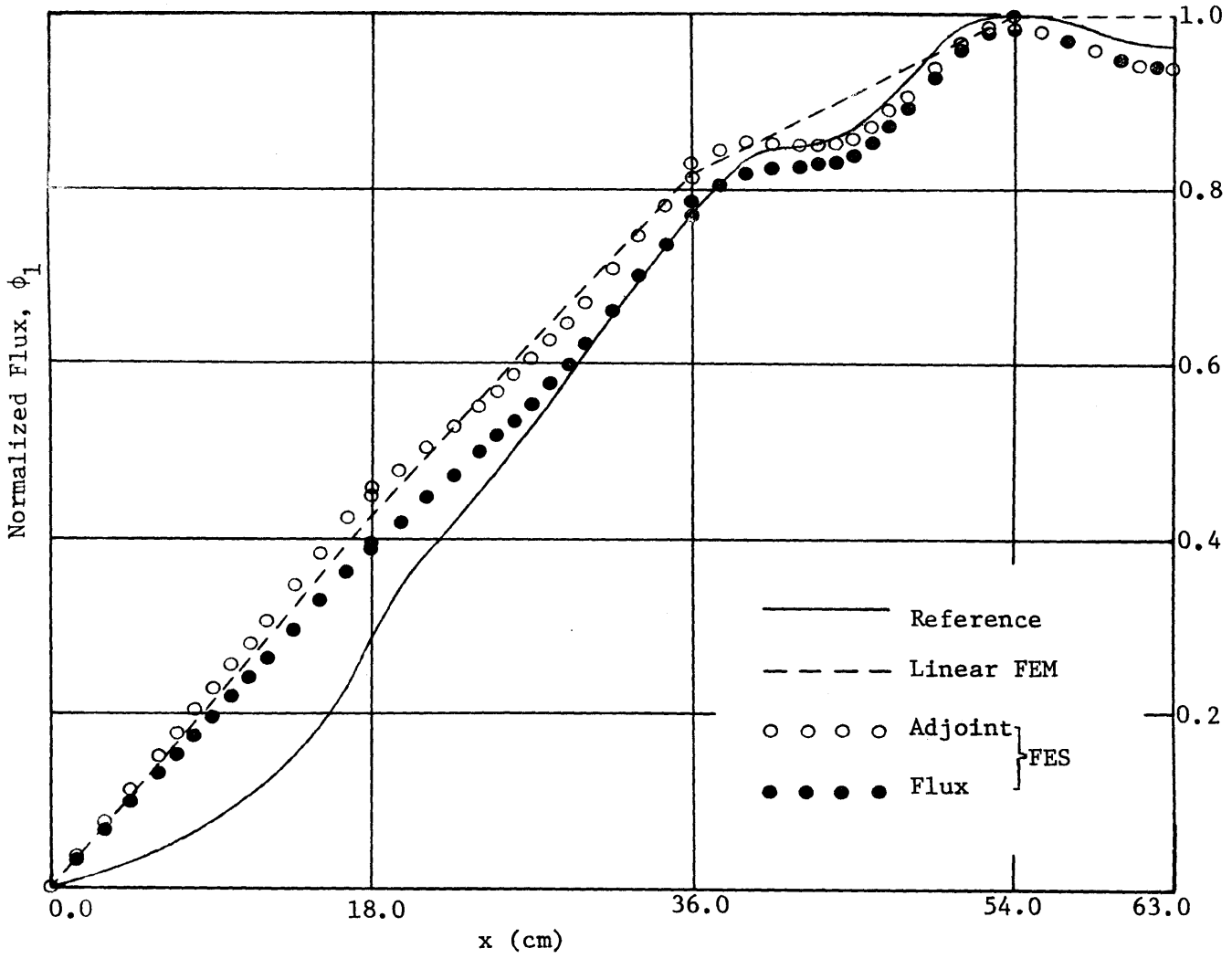

Figure 4.19 Fast Flux at Y = 63 cm - Case 3

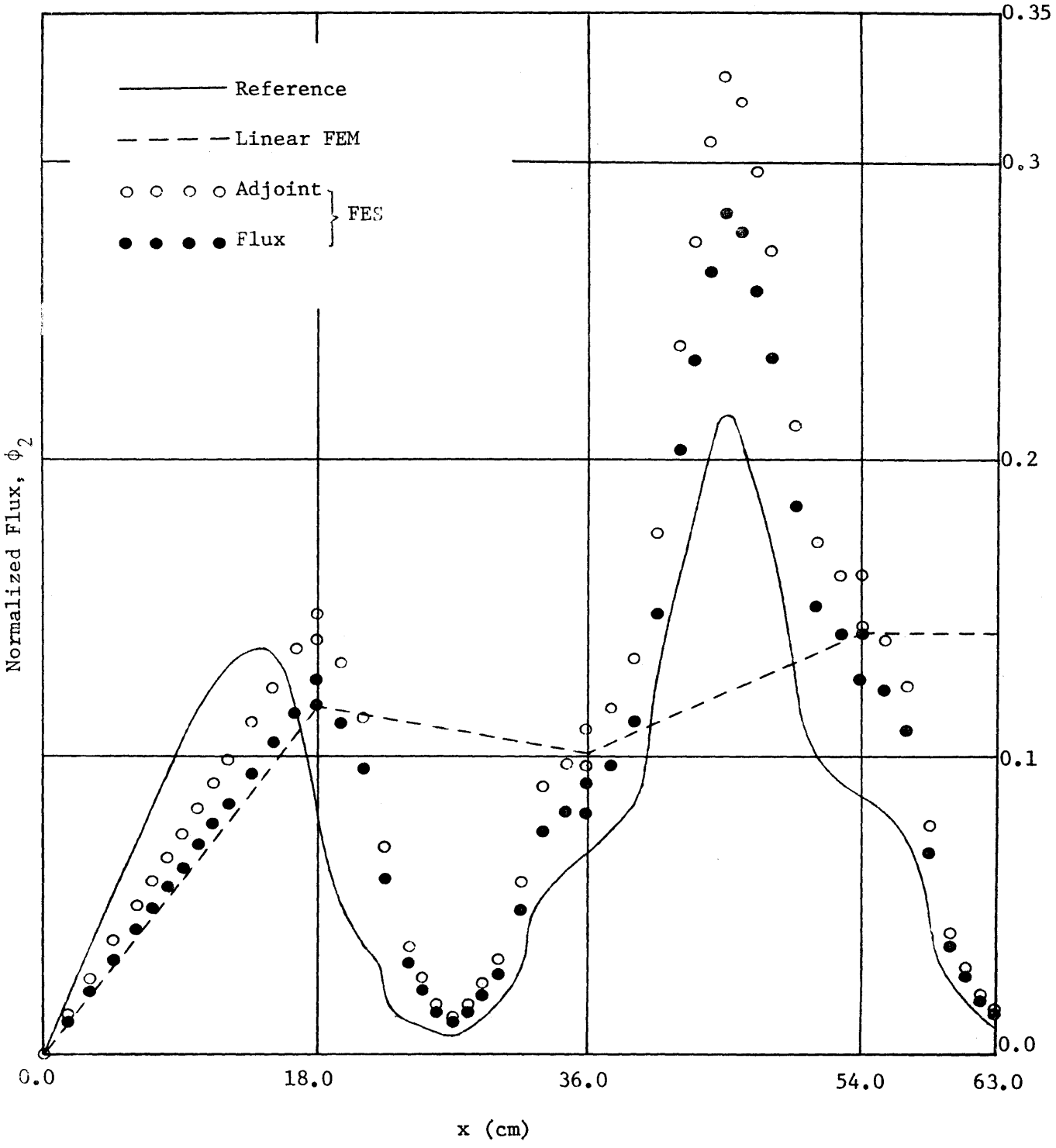

Figure 4.20 Thermal Flux at Y = 27 cm - Case 3

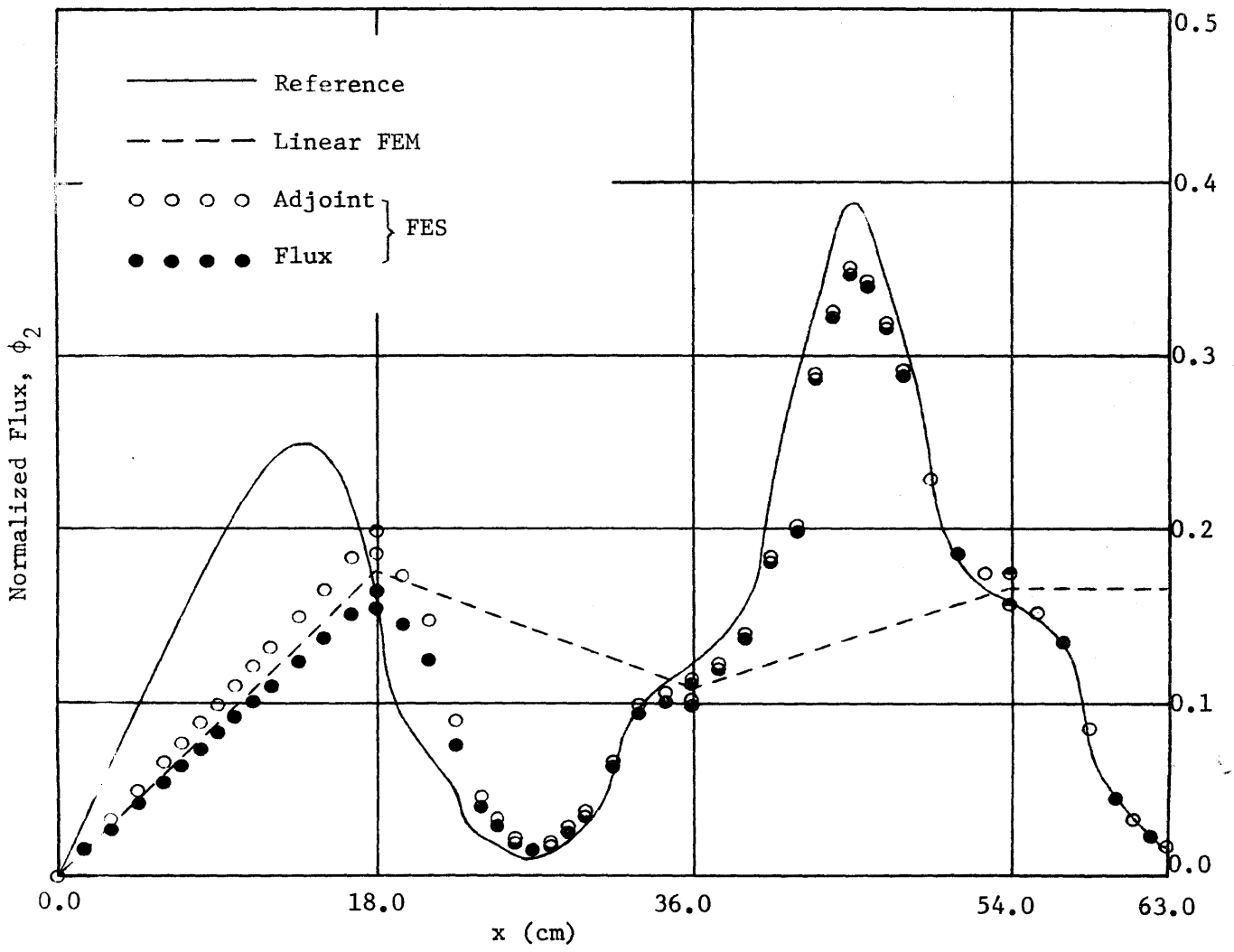

Figure 4.21 Thermal Flux at Y = 63 cm - Case 3

reflector subassemblies instead of flat shapes.

Figure 4.22 shows the average X-direction flux shapes for water subassemblies at the left side of the reactor, found from the reference solution. The Y-direction flux shapes are assumed to be flat. These fast and thermal flux shapes differ from those obtained by a simple 1-D calculation involving only one 18-cm region of water and one 18-cm region of fuel:

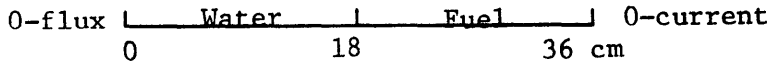

by 2% at most, using the same mesh intervals (14) in each region. Therefore, in the actual calculation where we normally would not have the reference solution in advance we can obtain the flux shapes from some simple auxiliary calculations. The flux shapes for water subassemblies at other three sides of the reactor can be found by symmetry considerations.

Figure 4.23 shows the flux shapes for the top-left corner water subassembly, again from the reference solution. Simple auxiliary 2-D calculation involving 3 water regions and 1 pure fuel region:

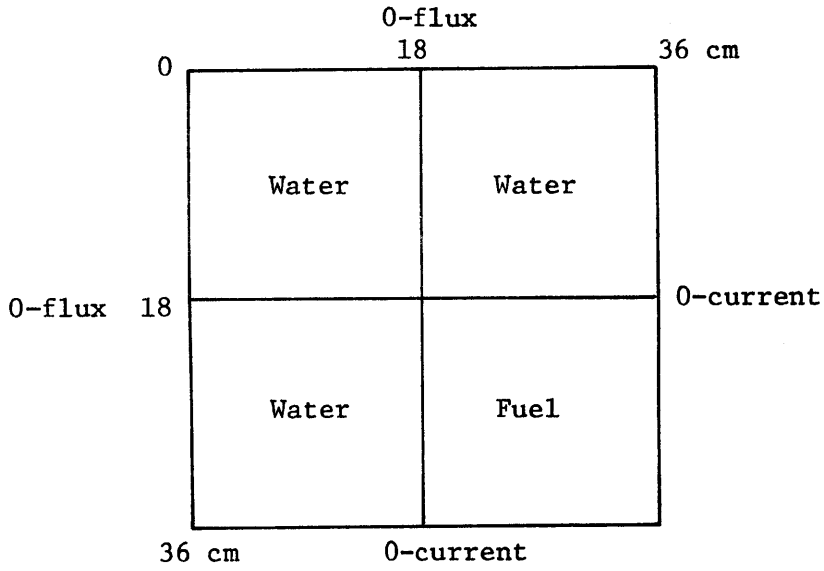

shows that these flux shapes differ only slightly (<3%) with each other.

For the modified calculation which follows below, we shall use Figures 4.22 and 4.23 as the regular flux as well as adjoint flux shapes for various water subassemblies.

The use of the flux shapes shown in Figures 4.22 and 4.23 is not legitimate in our present approximation, since these shapes do not have zero normal currents on all four subassembly boundaries. However, we can show that for the present case, use of these flux shapes merely adds some leakage terms to the calculations of those matrix elements (Appendix E) which correspond to reflector-core interfaces. These terms are of the form

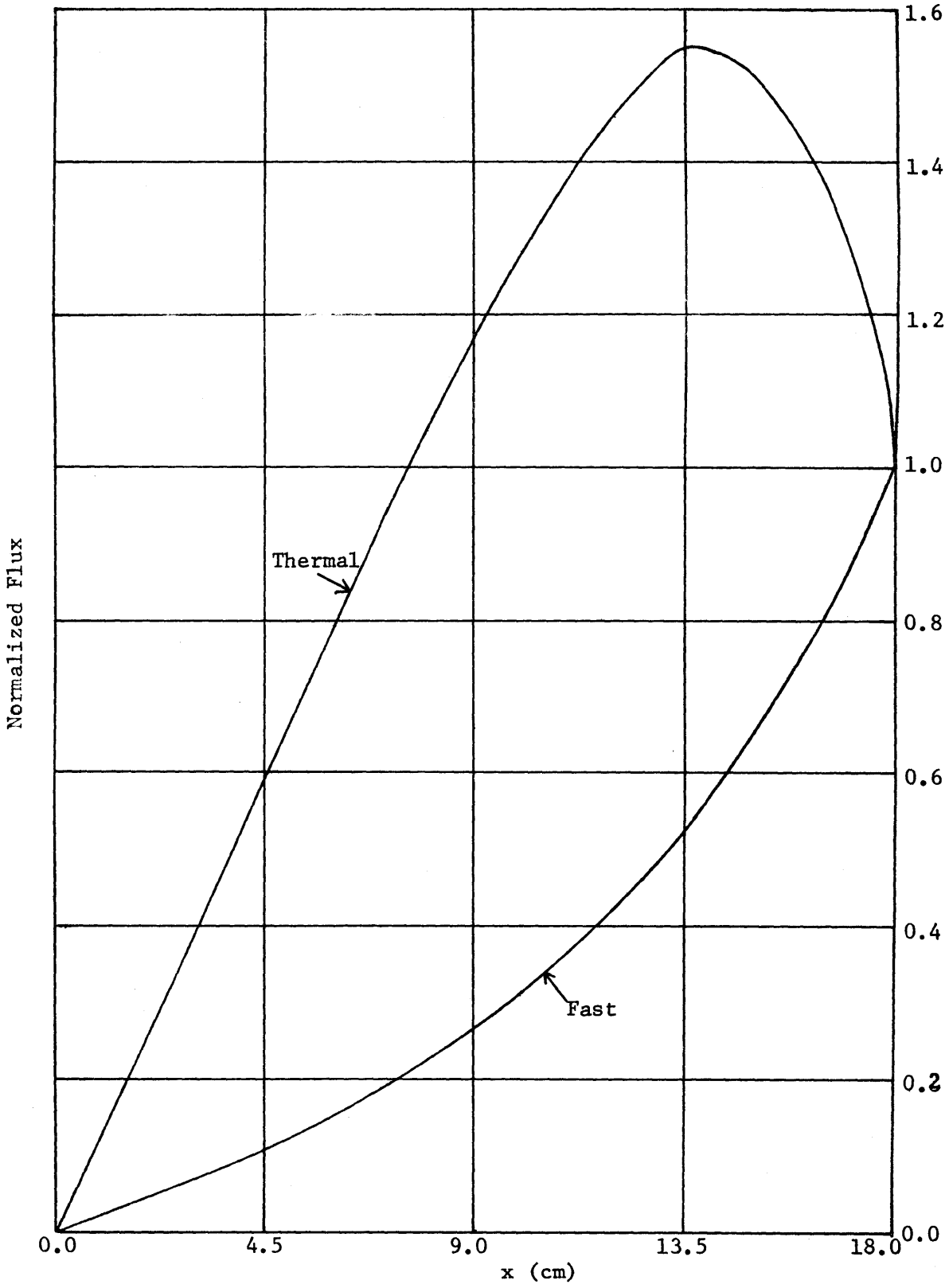

Figure 4.22 Flux Shapes for the Water Subassemblies at the Left Side Used in Modified Calculation - Case 3

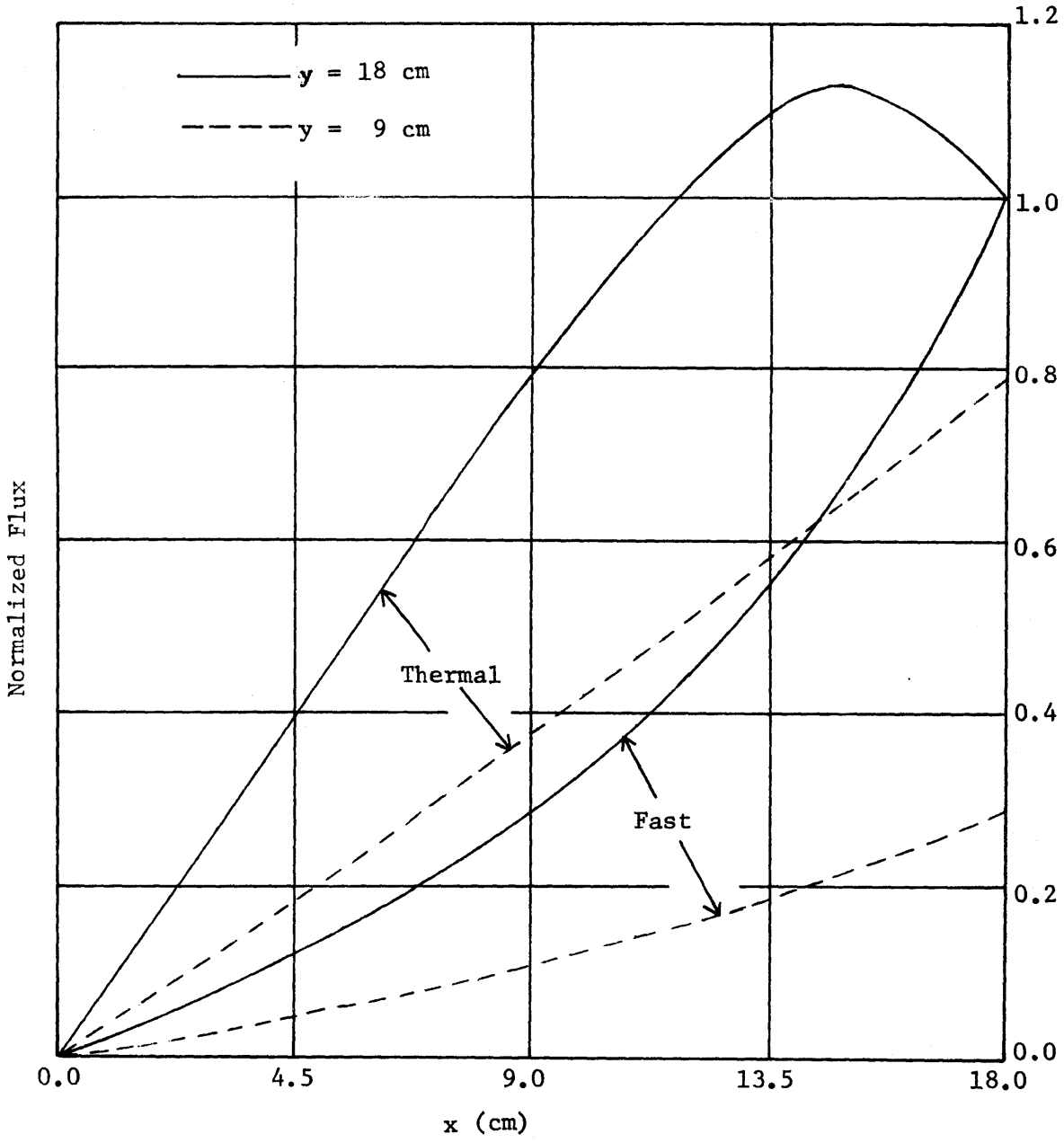

Figure 4.23 Flux Shapes for the Top-left Corner Water Subassembly Used in Modified Calculation - Case 3

$$\pm \frac{h_{yj}}{2} \int_0^1 dy P_m(y) P_n(y) [\psi^{*T^{-1}}_{2,j}(0,1)\psi^{*T}_{2,j}(0,y)\xi_{1,j}(1,y)\psi^{-1}_{1,j}(1,0)$$

$$- \psi^{T^{-1}}_{1,j}(1,0)\xi^{T}_{1,j}(1,y)\psi_{2,j}(0,y)\psi^{-1}_{2,j}(0,1)]$$

for the interface between subassemblies (1,j) and (2,j) for a particular j, and where m and n are either 1 or 2. The two terms in the square brackets are of the same sign.

A rough estimate, using the maximum absolute value for the first term and minimum absolute value for the second term, gives a largest value of

$$\frac{18}{2}\frac{1}{3}[(1.003)(0.0111) - (0.0111)(0.981)] = 0.00073$$

for the fast leakage and a largest value of

$$\frac{18}{2}\frac{1}{3}[(1.053)(0.00433) - (0.00433)(0.936)] = 0.00152$$

for the thermal leakage. These values are less than one tenth of one percent of the original leakage matrix elements. The results shown in the following pages are the results obtained by ignoring these additional small terms.

The results obtained by using these modified shapes for reflector subassemblies along with the previous shapes for core subassemblies are shown in Figures 4.24 - 4.27. It is seen that the flux shapes, especially the thermal flux shapes, improve significantly in the core region (X > 18 cm). The eigenvalues obtained from various methods are

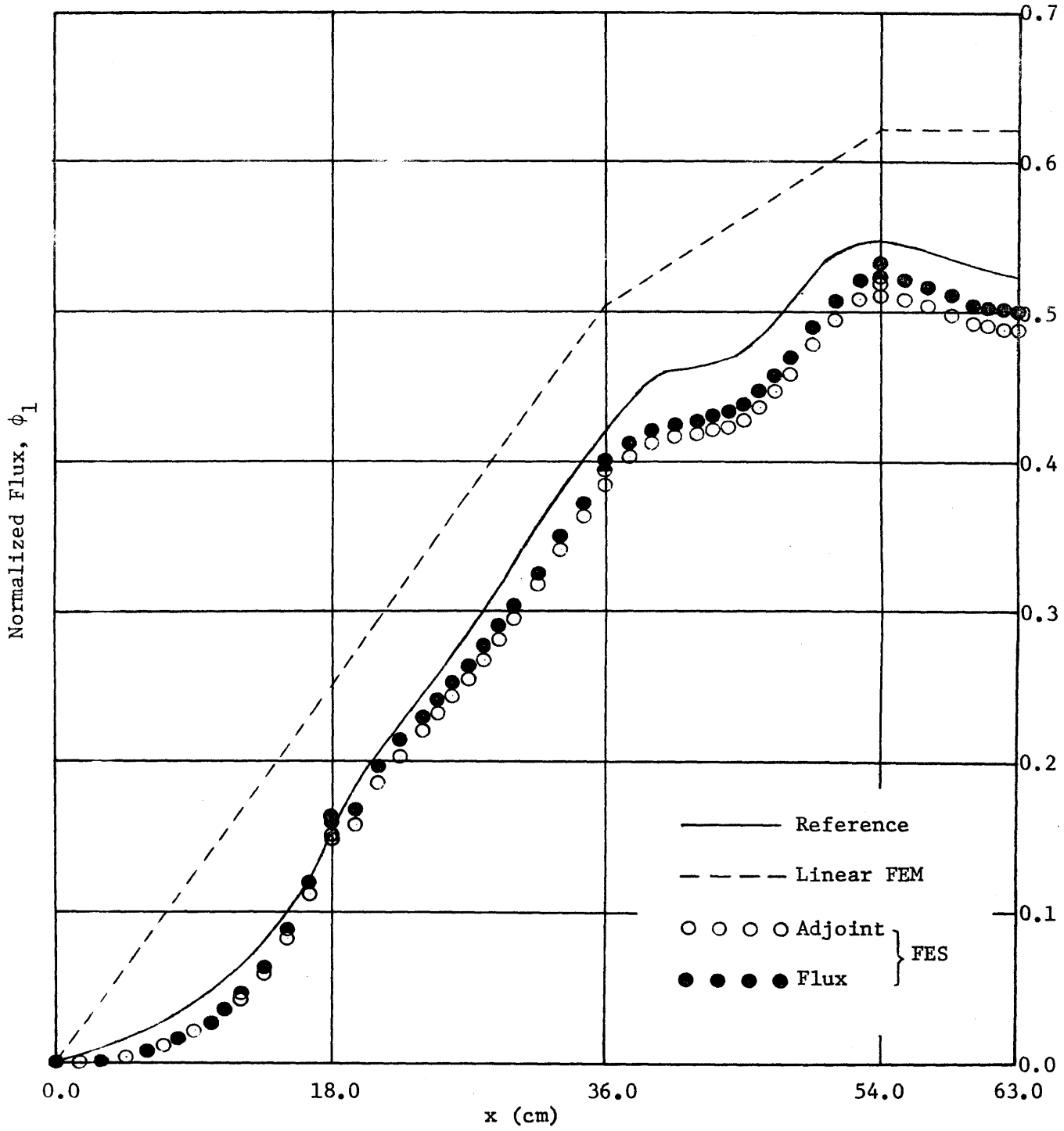

Figure 4.24 Fast Flux at Y = 27 cm - Case 3, Modified

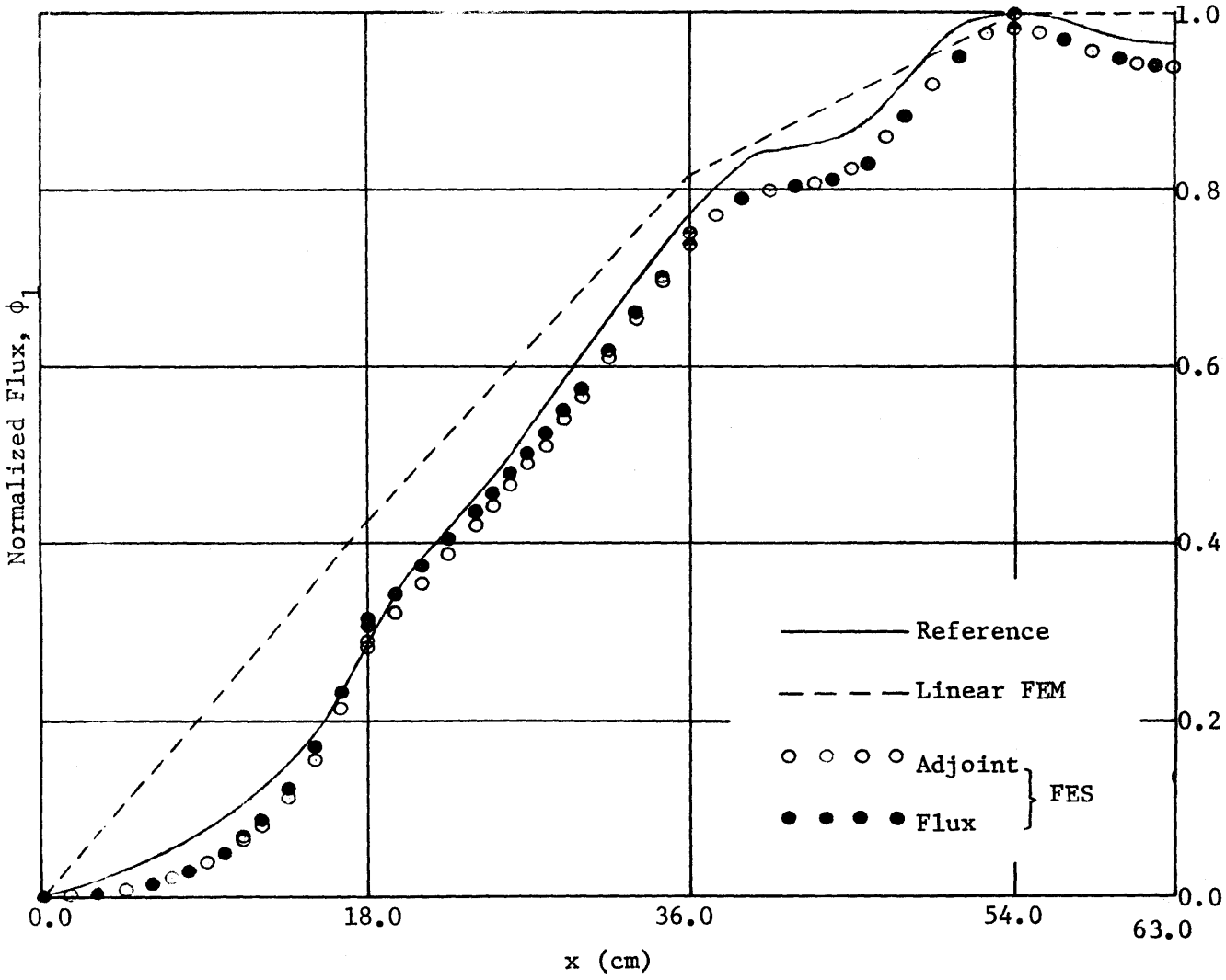

Figure 4.25 Fast Flux at Y = 63 cm - Case 3, Modified

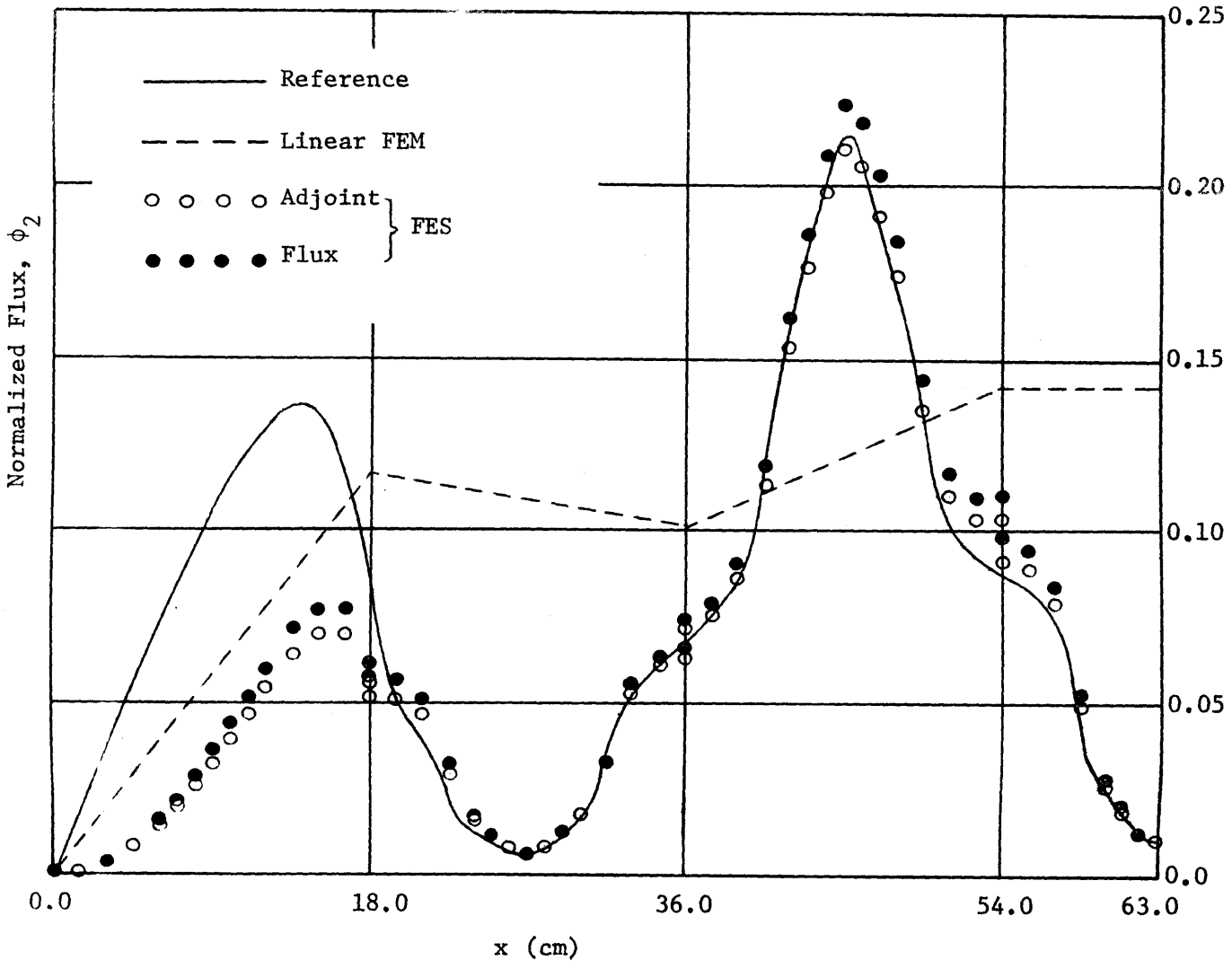

Figure 4.26 Thermal Flux at Y = 27 cm - Case 3, Modified

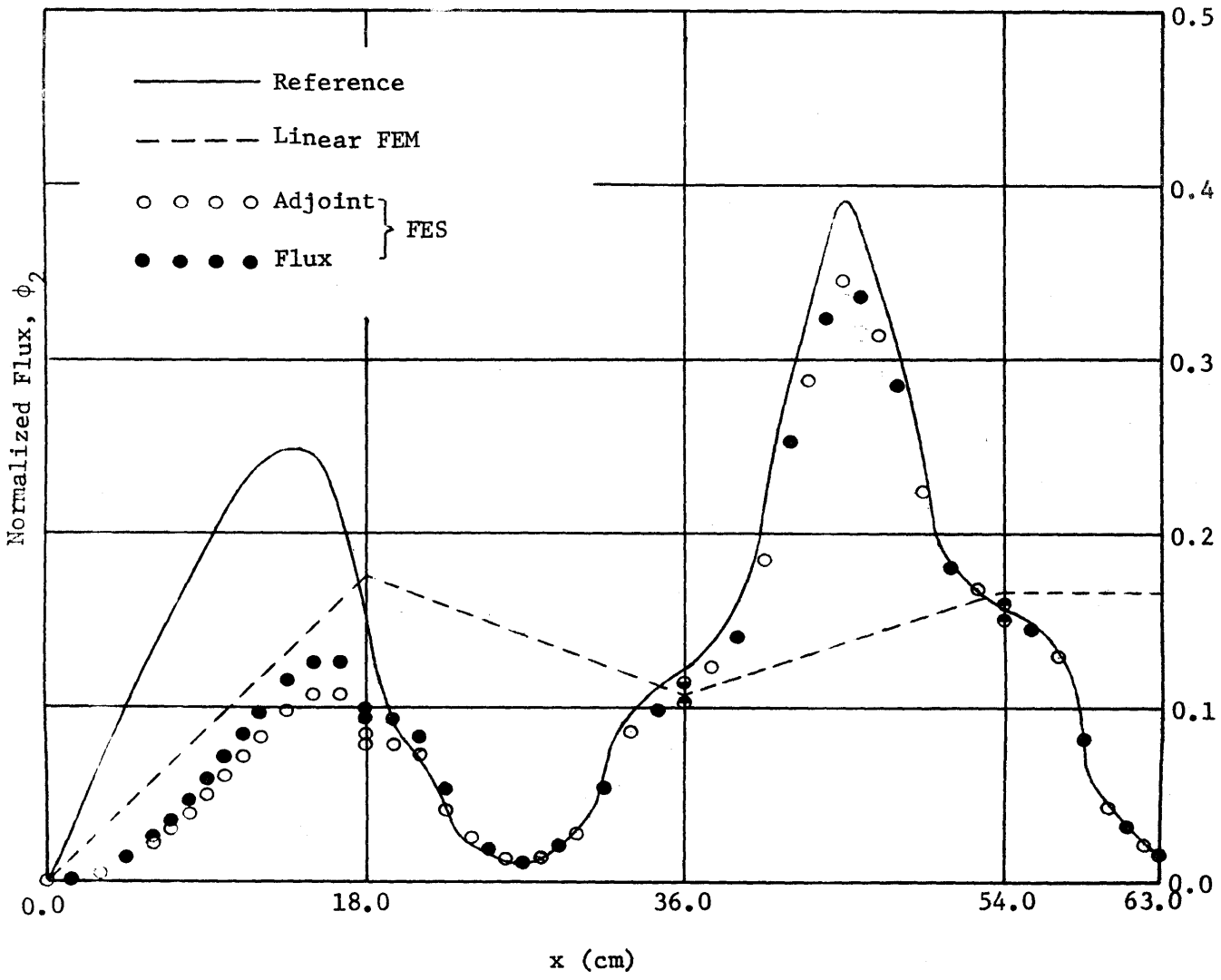

Figure 4.27 Thermal Flux at Y = 63 cm - Case 3, Modified

compared in Table 4.9. It is observed that: (i) the linear FEM using flux-weighted constants gives better results than the linear synthesis method and (ii) flux-weighted results are better than adjoint-weighted results in linear synthesis method. Although there is some mathematical reason to expect that the adjoint-weighted result should be better than the flux-weighted result, there is no proof of this expectation and it is common that in many numerical problems the reverse is true (as in this case).

From the above example, we conclude that the method of synthesizing detailed subassembly solutions with finite element basis functions in two-dimensional diffusion problems is quite encouraging. Thus, instead of the calculating of a large, fine-mesh problem to obtain the eigenvalue and detailed flux shape throughout a geometrically complicated core, we can solve the same problem by first determining a few, much smaller, fine-mesh subassembly solutions and then performing a very small coarse-mesh calculation.

Table 4.8 One-group Eigenvalue λ Obtained from Different Methods - Cases 1 and 2

	Case 1	Case 2
Reference	1.0081406	1.0071173
Linear FEM	0.9447535 (-6.29%)	0.9918033 (-1.52%)
Linear Synth.	1.0017971 (-0.63%)	0.9919463 (-1.51%)

Table 4.9 Two-group Eigenvalue λ Obtained from Different Methods - Case 3

		Case 3	
Reference		1.0428543	
Linear FEM		1.0397139 (-0.30%)	
Linear Synth.	Adjoint Weighted	1.0593464 (+1.58%)	1.0319060 (-1.05%)
	Flux Weighted	1.0510194 (+0.78%)	1.0380392 (-0.46%)
		Unmodified	Modified

CHAPTER 5

CONCLUSIONS AND RECOMMENDATIONS

5.1 Conclusions of the Study

Our proposed approximation, which couples detailed subassembly flux solutions together with bi-linear finite element basis functions, has a mathematical structure that is very similar to a coarse mesh bi-linear finite element approximation in which detailed flux shapes have been used beforehand to flux-weight the nuclear constants in each region. However, the two methods are conceptually different and become equivalent only when all of the coarse mesh regions are homogeneous. The proposed method is also similar to existing synthesis methods which use detailed flux solutions or other known flux shapes directly in the trial function for the flux. However, it is different in that it does not require full core, detailed flux shapes as input but instead stitches together a few fine-mesh subassembly solutions.

The numerical results indicate that the proposed scheme is able to predict criticality accurately as well as the detailed flux shapes for each group. The results indicate that although both the proposed scheme and the finite element method with flux-weighted constants give good criticality estimates, the actual detailed flux behavior is much better approximated by the proposed method than the finite element method using coarse meshes.

As in any coarse mesh approximation method, inaccurate results

can occur when the coarse mesh region sizes chosen are too large. Thus it would be useful if there were error bounds that could be ascribed to the finite-element synthesis method. The accuracy of finite element methods is known to improve geometrically as the mesh sizes is decreased. Thus there is a useful error criteria for the finite element methods. On the other hand, the inability to predict error estimates has always been a major drawback of synthesis techniques, even though through proper physical insight and experience, accurate results can be obtained. Whether or not error bounds can be found for solutions obtained by combining synthesis and finite element flux shapes is not yet known.

Another thing which is lacking in this study is the computation time comparison between various methods. This is because of our inability to generate computer code for which the eigenvalue and flux shapes of a problem can be obtained directly without any intermediate matrix elements calculations, and we have to obtain the results step by step.

In conjunction with the study, we found some interesting results related to the finite element Hermite basis functions approximations:

(i) Under certain conditions described in the end of Chapter 2, Fick's law is a natural consequence of using the variational functional F_3.

(ii) The solution that is found by applying a variational method using continuous cubic flux trial functions and

discontinuous Fick's law current trial functions is not necessarily the best. We found in Chapter 3 that the cubic Hermite method, which defines continuous flux trial functions in such a way that the current trial functions are also continuous throughout the problem domain except at singular points, yields more accurate results even though the trial functions space is more limited.

5.2 Recommendations for Future Study

For future study of the finite element synthesis method, some areas which deserve closer attention are:

i) Development of error bounds for the finite element-synthesis method. The close similarity between the present method and the finite element methods may allow an extension or generalization of error estimates previously developed for finite element methods.

ii) Examination of the matrix properties of the synthesis method. This is necessary in order to guarantee convergence to a positive eigenvalue and an everywhere positive flux solution.

The bi-linear finite element synthesis method can be extended to three-dimensional diffusion problems as well as to a higher degree of Hermite basis polynomials. The mathematical principles are the same as for the present method, and the main concern would be the algebraic complexity of handling large numbers of lengthy equations.

Also possible is the extension of using the proposed trial function forms in spatial overlapping synthesis methods for multi-dimensional reactor problems, where the discontinuities of flux and current trial functions occur at different places.

BIBLIOGRAPHY

1. T.J. Thompson and J.G. Beckerley, The Technology of Nuclear Reactor Safety, Vol. 1, M.I.T. Press, Cambridge, Mass. (1964)

2. A.M. Weinberg and E.P. Wigner, The Physical Theory of Neutron Chain Reactors, University of Chicago Press, Chicago, Ill. (1958)

3. B. Davison, Neutron Transport Theory, Oxford University Press (Clarendon), London (1958)

4. J.R. Lamarsh, Introduction to Nuclear Reactor Theory, Addison-Wesley, Reading, Mass. (1966)

5. M. Clark, Jr. and K.F. Hansen, Numerical Methods of Reactor Analysis, Academic Press, New York (1964)

6. M. Rose, "Finite Difference Schemes for Differential Equations", Math. of Comp., 18, 179 (1964)

7. D.S. Selengut, "Variational Analysis of a Multi-dimensional System", HW-59126, pp. 89-125, Hanford Atomic Products Operation (1959)

8. G.P. Calame and F.D. Federighi, "A Variational Procedure for Determining Spatially Dependent Thermal Spectra", Nucl. Sci. Eng., 10, 190 (1961)

9. S. Kaplan, "Some New Methods of Flux Synthesis", Nucl. Sci. Eng., 13, 22 (1962)

10. S. Kaplan, O.J. Marlowe, and J. Bewick, "Application of Synthesis Techniques to Problems Involving Time Dependence", Nucl. Sci. Eng., 18, 163 (1964)

11. S. Kaplan, "Synthesis Methods in Reactor Analysis", in Advances in Nuclear Science and Technology, Vol. III, P.R. Greebler, Ed., Academic Press, New York (1966)

12. W.M. Stacey, Jr., Modal Approximations: Theory and an Application to Reactor Physics, M.I.T. Press, Cambridge, Mass. (1967)

13. J.B. Yasinsky, "The Solution of the Space-time Neutron Group Diffusion Equations by a Time-discontinuous Synthesis Method", Nucl. Sci. Eng., 29, 381 (1967)

14. J.B. Yasinsky and S. Kaplan, "Synthesis of Three-dimensional Flux Shapes Using Discontinuous Sets of Trial Functions", Nucl. Sci. Eng., 28, 426 (1967)

15. R.A. Rydin, "Time Synthesis - A Study of Synthesis Modes and Weighting Functions", Trans. Am. Nucl. Soc., 10, 559 (1967)

16. J.E. Cockayne, K.O. Ott, "Successive Space-Energy Synthesis for Neutron Fluxes in Fast Reactors", Nucl. Sci. Eng., 43, 159 (1971)

17. M.J. Lancefield, "Space-Energy Flux Synthesis in Neutron Transport", Nucl. Sci. Eng., 37, 423(1969)

18. W.M. Stacey, Jr., "Variational Flux Synthesis Methods for Multigroup Neutron Diffusion Theory", Nucl. Sci. Eng., 47, 449 (1972)

19. M. Natelson, "Synthesis of Three-dimensional Transport Problems Using Two-dimensional Trial Functions", Nucl. Sci. Eng., 48. 16 (1972)

20. C.A. Felippe and R.W. Clough, "The Finite Element Method in Solid Mechanics", Numerical Solution of Field Problems in Continuum Physics, SIAM-AMS Proceedings, Vol. II, p. 210 (1970)

21. O.C. Zienkiewicz and Y.K. Cheung, The Finite Element Method in Structural and Continuum Mechanics, McGraw-Hill, New York (1967)

22. H.C. Martin, "Finite Element Analysis of Fluid Flows", Proc. Conf. Matrix Methods in Structural Mechanics, 2nd, Wright-Patterson Air Force Base (1968)

23. L.J. Doctors, Intern. J. Num. Meth. in Eng., 2, 243 (1970)

24. C.M. Kang and K.F. Hansen, Finite Element Methods for Space-Time Reactor Kinetics, Sc.D. Thesis, Department of Nuclear Engineering, M.I.T., MITNE-135 (November, 1971)

25. L.A. Semenza, E.E. Lewis, and E.C. Rossow, "The Application of the Finite Element Method to the Multigroup Neutron Diffusion Equations", Nucl. Sci. Eng., 47, 302 (1972)

26. L.O. Deppe and K.F. Hansen, The Finite Element Method Applied to Neutron Diffusion Problems, M.S. and N.E. Thesis, Department of Nuclear Engineering, M.I.T., MITNE-145 (February, 1973)

27. G. Fix and G. Strang, "Fourier Analysis of the Finite Element Method in Ritz-Galerkin Theory", Studies in Applied Math., 48, 265 (1969)

28. G. Strang, "The Finite Element Method and Approximation Theory", Numerical Solution of Partial Differential Equations - II, SYNSPADE 1970, Ed. B. Hubbard, p. 547, Academic Press, New York (1971)

29. M. Zlamal, "On the Finite Element Method", Numer. Math., 12, 394 (1968)

30. P.G. Bailey and A.F. Henry, Variational Derivation of Modal-Nodal Finite Difference Equations in Spatial Reactor Physics, Ph.D. Thesis, Department of Nuclear Engineering, M.I.T., MITNE-138 (July, 1972)

31. S. Glasstone and A. Sesonske, Nuclear Reactor Engineering, D. Van Nostrand, Princeton, N.J. (1963)

32. S. Glasstone and M.C. Edlund, Nuclear Reactor Theory, D. Van Nostrand, Princeton, N.J. (1952)

33. P.M. Morse and H. Feshbach, Methods of Theoretical Physics, Capt. 6, McGraw-Hill (1953)

34. R.S. Varga, "Hermite Interpolation-Type Ritz Methods for Two-Point Boundary Problems", Numerical Solution of Partial Differential Equations, Ed. J.H. Bramble, pp. 365-373, Academic Press, New York (1966)

35. P.G. Ciarlet, M.H. Schultz and R.S. Varga, "Numerical Methods of High-Order Accuracy for Nonlinear Boundary Value Problems I, One-Dimensional Problem", Numer. Math., 9, 394-403 (1967); also see III, Numer. Math., 12, 120-133 (1968); V.Numer. Math., 13, 51-77 (1969)

36. I.J. Schoenberg, "Contribution to the Problem of Approximation of Equidistat Data by Analytic Functions, Parts A and B", Quart. Appl. Math., 4, 45-99, 112-131 (1946)

37. J. Mathews and R.L. Walker, Mathematical Methods of Physics, W.A. Benjamin, New York (1965)

38. L.I. Schiff, Quantum Mechanics, McGraw-Hill, New York (1955)

39. R.P. Feynmann, R.B. Leighton, and M. Sands, The Feymann Lectures on Physics, Addison-Wesley, Reading, Mass. (1963)

40. H. Goldstein, Classical Mechanics, Addison-Wesley, Reading, Mass. (1962)

41. M. Becker, The Principles and Applications of Variational Methods, M.I.T. Press, Cambridge, Mass. (1964)

42. F.B. Hildebrand, Methods of Applied Mathematics, Prentice-Hall, Englewood Cliffs, New Jersey (1965)

43. A.F. Henry, "Variational Techniques as a Means of Deriving Approximation Methods", in M.I.T. Course 22.25 Notes, Advanced Reactor Physics, p. 96 (Fall, 1969)

44. V. Luco and P. Lambropoulos, "Functional for Discontinuous Trial Function Flux Synthesis", J. Nucl. Energy A/B, 24, 551 (1970)

45. A.F. Henry, "Few-group Approximations Based on a Variational Principle", Nucl. Sci. Eng., 27, 493 (1967)

46. W.M. Stacey, Jr., Variational Methods in Nuclear Reactor Physics, Academic Press, New York (1974)

47. G. Fix, "Higher Order Rayleigh-Ritz Approximation", J. Math. Mech., 18, 645-658 (1969). Also, Ph.D. Thesis, Harvard University (1968)

48. G.I. Wakoff, "Piecewise Polynomial Spaces and Their Use with Rayleigh-Ritz-Galerkin Method", Ph.D. Thesis, Harvard University (1970)

49. G. Strang and G. Fix, An Analysis of the Finite Element Method, Prentice-Hall, Englewood, New Jersey (1973)

50. G. Birkhoff, C. deBoor, B. Swartz, and B. Wendroff, "Rayleigh-Ritz Approximation by Piecewise Cubic Polynomials", J. SIAM Numer. Anal., Vol. 3, No. 2,p. 188 (1966)

51. J.J. Goel, "Construction of Basic Functions for Numerical Utilization of Ritz's Method", Numer. Math., 12, p. 435 (1968)

52. A.F. Henry, M.I.T. Course 22.213 Notes, Nuclear Reactor Physics III, p. 143 (Fall, 1971)

53. G. Birkhoff, "Angular Singularities of Piecewise Helmholtz Equations", N.S.F. Regional Research Conf. on Num. Sol. of Elliptic Diff. Eqs. at Rolla, Mo., Sept. 8-12, 1969

54. R.B. Kellog, "Singularities in Interface Problems", Numerical Solution of Partial Differential Equation-II, SYNSPADE 1970, Ed., B. Hubbard, pp. 351-400, Academic Press, New York (1971)

55. F.B. Hildebrand, Introduction to Numerical Analysis, McGraw-Hill, New York (1956)

56. E.L. Wachspress, Iterative Solution of Elliptic Systems, Prentice-Hall, Engelwood Cliffs, N.J. (1966)

57. R.S. Varga, Matrix Iterative Analysis, Prentics-Hall, Engelwood Cliffs, N.J. (1962)

58. G. Forsythe and C.B. Moler, Computer Solution of Linear Algebraic Systems, Prentice-Hall, Engelwood Cliffs, N.J. (1967)

59. J.H. Wilkinson, The Algebraic Eigenvalue Problems, Oxford University Press, London (1965)

60. G. Bilodeau and L. Hageman, "A Survey of Numerical Methods in the Solution of Differential Problems", WAPD-TM-64 (July, 1957)

61. A.F. Henry, M.I.T. Course 22.212 Notes, Nuclear Reactor Physics II, p. 32 (Spring 1971)

62. C.M. Kang and K.F. Hansen, "Finite Element Methods for the Neutron Diffusion Equations", Trans. Am. Nucl. Soc., Vol. 14, No. 1, p. 190 (1971)

63. A. Radkowsky, Editor, Naval Reactors Physics Handbook, Vol. 1, Selected Basis Techniques, "Homogenization Techniques", Chap. 4.3, USAEC, p. 620 (1964)

64. W.R. Cadwell, PDQ-7 Reference Manual, WAPD-TM-678 (Jan., 1967)

65. R.J. Breen, et al, HARMONY: System for Nuclear Reactor Depletion Computation, WAPD-TM-478 (Jan., 1965)

66. A.W. Brown, J.A. McClure, and R.J. Wagner, Summary of PDQ-7 (IBM-360-370 Version) Input Data Requirements and Operating Procedures, ANCR-1061, UC-32, Aerojet Nuclear Company, prepared for the USAEC (March 1972)

67. T.B. Fowler, D.R. Vondy, and G.W. Cunningham, Nuclear Reactor Core Analysis Code: CITATION, ORNL-TM-2496, Rev. 2 (July, 1971)

BIOGRAPHICAL NOTE

The author, Shi-tien Yang, was born on July 9, 1946 in the city of Hsinchu, Hsinchu County, Taiwan. He received elementary school education in his home town and then graduated from Taiwan Provincial Chien-kuo High School in Taipei, in July 1964.

He then attended Tunghai University in October 1964, without taking the usual requirements of College Entrance Examination because of his good academic performance in high school. In June 1968, he received his Bachelor of Science Degree in Physics. During his four years' stay in Tunghai University, he was honored as an outstanding student every year, and was given the highest honor for a student with his name engraved on the wall of the University Auditorium upon his graduation. He was also elected to the Phi Tau Phi Honorary Society in his senior year.

After one-year mandatory service in the Chinese Air Force, he came to the United States in August 1969 and enrolled at the Massachusetts Institute of Technology in February, 1970. The author completed this work and obtained the degree of Doctor of Philosophy in 1975.

The author is married to the former Yu-fen Lai and is expecting a baby in August 1975.

APPENDIX A

TABLE OF SYMBOLS

g	Energy group index which runs from the highest to the lowest energy group as g = 1 to G.
$\underline{r}$	The position vector.
$\phi_g(\underline{r})$	Scalar neutron flux in energy group g at $\underline{r}$ (neutrons/cm^2-sec).
$\underline{j}_g(\underline{r})$	Neutron current vector in energy group g at $\underline{r}$ (neutrons/cm^2-sec).
$D_g(\underline{r})$	Diffusion coefficient for neutrons in energy group g at $\underline{r}$ (cm).
$\Sigma_g(\underline{r})$	Macroscopic total neutron removal cross section in energy group g at $\underline{r}$ (cm^{-1}).
$\Sigma_{gg'}(\underline{r})$	Macroscopic neutron scattering cross section from energy group g' to energy group g at $\underline{r}$ (cm^{-1}).
λ	The eigenvalue of the diffusion problem.
χ_g	Fission spectrum yield in energy group g.
$\nu\Sigma_{fg}(\underline{r})$	Macroscopic fission neutron production cross section in energy group g at $\underline{r}$ (cm^{-1}).
$\Phi(\underline{r})$, $\Phi^*(\underline{r})$	Scalar group flux column vector of length G and the corresponding adjoint flux vector.
$\underline{J}(\underline{r})$, $\underline{J}^*(r)$	Vector group current column vector of length G and the corresponding adjoint current vector.

$\mathbb{D}(\underline{r})$ GxG diagonal group diffusion coefficient matrix.

$\mathbb{M}(\underline{r})$ GxG diagonal group removal cross section matrix.

$\mathbb{T}(\underline{r})$ GxG group scattering out cross section matrix.

$\mathbb{F}(\underline{r})$ GxG group fission-production cross section matrix.

$\mathbb{A}(\underline{r})$ GxG group removal, scattering, and production matrix.

k One-dimensional spatial index which runs from the left-most first region to the right-most K-th region, as k = 1 to K.

i,j Two-dimensional spatial indices. For horizontal direction, i runs from the left-most first region to the right-most I-th region as i = 1 to I and for vertical direction, j runs from the top first region to the bottom J-th region as j = 1 to J.

$\underline{i},\underline{j}$ Unit vectors in the X and Y directions in a 2-D problem.

z The one-dimensional axis variable divided into K regions such that each region k is bounded by nodes z_k and z_{k+1}.

X, Y The two-dimensional axis variables divided into I and J intervals, respectively, such that each region (i,j) is bounded by lines $X = X_i$, $X = X_{i+1}$, $Y = Y_j$, and $Y = Y_{j+1}$.

x A dimensionless variable defined in each region k as $x = (z-z_k)/(z_{k+1}-z_k)$, such that $0 \leq x \leq 1$ as $z_k \leq z \leq z_{k+1}$. It is also used as the dimensionless

variable in X-direction in a 2-D problem.

y — A dimensionless variable in Y-direction in a 2-D problem, defined in the same way as x.

$U(\underline{r}), U^*(\underline{r})$ — Scalar group flux and adjoint (or weighting) flux trial function (column vectors of length G).

$\underline{V}(\underline{r}), V^*(\underline{r})$ — Vector group current and adjoint (or weighting) current trial function (column vectors of length G).

$Q_{i,j}, Q_{i,j}^*$ — X-direction group current and adjoint current trial function (column vectors of length G in region (i,j)).

$R_{i,j}, R_{i,j}^*$ — Y-direction group current and adjoint current trial function (column vectors of length G in region (i,j)).

$\psi_k(z), \psi_k^*(z)$ — Detailed one-dimensional subassembly flux and weighting flux solutions in coarse mesh region k.

$\eta_k(z), \eta_k^*(z)$ — Detailed one-dimensional subassembly current and weighting current solutions in coarse mesh region k.

$\psi_{i,j}, \psi_{i,j}^*$ — Detailed two-dimensional subassembly flux and weighting flux solutions in coarse mesh region (i,j).

$\xi_{i,j}, \xi_{i,j}^*$ — Detailed two-dimensional subassembly X-direction current and weighting current solutions in coarse mesh region (i,j).

$\eta_{i,j}, \eta_{i,j}^*$ — Detailed two-dimensional subassembly Y-direction current and weighting current solutions in coarse mesh region (i,j).

A	Discretized matrix form of the GxG group diffusion, absorption, and scattering matrices.
B	Discretized matrix form of the GxG group fission-production matrix.
$\underline{P}$	The unknown approximate group flux solution vector which may contain group current unknowns.

APPENDIX B

INNER PRODUCTS FOR HERMITE BASIS FUNCTIONS

Nonvanishing inner products for the univariate basis functions $u_k^{p\pm}(x)$ for m = 1,2 (as defined by Eqs. 1.10 and 1.11) are listed below:

(i) m = 1

$$(u_k^{0-}, u_{k-1}^{0+}) = \frac{1}{6} \qquad (u_k^{0-}, u_k^{0-}) = \frac{1}{3}$$

$$(u_k^{0+}, u_k^{0+}) = \frac{1}{3} \qquad (u_k^{0+}, u_{k+1}^{0-}) = \frac{1}{6}$$

$$(\frac{d}{dx}u_k^{0-}, u_{k-1}^{0+}) = -\frac{1}{2} \qquad (\frac{d}{dx}u_k^{0-}, u_k^{0-}) = -\frac{1}{2}$$

$$(\frac{d}{dx}u_k^{0+}, u_k^{0+}) = \frac{1}{2} \qquad (\frac{d}{dx}u_k^{0+}, u_{k+1}^{0-}) = \frac{1}{2}$$

$$(\frac{d}{dx}u_k^{0-}, \frac{d}{dx}u_{k-1}^{0+}) = -1 \qquad (\frac{d}{dx}u_k^{0-}, \frac{d}{dx}u_k^{0-}) = 1$$

$$(\frac{d}{dx}u_k^{0+}, \frac{d}{dx}u_k^{0+}) = 1 \qquad (\frac{d}{dx}u_k^{0+}, \frac{d}{dx}u_{k+1}^{0-}) = -1$$

(ii) m = 2

$$(u_k^{0-}, u_{k-1}^{0+}) = \frac{9}{70} \qquad (u_k^{0-}, u_{k-1}^{1+}) = \frac{13}{420}$$

$$(u_k^{0-}, u_k^{0-}) = \frac{13}{35} \qquad (u_k^{0-}, u_k^{1-}) = -\frac{11}{210}$$

$$(u_k^{0+}, u_k^{0+}) = \frac{13}{35} \qquad (u_k^{0+}, u_k^{1+}) = \frac{11}{210}$$

$$(u_k^{0+}, u_{k+1}^{0-}) = \frac{9}{70} \qquad (u_k^{0+}, u_{k+1}^{1-}) = -\frac{13}{420}$$

$$(u_k^{1-}, u_{k-1}^{0+}) = -\frac{13}{420} \qquad (u_k^{1-}, u_{k-1}^{1+}) = -\frac{1}{140}$$

$$(u_k^{1-}, u_k^{0-}) = -\frac{11}{210} \qquad (u_k^{1-}, u_k^{1-}) = \frac{1}{105}$$

$$(u_k^{1+}, u_k^{0+}) = \frac{11}{210} \qquad (u_k^{1+}, u_k^{1+}) = \frac{1}{105}$$

$$(u_k^{1+}, u_{k+1}^{0-}) = \frac{13}{420} \qquad (u_k^{1+}, u_{k+1}^{1-}) = -\frac{1}{140}$$

$$(\frac{d}{dx} u_k^{0-}, u_{k-1}^{0+}) = \frac{1}{2} \qquad (\frac{d}{dx} u_k^{0-}, u_{k-1}^{1+}) = \frac{1}{10}$$

$$(\frac{d}{dx} u_k^{0-}, u_k^{0-}) = \frac{1}{2} \qquad (\frac{d}{dx} u_k^{0-}, u_k^{1-}) = -\frac{1}{10}$$

$$(\frac{d}{dx} u_k^{0+}, u_k^{0+}) = -\frac{1}{2} \qquad (\frac{d}{dx} u_k^{0+}, u_k^{1+}) = -\frac{1}{10}$$

$$(\frac{d}{dx} u_k^{0+}, u_{k+1}^{0-}) = -\frac{1}{2} \qquad (\frac{d}{dx} u_k^{0+}, u_{k+1}^{1-}) = \frac{1}{10}$$

$$(\frac{d}{dx} u_k^{1-}, u_{k-1}^{0+}) = -\frac{1}{10} \qquad (\frac{d}{dx} u_k^{1-}, u_{k-1}^{1+}) = -\frac{1}{60}$$

$$(\frac{d}{dx} u_k^{1-}, u_k^{0-}) = \frac{1}{10} \qquad (\frac{d}{dx} u_k^{1-}, u_k^{1-}) = 0$$

$$\left(\frac{d}{dx} u_k^{1+}, u_k^{0+}\right) = \frac{1}{10} \qquad \left(\frac{d}{dx} u_k^{1+}, u_k^{1+}\right) = 0$$

$$\left(\frac{d}{dx} u_k^{1+}, u_{k+1}^{0-}\right) = -\frac{1}{10} \qquad \left(\frac{d}{dx} u_k^{1+}, u_{k+1}^{1-}\right) = \frac{1}{60}$$

$$\left(\frac{d}{dx} u_k^{0-}, \frac{d}{dx} u_{k-1}^{0+}\right) = -\frac{6}{5} \qquad \left(\frac{d}{dx} u_k^{0-}, \frac{d}{dx} u_{k-1}^{1+}\right) = -\frac{1}{10}$$

$$\left(\frac{d}{dx} u_k^{0-}, \frac{d}{dx} u_k^{0-}\right) = \frac{6}{5} \qquad \left(\frac{d}{dx} u_k^{0-}, \frac{d}{dx} u_k^{1-}\right) = -\frac{1}{10}$$

$$\left(\frac{d}{dx} u_k^{0+}, \frac{d}{dx} u_k^{0+}\right) = \frac{6}{5} \qquad \left(\frac{d}{dx} u_k^{0+}, \frac{d}{dx} u_k^{1+}\right) = \frac{1}{10}$$

$$\left(\frac{d}{dx} u_k^{0+}, \frac{d}{dx} u_{k+1}^{0-}\right) = -\frac{6}{5} \qquad \left(\frac{d}{dx} u_k^{0+}, \frac{d}{dx} u_{k+1}^{1-}\right) = \frac{1}{10}$$

$$\left(\frac{d}{dx} u_k^{1-}, \frac{d}{dx} u_{k-1}^{0+}\right) = \frac{1}{10} \qquad \left(\frac{d}{dx} u_k^{1-}, \frac{d}{dx} u_{k-1}^{1+}\right) = -\frac{1}{30}$$

$$\left(\frac{d}{dx} u_k^{1-}, \frac{d}{dx} u_k^{0-}\right) = -\frac{1}{10} \qquad \left(\frac{d}{dx} u_k^{1-}, \frac{d}{dx} u_k^{1-}\right) = \frac{2}{15}$$

$$\left(\frac{d}{dx} u_k^{1+}, \frac{d}{dx} u_k^{0+}\right) = \frac{1}{10} \qquad \left(\frac{d}{dx} u_k^{1+}, \frac{d}{dx} u_k^{1+}\right) = \frac{2}{15}$$

$$\left(\frac{d}{dx} u_k^{1+}, \frac{d}{dx} u_{k+1}^{0-}\right) = -\frac{1}{10} \qquad \left(\frac{d}{dx} u_k^{1+}, \frac{d}{dx} u_{k+1}^{1-}\right) = -\frac{1}{30}$$

The inner products for multivariate basis functions can be determined using the univariate inner products.

APPENDIX C

DIFFERENCE EQUATION COEFFICIENTS RESULTING FROM USE OF THE FINITE ELEMENT APPROXIMATION METHODS IN CHAPTER 2

The GxG matrix coefficients resulting from the linear finite element approximation and the cubic Hermite finite element approximation in multigroup diffusion theory are defined below in various sections. The coefficients are given in terms of assumed homogeneous regional nuclear constants through the use of the GxG group matrices $\mathbb{D}_k$ and $\mathbb{A}_k$. Since $\mathbb{A}_k = \mathbb{M}_k - \mathbb{T}_k - \frac{1}{\lambda}\mathbb{F}_k$, these coefficients are of the form $A - \frac{1}{\lambda} B$. Various inner products of the finite element basis functions used to facilitate the calculation are listed in Appendix B.

C.1 Coefficients of the Linear Finite Element Method Equations

(as defined by Eqs. 2.20)

Interior Coefficients; k = 2 to K:

$$a_k = \frac{1}{6}\,\mathbb{A}_{k-1}\,h_{k-1} - \mathbb{D}_{k-1}/h_{k-1}$$

$$b_k = \frac{1}{3}\,(\mathbb{A}_{k-1}\,h_{k-1} + \mathbb{A}_k h_k) + (\mathbb{D}_{k-1}/h_{k-1} + \mathbb{D}_k/h_k)$$

$$c_k = \frac{1}{6}\,\mathbb{A}_k\,h_k - \mathbb{D}_k/h_k$$

Symmetry Boundary Condition Coefficients:

$$b_1 = \frac{1}{3}\,\mathbb{A}_1\,h_1 + \mathbb{D}_1/h_1$$

$$c_1 = \frac{1}{6}\,\mathbb{\Lambda}_1 h_1 - \mathbb{D}_1/h_1 = c_k \quad (k=1)$$

$$a_{K+1} = \frac{1}{6}\,\mathbb{\Lambda}_K h_K - \mathbb{D}_K/h_K = a_k \quad (k = K+1)$$

$$b_{K+1} = \frac{1}{3}\,\mathbb{\Lambda}_K h_K + \mathbb{D}_K/h_K$$

C.2 Coefficients of the Cubic Hermite Finite Element Method Equations

(as defined by Eq. 2.38)

Interior Coefficients; k = 2 to K:

$$a1_k = \frac{9}{70}\,\mathbb{\Lambda}_{k-1}\,h_{k-1} - \frac{6}{5}\,\mathbb{D}_{k-1}/h_{k-1}$$

$$a2_k = -\frac{13}{420}\,\mathbb{\Lambda}_{k-1}\,h_{k-1}^2\,\mathbb{D}_{k-1}^{-1} + \frac{1}{10}$$

$$b1_k = \frac{13}{35}(\,\mathbb{\Lambda}_{k-1}h_{k-1} + \mathbb{\Lambda}_k\,h_k\,) + \frac{6}{5}(\,\mathbb{D}_{k-1}/h_{k-1} + \mathbb{D}_k/h_k)$$

$$b2_k = \frac{11}{210}\,(\,\mathbb{\Lambda}_{k-1}h_{k-1}^2\,\mathbb{D}_{k-1}^{-1} - \mathbb{\Lambda}_k h_k^2\,\mathbb{D}_k^{-1})$$

$$c1_k = \frac{9}{70}\,\mathbb{\Lambda}_k h_k - \frac{6}{5}\,\mathbb{D}_k/h_k$$

$$c2_k = \frac{13}{420}\,\mathbb{\Lambda}_k h_k^2\,\mathbb{D}_k^{-1} - \frac{1}{10}$$

$$a3_k = \frac{13}{420}\,\mathbb{D}_{k-1}^{-1}\,h_{k-1}^2\,\mathbb{\Lambda}_{k-1} - \frac{1}{10}$$

$$a4_k = -\frac{1}{140}\mathbb{D}_{k-1}^{-1} h_{k-1}^3 \mathbb{\Lambda}_{k-1}\mathbb{D}_{k-1}^{-1} - \frac{1}{30} h_{k-1}\mathbb{D}_{k-1}^{-1}$$

$$b3_k = \frac{11}{210}\left(\mathbb{D}_{k-1}^{-1} h_{k-1}^2 \mathbb{\Lambda}_{k-1} - \mathbb{D}_k^{-1} h_k^2 \mathbb{\Lambda}_k\right)$$

$$b4_k = \frac{1}{105}\left(\mathbb{D}_{k-1}^{-1} h_{k-1}^3 \mathbb{\Lambda}_{k-1}\mathbb{D}_{k-1}^{-1} + \mathbb{D}_k^{-1} h_k^3 \mathbb{\Lambda}_k \mathbb{D}_k^{-1}\right) + \frac{2}{15}\left(h_{k-1}\mathbb{D}_{k-1}^{-1} + h_k\mathbb{D}_k^{-1}\right)$$

$$c3_k = -\frac{13}{420}\mathbb{D}_k^{-1} h_k^2 \mathbb{\Lambda}_k + \frac{1}{10}$$

$$c4_k = -\frac{1}{140}\mathbb{D}_k^{-1} h_k^3 \mathbb{\Lambda}_k \mathbb{D}_k^{-1} - \frac{1}{30} h_k \mathbb{D}_k^{-1}$$

Zero Flux Boundary Condition Coefficients:

$$b4_1 = \frac{1}{105}\mathbb{D}_1^{-1} h_1^3 \mathbb{\Lambda}_1 \mathbb{D}_1^{-1} + \frac{2}{15} h_1 \mathbb{D}_1^{-1}$$

$$c3_1 = -\frac{13}{420}\mathbb{D}_1^{-1} h_1^2 \mathbb{\Lambda}_1 + \frac{1}{10} = c3_k \quad (k = 1)$$

$$c4_1 = -\frac{1}{140}\mathbb{D}_1^{-1} h_1^3 \mathbb{\Lambda}_1 \mathbb{D}_1 - \frac{1}{30} h_1 \mathbb{D}_1^{-1} = c4_k \quad (k = 1)$$

$$a3_{K+1} = \frac{13}{420}\mathbb{D}_K^{-1} h_K^2 \mathbb{\Lambda}_K - \frac{1}{10} = a3_k \quad (k = K+1)$$

$$a4_{K+1} = -\frac{1}{140}\mathbb{D}_K^{-1} h_K^3 \mathbb{\Lambda}_K \mathbb{D}_K^{-1} - \frac{1}{30} h_K \mathbb{D}_K^{-1} = a4_k \quad (k = K+1)$$

$$b4_{K+1} = \frac{1}{105}\mathbb{D}_K^{-1} h_K^3 \mathbb{\Lambda}_K \mathbb{D}_K^{-1} + \frac{2}{15} h_K \mathbb{D}_K^{-1}$$

Symmetry Boundary Condition Coefficients:

$$b1_1 = \frac{13}{35} \mathbb{\Lambda}_1 \, h_1 + \frac{6}{5} \mathbb{D}_1 / h_1$$

$$c1_1 = \frac{9}{70} \mathbb{\Lambda}_1 \, h_1 = \frac{6}{5} \mathbb{D}_1 / h_1 = c1_k \quad (k = 1)$$

$$c2_1 = \frac{13}{420} \mathbb{\Lambda}_1 \, h_1^2 \, \mathbb{D}_1^{-1} - \frac{1}{10} = c2_k \quad (k = 1)$$

$$a1_{K+1} = \frac{9}{70} \mathbb{\Lambda}_K \, h_K - \frac{6}{5} \mathbb{D}_K / h_K = a1_k \quad (k = K+1)$$

$$a2_{K+1} = - \frac{13}{420} \mathbb{\Lambda}_K \, h_K^2 \, \mathbb{D}_K^{-1} + \frac{1}{10} = a2_k \quad (k = K+1)$$

$$b1_{K+1} = \frac{13}{35} \mathbb{\Lambda}_K \, h_K + \frac{6}{5} \mathbb{D}_K / h_K$$

APPENDIX D

DIFFERENCE EQUATIONS RESULTING FROM USE OF CUBIC FINITE ELEMENT APPROXIMATIONS WITH DISCONTINUOUS FICK'S LAW CURRENT TRIAL FUNCTIONS

The difference equations resulting from the cubic (and bi-cubic) finite element approximations with discontinuous Fick's Law current trial functions in 1-D and 2-D are given below. The nuclear constants are assumed to be homogeneous in each region.

D.1 Difference Equations in 1-D (derived from Eq. 3.3)

For simplicity we define

$$d[a,b]_k \equiv dah_k \Sigma_k + db\, D_k/h_k$$

and

$$d[a,b]_{(k,k')} \equiv d[a,b]_k + d[a,b]_{k'},$$

and with the understanding that all nuclear constants outside the reactor region should be set equal to zero, we have

(i) From taking arbitrary variations in all P_k^*, k=1 to K+1:

$$\frac{3}{5}\left[\frac{3}{14}, -2\right]_{k-1} P_{k-1} + \frac{1}{10}\left[\frac{13}{42}, -1\right]_{k-1} Q_{k-1,+}$$

$$+ \frac{1}{5}\left[\frac{13}{7}, 6\right]_{(k-1,k)} P_k + \frac{1}{10}\left[\frac{11}{21}, 1\right]_k Q_{k,+}$$

$$- \frac{1}{10}\left[\frac{11}{21}, 1\right]_{k-1} Q_{k,-} + \frac{3}{5}\left[\frac{3}{14}, -2\right]_k P_{k+1}$$

$$- \frac{1}{10}\left[\frac{13}{42}, -1\right]_k Q_{k+1,-} = 0 \quad ; \qquad k = 1 \text{ to } K+1 \qquad \text{(D1.1)}$$

(ii) From taking arbitrary variations in all $Q^*_{k,+}$, k = 1 to K:

$$\frac{1}{10}\left[\frac{11}{21}, 1\right]_k P_k + \frac{1}{15}\left[\frac{1}{7}, 2\right]_k Q_{k,+} + \frac{1}{10}\left[\frac{13}{42}, -1\right]_k P_{k+1}$$

$$- \frac{1}{30}\left[\frac{3}{14}, 1\right]_k Q_{k+1,-} = 0 \quad ; \quad k = 1 \text{ to } K \qquad \text{(D1.2)}$$

(iii) From taking arbitrary variations in all $Q^*_{k,-}$, k = 2 to K+1:

$$-\frac{1}{10}\left[\frac{13}{42}, -1\right]_{k-1} P_{k-1} - \frac{1}{30}\left[\frac{3}{14}, 1\right]_{k-1} Q_{k-1,+} - \frac{1}{10}\left[\frac{11}{21}, 1\right]_{k-1} P_k$$

$$+ \frac{1}{15}\left[\frac{1}{7}, 2\right]_{k-1} Q_{k,-} = 0 \quad ; \quad k = 2 \text{ to } K + 1 \qquad \text{(D1.3)}$$

(iv) Zero flux boundary conditions:

Eliminate k = 1 and k = K + 1 equations from Eqs. D1.1 and set $P_1 = P_{K+1} = 0$.

(v) Zero current boundary conditions:

Eliminate k = 1 from Eq. D1.2 and k = K + 1 from Eq. D1.3 and set $Q_{1,+} = Q_{K+1,-} = 0$

D.2 Difference Equations in 2-D (derived from Eq. 3.8)

For simplicity we define

$$d[a,b,c]_{i,j} \equiv dah_{xi}h_{yj}\Lambda_{i,j} + db\frac{h_{yj}}{h_{xi}}D_{i,j} + dc\frac{h_{xi}}{h_{yj}}D_{i,j}$$

$$d[a,b,c]_{(i,j+i',j')} \equiv d[a,b,c]_{i,j} + d[a,b,c]_{i',j'}$$

With the understanding that all nuclear constants outside the reactor region should be set equal to zero, we have

(i) From taking arbitrary variation in all $P^{(0,0)*}_{i,j}$, i=1 to I+1, j=1 to J+1:

$$\frac{27}{175}\left[\frac{3}{28},-1,-1\right]_{i-1,j-1} P^{(0,0)}_{i-1,j-1}$$

$$+ \frac{1}{350}\left[\frac{39}{28}, -\frac{9}{2}, -13\right]_{i-1,j-1} P^{(1,0)}_{i-1,j-1} \quad (+)$$

$$+ \frac{1}{350}\left[\frac{39}{28}, -13, -\frac{9}{2}\right]_{i-1,j-1} P^{(0,1)}_{i-1,j-1} \quad (+)$$

$$+ \frac{13}{4200}\left[\frac{13}{42},-1,-1\right]_{i-1,j-1} P^{(1,1)}_{i-1,j-1} \quad (1)$$

$$+ \frac{3}{175}\left[\frac{39}{14},9,-26\right]_{(i-1,j-1+i,j-1)} P^{(0,0)}_{i,j-1}$$

$$+ \frac{1}{175}\left[\frac{33}{28}, \frac{9}{4}, -11\right]_{i,j-1} P^{(1,0)}_{i,j-1} \quad (+)$$

$$- \frac{1}{175}\left[\frac{33}{28}, \frac{9}{4}, -11\right]_{i-1,j-1} P^{(1,0)}_{i,j-1} \quad (-)$$

$$+ \frac{13}{350}\left[\frac{13}{42},1,-1\right]_{(i-1,j-1+i,j-1)} P_{i,j-1}^{(0,1)} \quad (+)$$

$$+ \frac{1}{2100}\left[\frac{143}{42}, \frac{13}{2}, -11\right]_{i,j-1} P_{i,j-1}^{(1,1)} \quad (1)$$

$$- \frac{1}{2100}\left[\frac{143}{42}, \frac{13}{2}, -11\right]_{i-1,j-1} P_{i,j-1}^{(1,1)} \quad (2)$$

$$+ \frac{27}{175}\left[\frac{3}{28},-1,-1\right]_{i,j-1} P_{i+1,j-1}^{(0,0)}$$

$$- \frac{1}{350}\left[\frac{39}{28}, \frac{9}{2}, -13\right]_{i,j-1} P_{i+1,j-1}^{(1,0)} \quad (-)$$

$$+ \frac{1}{350}\left[\frac{39}{28},-13,-\frac{9}{2}\right]_{i,j-1} P_{i+1,j-1}^{(0,1)} \quad (+)$$

$$- \frac{13}{4200}\left[\frac{13}{42}, -1,-1\right]_{i,j-1} P_{i+1,j-1}^{(1,1)} \quad (2)$$

$$+ \frac{3}{175}\left[\frac{39}{14},-26,9\right]_{(i-1,j-1+i-1,j)} P_{i-1,j}^{(0,0)}$$

$$+ \frac{13}{350}\left[\frac{13}{42},-1,1\right]_{(i-1,j-1+j-1,j)} P_{i-1,j}^{(1,0)} \quad (+)$$

$$+ \frac{1}{175}\left[\frac{33}{28},-11,\frac{9}{4}\right]_{i-1,j} P_{i-1,j}^{(0,1)} \quad (+)$$

$$- \frac{1}{175}\left[\frac{33}{28},-11,\frac{9}{4}\right]_{i-1,j-1} P_{i-1,j}^{(0,1)} \quad (-)$$

$$+ \frac{1}{2100}\left[\frac{143}{42},-11,\frac{13}{2}\right]_{i-1,j} P_{i-1,j}^{(1,1)} \quad (1)$$

$$- \frac{1}{2100}\left[\frac{143}{42}, -11, \frac{13}{2}\right]_{i-1,j} P^{(1,1)}_{i-1,j} \quad (4)$$

$$+ \frac{78}{175}\left[\frac{13}{42}, 1, \right]_{(i-1,j-1+i,j-1+i-1,j+i,j)} P^{(0,0)}_{i,j}$$

$$+ \frac{1}{175}\left[\frac{143}{42}, \frac{13}{2}, 11\right]_{(i,j-1+i,j)} P^{(1,0)}_{i,j} \quad (+)$$

$$- \frac{1}{175}\left[\frac{143}{42}, \frac{13}{2}, 11\right]_{(i-1,j-1+i-1,j)} P^{(1,0)}_{i,j} \quad (-)$$

$$+ \frac{1}{175}\left[\frac{143}{42}, 11, \frac{13}{2}\right]_{(i-1,j+i,j)} P^{(0,1)}_{i,j} \quad (+)$$

$$- \frac{1}{175}\left[\frac{143}{42}, 11, \frac{13}{2}\right]_{(i-1,j-1+i,j-1)} P^{(0,1)}_{i,j} \quad (-)$$

$$+ \frac{11}{2100}\left[\frac{11}{21}, 1, 1\right]_{i,j} P^{(1,1)}_{i,j} \quad (1)$$

$$- \frac{11}{2100}\left[\frac{11}{21}, 1, 1\right]_{i-1,j} P^{(1,1)}_{i,j} \quad (2)$$

$$+ \frac{11}{2100}\left[\frac{11}{21}, 1, 1\right]_{i-1,j-1} P^{(1,1)}_{i,j} \quad (3)$$

$$- \frac{11}{2100}\left[\frac{11}{21}, 1, 1\right]_{i,j-1} P^{(1,1)}_{i,j} \quad (4)$$

$$+ \frac{3}{175}\left[\frac{39}{14}, -26, 9\right]_{(i,j-1+i,j)} P^{(0,0)}_{i+1,j}$$

$$- \frac{13}{350}\left[\frac{13}{42}, -1, 1\right]_{(i,j-1+i,j)} P_{i,j}^{(1,0)} (-)$$

$$+ \frac{1}{175}\left[\frac{33}{28}, -11, \frac{9}{4}\right]_{i,j} P_{i+1,j}^{(0,1)} (+)$$

$$- \frac{1}{175}\left[\frac{33}{28}, -11, \frac{9}{4}\right]_{i,j-1} P_{i+1,j}^{(0,1)} (-)$$

$$- \frac{1}{2100}\left[\frac{143}{42}, -11, \frac{13}{2}\right]_{i,j} P_{i+1,j}^{(1,1)} (2)$$

$$+ \frac{1}{2100}\left[\frac{143}{42}, -11, \frac{13}{2}\right]_{i,j-1} P_{i+1,j}^{(1,1)} (3)$$

$$+ \frac{27}{175}\left[\frac{3}{28}, -1, -1\right]_{i-1,j} P_{i-1,j+1}^{(0,0)}$$

$$+ \frac{1}{350}\left[\frac{39}{28}, -\frac{9}{2}, -13\right]_{i-1,j} P_{i-1,j+1}^{(1,0)} (+)$$

$$- \frac{1}{350}\left[\frac{39}{28}, -13, -\frac{9}{2}\right]_{i-1,j} P_{i-1,j+1}^{(0,1)} (-)$$

$$- \frac{13}{4200}\left[\frac{13}{42}, -1, -1\right]_{i-1,j} P_{i-1,j+1}^{(1,1)} (4)$$

$$+ \frac{3}{175}\left[\frac{39}{14}, 9, -26\right]_{(i-1,j+i,j)} P_{i,j+1}^{(0,0)}$$

$$+ \frac{1}{175}\left[\frac{33}{28}, \frac{9}{4}, -11\right]_{i,j} P_{i,j+1}^{(1,0)} (+)$$

$$- \frac{1}{175}\left[\frac{33}{28}, \frac{9}{4}, -11\right]_{i-1,j} P_{i,j+1}^{(1,0)} (-)$$

$$-\frac{13}{350}[\frac{13}{42},\ 1,\ -1]_{(i-1,j+i,j)}\ P^{(0,1)}_{i,j+1}\ (-)$$

$$+\frac{1}{2100}[\frac{143}{42},\ \frac{13}{2},\ -11]_{i-1,j}\ P^{(1,1)}_{i,j+1}\ (3)$$

$$-\frac{1}{2100}[\frac{143}{42},\ \frac{13}{2},\ -11]_{i,j}\ P^{(1,1)}_{i,j+1}\ (4)$$

$$+\frac{27}{175}[\frac{3}{28},\ -1,\ -1]_{i,j}\ P^{(0,0)}_{i+1,j+1}$$

$$-\frac{1}{350}[\frac{39}{28},\ -\frac{9}{2},\ -13]_{i,j}\ P^{(1,0)}_{i+1,j+1}\ (-)$$

$$-\frac{1}{350}[\frac{39}{28},\ -13,\ -\frac{9}{2}]_{i,j}\ P^{(0,1)}_{i+1,j+1}\ (-)$$

$$+\frac{13}{4200}[\frac{13}{42},\ -1,\ -1]_{i,j}\ P^{(1,1)}_{i+1,j+1}(3)\ =\ 0$$

$$i = 1 \text{ to } I + 1,\ j = 1 \text{ to } J + 1 \qquad \text{(D2.1)}$$

(ii) From taking arbitrary variations in all $P^{(1,0)*}_{i,j}$ (+), $i = 1$ to I, $j = 1$ to $J + 1$:

$$\frac{1}{175}[\frac{33}{28},\ \frac{9}{4},\ -11]_{i,j-1}\ P^{(0,0)}_{i,j-1}$$

$$+\frac{1}{175}[\frac{3}{14},\ 3,\ -2]_{i,j-1}\ P^{(1,0)}_{i,j-1}\ (+)$$

$$+ \frac{1}{2100}\left[\frac{143}{42}, \frac{13}{2}, -11\right]_{i,j-1} P^{(0,1)}_{i,j-1} \quad (+)$$

$$+ \frac{1}{1050}\left[\frac{13}{42}, \frac{13}{3}, -1\right]_{i,j-1} P^{(1,1)}_{i,j-1} \quad (1)$$

$$+ \frac{1}{350}\left[\frac{39}{28}, -\frac{9}{2}, -13\right]_{i,j-1} P^{(0,0)}_{i+1,j-1}$$

$$- \frac{3}{350}\left[\frac{3}{28}, \frac{1}{2}, -1\right]_{i,j-1} P^{(1,0)}_{i+1,j-1} \quad (-)$$

$$+ \frac{13}{4200}\left[\frac{13}{42}, -1, -1\right]_{i,j-1} P^{(0,1)}_{i+1,j-1} \quad (+)$$

$$- \frac{1}{1400}\left[\frac{13}{42}, \frac{13}{9}, -1\right]_{i,j-1} P^{(1,1)}_{i+1,j-1} \quad (2)$$

$$+ \frac{1}{175}\left[\frac{143}{42}, \frac{13}{2}, 11\right]_{(i,j-1+i,j)} P^{(0,0)}_{i,j}$$

$$+ \frac{2}{525}\left[\frac{13}{14}, 13, 3\right]_{(i,j-1+i,j)} P^{(1,0)}_{i,j} \quad (+)$$

$$+ \frac{11}{2100}\left[\frac{11}{21}, 1, 1\right]_{i,j} P^{(0,1)}_{i,j} \quad (+)$$

$$- \frac{11}{2100}\left[\frac{11}{21}, 1, 1\right]_{i,j-1} P^{(0,1)}_{i,j} \quad (-)$$

$$+ \frac{1}{1050}\left[\frac{11}{21}, \frac{22}{3}, 1\right]_{i,j} P^{(1,1)}_{i,j} \quad (1)$$

$$- \frac{1}{1050}\left[\frac{11}{21}, \frac{22}{3}, 1\right]_{i,j-1} P^{(1,1)}_{i,j} \quad (4)$$

$$+\frac{13}{350}\left[\frac{13}{42},\ -1,1\right]_{(i,j-1+i,j)}\ P^{(0,0)}_{i+1,j}$$

$$-\frac{3}{350}\left[\frac{13}{42},\ \frac{13}{9},\ 1\right]_{(i,j-1+i,j)}\ P^{(1,0)}_{i+1,j}\quad (-)$$

$$+\frac{1}{2100}\left[\frac{143}{42},\ -11,\ \frac{13}{2}\right]_{i,j}\ P^{(0,1)}_{i+1,j}\quad (+)$$

$$-\frac{1}{2100}\left[\frac{143}{42},\ -11,\ \frac{13}{2}\right]_{i,j-1}\ P^{(0,1)}_{i+1,j}\quad (-)$$

$$-\frac{1}{1400}\left[\frac{11}{21},\ \frac{22}{9},\ 1\right]_{i,j}\ P^{(1,1)}_{i+1,j}\quad (2)$$

$$+\frac{1}{1400}\left[\frac{11}{21},\ \frac{22}{9},\ 1\right]_{i,j-1}\ P^{(1,1)}_{i+1,j}\quad (3)$$

$$+\frac{1}{175}\left[\frac{33}{28},\ \frac{9}{4},\ -11\right]_{i,j}P^{(0,0)}_{i,j+1}$$

$$+\frac{1}{175}\left[\frac{3}{14},\ 3,\ -2\right]_{i,j}\ P^{(1,0)}_{i,j+1}\quad (+)$$

$$-\frac{1}{2100}\left[\frac{143}{42},\ \frac{13}{2},\ -11\right]_{i,j}\ P^{(0,1)}_{i,j+1}\quad (-)$$

$$-\frac{1}{1050}\left[\frac{13}{42},\ \frac{13}{3},\ -1\right]_{i,j}\ P^{(1,1)}_{i,j+1}\quad (4)$$

$$+\frac{1}{350}\left[\frac{39}{28},\ -\frac{9}{2},\ -13\right]_{i,j}\ P^{(0,0)}_{i+1,j+1}$$

$$-\frac{3}{350}\left[\frac{3}{28},\ \frac{1}{2},\ -1\right]_{i,j}\ P^{(1,0)}_{i+1,j+1}\quad (-)$$

$$- \frac{13}{4200}\left[\frac{13}{42}, -1, -1\right]_{i,j} P^{(0,1)}_{i+1,j+1} \quad (-)$$

$$+ \frac{1}{1400}\left[\frac{13}{42}, \frac{13}{9}, -1\right]_{i,j} P^{(1,1)}_{i+1,j+1} \quad (3) \quad = \quad 0$$

$$i = 1 \text{ to } I, \; j = 1 \text{ to } J + 1 \qquad \text{(D2.2)}$$

(iii) From taking arbitrary variations in all $P^{(1,0)*}_{i,j}(-)$,

$i = 2$ to $I + 1$, $j = 1$ to $J + 1$:

$$- \frac{1}{350}\left[\frac{39}{28}, -\frac{9}{2}, -13\right]_{i-1,j-1} P^{(0,0)}_{i-1,j-1}$$

$$- \frac{3}{350}\left[\frac{3}{28}, \frac{1}{2}, -1\right]_{i-1,j-1} P^{(1,0)}_{i-1,j-1} (+)$$

$$- \frac{13}{4200}\left[\frac{13}{42}, -1, -1\right]_{i-1,j-1} P^{(0,1)}_{i-1,j-1} \quad (+)$$

$$- \frac{1}{1400}\left[\frac{13}{42}, \frac{13}{9}, -1\right]_{i-1,j-1} P^{(1,1)}_{i-1,j-1} (1)$$

$$- \frac{1}{175}\left[\frac{33}{28}, \frac{9}{4}, -11\right]_{i-1,j-1} P^{(0,0)}_{i,j-1}$$

$$+ \frac{1}{175}\left[\frac{3}{14}, 3, -2\right]_{i-1,j-1} P^{(1,0)}_{i,j-1} \quad (-)$$

$$- \frac{1}{2100}\left[\frac{143}{42}, \frac{13}{2}, -11\right]_{i-1,j-1} P^{(0,1)}_{i,j-1} \quad (+)$$

$$+ \frac{1}{1050}\left[\frac{13}{42}, \frac{13}{3}, -1\right]_{i-1,j-1} P^{(1,1)}_{i,j-1} \quad (2)$$

$$- \frac{13}{350}\left[\frac{13}{42}, -1, +1\right]_{(i-1,j-1+i-1,j)} P^{(0,0)}_{i-1,j}$$

$$- \frac{3}{350}\left[\frac{13}{42}, \frac{13}{9}, 1\right]_{(i-1,j-1+i-1,j)} P^{(1,0)}_{i-1,j} \quad (+)$$

$$- \frac{1}{2100}\left[\frac{143}{42}, -11, \frac{13}{2}\right]_{i-1,j} P^{(0,1)}_{i-1,j} \quad (+)$$

$$+ \frac{1}{2100}\left[\frac{143}{42}, -11, \frac{13}{2}\right]_{i-1,j-1} P^{(0,1)}_{i-1,j} \quad (-)$$

$$- \frac{1}{1400}\left[\frac{11}{21}, \frac{22}{9}, 1\right]_{i-1,j} P^{(1,1)}_{i-1,j} \quad (1)$$

$$+ \frac{1}{1400}\left[\frac{11}{21}, \frac{22}{9}, 1\right]_{i-1,j-1} P^{(1,1)}_{i-1,j} \quad (4)$$

$$- \frac{1}{175}\left[\frac{143}{42}, \frac{13}{2}, 11\right]_{(i-1,j-1+i-1,j)} P^{(0,0)}_{i,j}$$

$$+ \frac{2}{525}\left[\frac{13}{14}, 13, 3\right]_{(i-1,j-1+i-1,j)} P^{(1,0)}_{i,j} \quad (-)$$

$$- \frac{11}{2100}\left[\frac{11}{21}, 1, 1\right]_{i-1,j} P^{(0,1)}_{i,j} \quad (+)$$

$$+ \frac{11}{2100}\left[\frac{11}{21}, 1, 1\right]_{i-1,j-1} P^{(0,1)}_{i,j} \quad (-)$$

$$+ \frac{1}{1050}\left[\frac{11}{21}, \frac{22}{3}, 1\right]_{i-1,j} P^{(1,1)}_{i,j} \quad (2)$$

$$- \frac{1}{1050}\left[\frac{11}{21}, \frac{22}{3}, 1\right]_{i-1,j-1} P^{(1,1)}_{i,j} \quad (3)$$

$$- \frac{1}{350}\left[\frac{39}{28}, -\frac{9}{2}, -13\right]_{i-1,j} P^{(0,0)}_{i-1,j+1}$$

$$- \frac{3}{350}\left[\frac{3}{28}, \frac{1}{2}, -1\right]_{i-1,j} P^{(1,0)}_{i-1,j+1}(+)$$

$$+ \frac{13}{4200}\left[\frac{13}{42}, -1, -1\right]_{i-1,j} P^{(0,1)}_{i-1,j+1}(-)$$

$$+ \frac{1}{1400}\left[\frac{13}{42}, \frac{13}{9}, -1\right]_{i-1,j} P^{(1,1)}_{i-1,j+1}(4)$$

$$- \frac{1}{175}\left[\frac{33}{28}, \frac{9}{4}, -11\right]_{i-1,j} P^{(0,0)}_{i,j+1}$$

$$+ \frac{1}{175}\left[\frac{3}{14}, 3, -2\right]_{i-1,j} P^{(1,0)}_{i,j+1}(-)$$

$$+ \frac{1}{2100}\left[\frac{143}{42}, \frac{13}{2}, -11\right]_{i-1,j} P^{(0,1)}_{i,j+1}(-)$$

$$- \frac{1}{1050}\left[\frac{13}{42}, \frac{13}{3}, -1\right]_{i-1,j} P^{(1,1)}_{i,j+1}(3) = 0$$

$$i = 2 \text{ to } I+1,\ j = 1 \text{ to } J+1 \qquad \text{(D2.3)}$$

(iv) From taking arbitrary variations in all $P^{(0,1)*}_{i,j}(+)$, $i = 1$ to $I + 1$, $j = 1$ to J:

$$\frac{1}{175}\left[\frac{33}{28}, -11, \frac{9}{4}\right]_{i-1,j} P^{(0,0)}_{i-1,j}$$

$$+ \frac{1}{2100}\left[\frac{143}{42}, -11, \frac{13}{2}\right]_{i-1,j} P^{(1,0)}_{i-1,j}(+)$$

$$+ \frac{1}{175}\left[\frac{3}{14}, -2, 3\right]_{i-1,j} P^{(0,1)}_{i-1,j} \quad (+)$$

$$+ \frac{1}{1050}\left[\frac{13}{42}, -1, \frac{13}{3}\right]_{i-1,j} P^{(1,1)}_{i-1,j} \quad (1)$$

$$+ \frac{1}{175}\left[\frac{143}{42}, 11, \frac{13}{2}\right]_{(i-1,j+i,j)} P^{(0,0)}_{i,j}$$

$$+ \frac{11}{2100}\left[\frac{11}{21}, 1, 1\right]_{i,j} P^{(1,0)}_{i,j} \quad (+)$$

$$- \frac{11}{2100}\left[\frac{11}{21}, 1, 1\right]_{i-1,j} P^{(1,0)}_{i,j} (-)$$

$$+ \frac{2}{525}\left[\frac{13}{14}, 3, 13\right]_{(i-1,j+i,j)} P^{(0,1)}_{i,j} \quad (+)$$

$$+ \frac{1}{1050}\left[\frac{11}{21}, 1, \frac{22}{3}\right]_{i,j} P^{(1,1)}_{i,j} \quad (1)$$

$$- \frac{1}{1050}\left[\frac{11}{21}, 1, \frac{22}{3}\right]_{i-1,j} P^{(1,1)}_{i,j} \quad (2)$$

$$+ \frac{1}{175}\left[\frac{33}{28}, -11, \frac{9}{4}\right]_{i,j} P^{(0,0)}_{i+1,j}$$

$$- \frac{1}{2100}\left[\frac{143}{42}, -11, \frac{13}{2}\right]_{i,j} P^{(1,0)}_{i+1,j} \quad (-)$$

$$+ \frac{1}{175}\left[\frac{3}{14}, -2, 3\right]_{i,j} P^{(0,1)}_{i+1,j} \quad (+)$$

$$- \frac{1}{1050}\left[\frac{13}{42}, -1, \frac{13}{3}\right]_{i,j} P^{(1,1)}_{i+1,j} \quad (2)$$

$$+\frac{1}{350}\left[\frac{39}{28},\ -13,\ -\frac{9}{2}\right]_{i-1,j}\ P^{(0,0)}_{i-1,j+1}$$

$$+\frac{13}{4200}\left[\frac{13}{42},\ -1,\ -1\right]_{i-1,j}\ P^{(1,0)}_{i-1,j+1}\ (+)$$

$$-\frac{3}{350}\left[\frac{3}{28},\ -1,\ \frac{1}{2}\right]_{i-1,j}\ P^{(0,1)}_{i-1,j+1}\ (-)$$

$$-\frac{1}{1400}\left[\frac{13}{42},\ -1,\ \frac{13}{9}\right]_{i-1,j}\ P^{(1,1)}_{i-1,j+1}\ (4)$$

$$+\frac{13}{350}\left[\frac{13}{42},\ 1,\ -1\right]_{(i-1,j+i,j)}\ P^{(0,0)}_{i,j+1}$$

$$+\frac{1}{2100}\left[\frac{143}{42},\ \frac{13}{2},\ -11\right]_{i,j}\ P^{(1,0)}_{i,j+1}\ (+)$$

$$-\frac{1}{2100}\left[\frac{143}{42},\ \frac{13}{2},\ -11\right]_{i-1,j}\ P^{(1,0)}_{i,j+1}\ (-)$$

$$-\frac{3}{350}\left[\frac{13}{42},\ 1,\ \frac{13}{9}\right]_{(i-1,j+i,j)}\ P^{(0,1)}_{i,j+1}\ (-)$$

$$+\frac{1}{1400}\left[\frac{11}{21},\ 1,\ \frac{22}{9}\right]_{i-1,j}\ P^{(1,1)}_{i,j+1}\ (3)$$

$$-\frac{1}{1400}\left[\frac{11}{21},\ 1,\ \frac{22}{9}\right]_{i,j}\ P^{(1,1)}_{i,j+1}\ (4)$$

$$+\frac{1}{350}\left[\frac{39}{28},\ -13,\ -\frac{9}{2}\right]_{i,j}\ P^{(0,0)}_{i+1,j+1}$$

$$-\frac{13}{4200}\left[\frac{13}{42},\ -1,\ -1\right]_{i,j}\ P^{(1,0)}_{i+1,j+1}\ (-)$$

$$- \frac{3}{350}\left[\frac{3}{28}, -1, \frac{1}{2}\right]_{i,j} P^{(0,1)}_{i+1,j+1} \quad (-)$$

$$+ \frac{1}{1400}\left[\frac{13}{42}, -1, \frac{13}{9}\right]_{i,j} P^{(1,1)}_{i+1,j+1} \quad (3) \quad = \quad 0$$

$$i = 1 \text{ to } I + 1, \; j = 1 \text{ to } J \qquad \text{(D2.4)}$$

(v) From taking arbitrary variations in all $P^{(0,1)*}_{i,j}(-)$,

$i = 1$ to $I + 1$, $j = 2$ to $J + 1$:

$$- \frac{1}{350}\left[\frac{39}{28}, -13, -\frac{9}{2}\right]_{i-1,j-1} P^{(0,0)}_{i-1,j-1}$$

$$- \frac{13}{4200}\left[\frac{13}{42}, -1, -1\right]_{i-1,j-1} P^{(1,0)}_{i-1,j-1} \quad (+)$$

$$- \frac{3}{350}\left[\frac{3}{28}, -1, \frac{1}{2}\right]_{i-1,j-1} P^{(0,1)}_{i-1,j-1} \quad (+)$$

$$- \frac{1}{1400}\left[\frac{13}{42}, -1, \frac{13}{9}\right]_{i-1,j-1} P^{(1,1)}_{i-1,j-1} (1)$$

$$- \frac{13}{350}\left[\frac{13}{42}, 1, -1\right]_{(i-1,j-1+i,j-1)} P^{(0,0)}_{i,j-1}$$

$$- \frac{1}{2100}\left[\frac{143}{42}, \frac{13}{2}, -11\right]_{i,j-1} P^{(1,0)}_{i,j-1} \quad (+)$$

$$+ \frac{1}{2100}\left[\frac{143}{42}, \frac{13}{2}, -11\right]_{i-1,j-1} P^{(1,0)}_{i,j-1} \quad (-)$$

$$- \frac{3}{350}\left[\frac{13}{42}, 1, \frac{13}{9}\right]_{(i-1,j-1+i,j-1)} P^{(0,1)}_{i,j-1} \quad (+)$$

$$- \frac{1}{1400}\left[\frac{11}{21}, 1, \frac{22}{9}\right]_{i,j-1} P^{(1,1)}_{i,j-1} \quad (1)$$

$$+ \frac{1}{1400}\left[\frac{11}{21}, 1, \frac{22}{9}\right]_{i-1,j-1} P^{(1,1)}_{i,j-1} \quad (2)$$

$$- \frac{1}{350}\left[\frac{39}{28}, -13, -\frac{9}{2}\right]_{i,j-1} P^{(0,0)}_{i+1,j-1}$$

$$+ \frac{13}{4200}\left[\frac{13}{42}, -1, -1\right]_{i,j-1} P^{(1,0)}_{i+1,j-1} (-)$$

$$- \frac{3}{350}\left[\frac{3}{28}, -1, \frac{1}{2}\right]_{i,j-1} P^{(0,1)}_{i+1,j-1} \quad (+)$$

$$+ \frac{1}{1400}\left[\frac{13}{42}, -1, \frac{13}{9}\right]_{i,j-1} P^{(1,1)}_{i+1,j-1} \quad (2)$$

$$- \frac{1}{175}\left[\frac{33}{28}, -11, \frac{9}{4}\right]_{i-1,j-1} P^{(0,0)}_{i-1,j}$$

$$- \frac{1}{2100}\left[\frac{143}{42}, -11, \frac{13}{2}\right]_{i-1,j-1} P^{(1,0)}_{i-1,j} \quad (+)$$

$$+ \frac{1}{175}\left[\frac{3}{14}, -2, 3\right]_{i-1,j-1} P^{(0,1)}_{i-1,j} \quad (-)$$

$$+ \frac{1}{1050}\left[\frac{13}{42}, -1, \frac{13}{3}\right]_{i-1,j-1} P^{(1,1)}_{i-1,j} \quad (4)$$

$$- \frac{1}{175}\left[\frac{143}{42}, 11, \frac{13}{2}\right]_{(i-1,j-1+i,j-1)} P^{(0,0)}_{i,j}$$

$$- \frac{11}{2100}\left[\frac{11}{21}, 1, 1\right]_{i,j-1} P^{(1,0)}_{i,j} \quad (+)$$

$$+ \frac{11}{2100}\left[\frac{11}{21},\ 1,\ 1\right]_{i-1,j-1} P^{(1,0)}_{i,j} \quad (-)$$

$$+ \frac{2}{525}\left[\frac{13}{14},\ 3,13\right]_{(i-1,j-1+i,j-1)} P^{(0,1)}_{i,j} \quad (-)$$

$$- \frac{1}{1050}\left[\frac{11}{21},\ 1,\ \frac{22}{3}\right]_{i-1,j-1} P^{(1,1)}_{i,j} \quad (3)$$

$$+ \frac{1}{1050}\left[\frac{11}{21},\ 1,\ \frac{22}{3}\right]_{i,j-1} P^{(1,1)}_{i,j} \quad (4)$$

$$- \frac{1}{175}\left[\frac{33}{28},\ -11,\ \frac{9}{4}\right]_{i,j-1} P^{(0,0)}_{i+1,j}$$

$$+ \frac{1}{2100}\left[\frac{143}{42},\ -11,\ \frac{13}{2}\right]_{i,j-1} P^{(1,0)}_{i+1,j} \quad (-)$$

$$+ \frac{1}{175}\left[\frac{3}{14},\ -2,\ 3\right]_{i,j-1} P^{(0,1)}_{i+1,j} \quad (-)$$

$$- \frac{1}{1050}\left[\frac{13}{42},\ -1,\ \frac{13}{3}\right]_{i,j-1} P^{(1,1)}_{i+1,j} \quad (3) \quad = \quad 0$$

$$i = 1 \text{ to } I + 1,\ j = 2 \text{ to } J + 1 \qquad \text{(D2.5)}$$

(vi) From taking arbitrary variations in all $P^{(1,1)*}_{i,j}(1)$

$i = 1$ to I, $j = 1$ to J:

$$\frac{11}{2100}\left[\frac{11}{21},\ 1,\ 1\right]_{i,j} P^{(0,0)}_{i,j}$$

$$+ \frac{1}{1050}\left[\frac{11}{21},\ \frac{22}{3},\ 1\right]_{i,j} P^{(1,0)}_{i,j} \quad (+)$$

$$+\frac{1}{1050}\left[\frac{11}{21},\ 1,\ \frac{22}{3}\right]_{i,j} P_{i,j}^{(0,1)} \quad (+)$$

$$+\frac{2}{1575}\left[\frac{1}{14},\ 1,\ 1\right]_{i,j} P_{i,j}^{(1,1)} \quad (1)$$

$$+\frac{1}{2100}\left[\frac{143}{42},\ -11,\ \frac{13}{2}\right]_{i,j} P_{i+1,j}^{(0,0)}$$

$$-\frac{1}{1400}\left[\frac{11}{21},\ \frac{22}{9},\ 1\right]_{i,j} P_{i+1,j}^{(1,0)} \quad (-)$$

$$+\frac{1}{1050}\left[\frac{13}{42},\ -1,\ \frac{13}{3}\right]_{i,j} P_{i+1,j}^{(0,1)} \quad (+)$$

$$-\frac{1}{1050}\left[\frac{1}{14},\ \frac{1}{3},\ 1\right]_{i,j} P_{i+1,j}^{(1,1)} \quad (2)$$

$$+\frac{1}{2100}\left[\frac{143}{42},\ \frac{13}{2},\ -11\right]_{i,j} P_{i,j+1}^{(0,0)}$$

$$+\frac{1}{1050}\left[\frac{13}{42},\ \frac{13}{3},\ -1\right]_{i,j} P_{i,j+1}^{(1,0)} \quad (+)$$

$$-\frac{1}{1400}\left[\frac{11}{21},\ 1,\ \frac{22}{9}\right]_{i,j} P_{i,j+1}^{(0,1)} \quad (-)$$

$$-\frac{1}{1050}\left[\frac{1}{14},\ 1,\ \frac{1}{3}\right]_{i,j} P_{i,j+1}^{(1,1)} \quad (4)$$

$$+\frac{13}{4200}\left[\frac{13}{42},\ -1,\ -1\right]_{i,j} P_{i+1,j+1}^{(0,0)}$$

$$-\frac{1}{1400}\left[\frac{13}{42},\ \frac{13}{9},\ -1\right]_{i,j} P_{i+1,j+1}^{(1,0)} \quad (-)$$

$$- \frac{1}{1400}\left[\frac{13}{42}, -1, \frac{13}{9}\right]_{i,j} P^{(0,1)}_{i+1,j+1}(-)$$

$$+ \frac{1}{4200}\left[\frac{3}{14}, 1, 1\right]_{i,j} P^{(1,1)}_{i+1,j+1}(3) = 0$$

$$i = 1 \text{ to } I,\ j = 1 \text{ to } J \qquad \text{(D2.6)}$$

(vii) From taking arbitrary variations in all $P^{(1,1)*}_{i,j}(2)$, $i = 2$ to $I + 1$, $j = 1$ to J:

$$- \frac{1}{2100}\left[\frac{143}{42}, -11, \frac{13}{2}\right]_{i-1,j} P^{(0,0)}_{i-1,j}$$

$$- \frac{1}{1400}\left[\frac{11}{21}, \frac{22}{9}, 1\right]_{i-1,j} P^{(1,0)}_{i-1,j}\ (+)$$

$$- \frac{1}{1050}\left[\frac{13}{42}, -1, \frac{13}{3}\right]_{i-1,j} P^{(0,1)}_{i-1,j}\ (+)$$

$$- \frac{1}{1050}\left[\frac{1}{14}, \frac{1}{3}, 1\right]_{i-1,j} P^{(1,1)}_{i-1,j}\ (1)$$

$$- \frac{11}{2100}\left[\frac{11}{21}, 1, 1\right]_{i-1,j} P^{(0,0)}_{i,j}$$

$$+ \frac{1}{1050}\left[\frac{11}{21}, \frac{22}{3}, 1\right]_{i-1,j} P^{(1,0)}_{i,j}\ (-)$$

$$- \frac{1}{1050}\left[\frac{11}{21}, 1, \frac{22}{3}\right]_{i-1,j} P^{(0,1)}_{i,j}\ (+)$$

$$+ \frac{2}{1575}\left[\frac{1}{14}, 1, 1\right]_{i-1,j} P^{(1,1)}_{i,j}(2)$$

$$- \frac{13}{4200}\left[\frac{13}{42}, -1, -1\right]_{i-1,j} P^{(0,0)}_{i-1,j+1}$$

$$- \frac{1}{1400}\left[\frac{13}{42}, \frac{13}{9}, -1\right]_{i-1,j} P^{(1,0)}_{i-1,j+1} \quad (+)$$

$$+ \frac{1}{1400}\left[\frac{13}{42}, -1, \frac{13}{9}\right]_{i-1,j} P^{(0,1)}_{i-1,j+1} \quad (-)$$

$$+ \frac{1}{4200}\left[\frac{3}{14}, 1, 1\right]_{i-1,j} P^{(1,1)}_{i-1,j+1} (4)$$

$$- \frac{1}{2100}\left[\frac{143}{42}, \frac{13}{2}, -11\right]_{i-1,j} P^{(0,0)}_{i,j+1}$$

$$+ \frac{1}{1050}\left[\frac{13}{42}, \frac{13}{3}, -1\right]_{i-1,j} P^{(1,0)}_{i,j+1} \quad (-)$$

$$+ \frac{1}{1400}\left[\frac{11}{21}, 1, \frac{22}{9}\right]_{i-1,j} P^{(0,1)}_{i,j+1} \quad (-)$$

$$- \frac{1}{1050}\left[\frac{1}{14}, 1, \frac{1}{3}\right]_{i-1,j} P^{(1,1)}_{i,j+1} (3) = 0$$

$$i = 2 \text{ to } I + 1, \; j = 1 \text{ to } J \qquad \text{(D2.7)}$$

(viii) From taking arbitrary variations in all $P^{(1,1)*}_{i,j}$ (3),
$i = 2$ to $I + 1$, $j = 2$ to $J + 1$:

$$\frac{13}{4200}\left[\frac{13}{42}, -1, -1\right]_{i-1,j-1} P^{(0,0)}_{i-1,j-1}$$

$$+ \frac{1}{1400}\left[\frac{13}{42}, \frac{13}{9}, -1\right]_{i-1,j-1} P^{(1,0)}_{i-1,j-1} (+)$$

$$+\frac{1}{1400}\left[\frac{13}{42},\ -1,\ \frac{13}{9}\right]_{i-1,j-1} P^{(0,1)}_{i-1,j-1} (+)$$

$$+\frac{1}{4200}\left[\frac{3}{14},\ 1,\ 1\right]_{i-1,j-1} P^{(1,1)}_{i-1,j-1} \quad (1)$$

$$+\frac{1}{2100}\left[\frac{13}{42},\ \frac{13}{2},\ -11\right]_{i-1,j-1} P^{(0,0)}_{i,j-1}$$

$$-\frac{1}{1050}\left[\frac{13}{42},\ \frac{13}{3},\ -1\right]_{i-1,j-1} P^{(1,0)}_{i,j-1} \quad (-)$$

$$+\frac{1}{1400}\left[\frac{11}{21},\ 1,\ \frac{22}{9}\right]_{i-1,j-1} P^{(0,1)}_{i,j-1} \quad (+)$$

$$-\frac{1}{1050}\left[\frac{1}{14},\ 1,\ \frac{1}{3}\right]_{i-1,j-1} P^{(1,1)}_{i,j-1} \quad (2)$$

$$+\frac{1}{2100}\left[\frac{143}{42},\ -11,\ \frac{13}{2}\right]_{i-1,j-1} P^{(0,0)}_{i-1,j}$$

$$+\frac{1}{1400}\left[\frac{11}{21},\ \frac{22}{9},\ 1\right]_{i-1,j-1} P^{(1,0)}_{i-1,j} \quad (+)$$

$$-\frac{1}{1050}\left[\frac{13}{42},\ -1,\ \frac{13}{3}\right]_{i-1,j-1} P^{(0,1)}_{i-1,j} \quad (-)$$

$$-\frac{1}{1050}\left[\frac{1}{14},\ \frac{1}{3},\ 1\right]_{i-1,j-1} P^{(1,1)}_{i-1,j} \quad (4)$$

$$+\frac{11}{2100}\left[\frac{11}{21},\ 1,\ 1\right]_{i-1,j-1} P^{(0,0)}_{i,j}$$

$$-\frac{1}{1050}\left[\frac{11}{21},\ \frac{22}{3},\ 1\right]_{i-1,j-1} P^{(1,0)}_{i,j} \quad (-)$$

$$- \frac{1}{1050}\left[\frac{11}{21}, 1, \frac{22}{3}\right]_{i-1,j-1} P_{i,j}^{(0,1)} \quad (-)$$

$$+ \frac{2}{1575}\left[\frac{1}{14}, 1, 1\right]_{i-1,j-1} P_{i,j}^{(1,1)} \quad (3) \quad = \quad 0$$

$$i = 2 \text{ to } I + 1, \; j = 2 \text{ to } J + 1 \qquad \text{(D2.8)}$$

(ix) From taking arbitrary variations in all $P_{i,j}^{(1,1)*}$ (4),

$i = 1$ to I, $j = 2$ to $J + 1$:

$$- \frac{1}{2100}\left[\frac{143}{42}, \frac{13}{2}, -11\right]_{i,j-1} P_{i,j-1}^{(0,0)}$$

$$- \frac{1}{1050}\left[\frac{13}{42}, \frac{13}{3}, -1\right]_{i,j-1} P_{i,j-1}^{(1,0)} \quad (+)$$

$$- \frac{1}{1400}\left[\frac{11}{21}, 1, \frac{22}{9}\right]_{i,j-1} P_{i,j-1}^{(0,1)} \quad (+)$$

$$- \frac{1}{1050}\left[\frac{1}{14}, 1, \frac{1}{3}\right]_{i,j-1} P_{i,j-1}^{(1,1)} \quad (1)$$

$$- \frac{13}{4200}\left[\frac{13}{42}, -1, -1\right]_{i,j-1} P_{i+1,j-1}^{(0,0)}$$

$$+ \frac{1}{1400}\left[\frac{13}{42}, \frac{13}{9}, -1\right]_{i,j-1} P_{i+1,j-1}^{(1,0)} \quad (-)$$

$$- \frac{1}{1400}\left[\frac{13}{42}, -1, \frac{13}{9}\right]_{i,j-1} P_{i+1,j-1}^{(0,1)} \quad (+)$$

$$+ \frac{1}{4200}\left[\frac{13}{14}, 1, 1\right]_{i,j-1} P_{i+1,j-1}^{(1,1)} \quad (2)$$

$$- \frac{11}{2100}\left[\frac{11}{21},\ 1,\ 1\right]_{i,j-1} P_{i,j}^{(0,0)}$$

$$- \frac{1}{1050}\left[\frac{11}{21},\ \frac{22}{3},\ 1\right]_{i,j-1} P_{i,j}^{(1,0)} \quad (+)$$

$$+ \frac{1}{1050}\left[\frac{11}{21},\ 1,\ \frac{22}{3}\right]_{i,j-1} P_{i,j}^{(0,1)} \quad (-)$$

$$+ \frac{2}{1575}\left[\frac{1}{14},\ 1,\ 1\right]_{i,j-1} P_{i,j}^{(1,1)} \quad (4)$$

$$- \frac{1}{2100}\left[\frac{143}{42},\ -11,\ \frac{13}{2}\right]_{i,j-1} P_{i+1,j}^{(0,0)}$$

$$+ \frac{1}{1400}\left[\frac{11}{21},\ \frac{22}{9},\ 1\right]_{i,j-1} P_{i+1,j}^{(1,0)} \quad (-)$$

$$+ \frac{1}{1050}\left[\frac{13}{42},\ -1,\ \frac{13}{3}\right]_{i,j-1} P_{i+1,j}^{(0,1)} \quad (-)$$

$$- \frac{1}{1050}\left[\frac{1}{14},\ \frac{1}{3},\ 1\right]_{i,j-1} P_{i+1,j}^{(1,1)} \quad (3) \quad = \quad 0$$

$$i = 1 \text{ to } I,\ j = 2 \text{ to } J + 1 \qquad \text{(D2.9)}$$

(x) Zero flux boundary condition on the left:

Set $P_{1,j}^{(0,0)} = \delta P_{1,j}^{(0,0)*} = 0$, $j = 1$ to $J + 1$, this will eliminate $J + 1$ equations from Eq. D2.1. Zero flux boundary conditions on other edges can be treated in the same way.

(xi) Zero current boundary conditions on the left:

Set $P^{(1,0)}_{1,j}(+) = \delta P^{(1,0)}_{1,j}(+)^* = 0$, $j = 1$ to $J + 1$,

this will eliminate $J + 1$ equations from Eq. D2.2.

Zero current b. c. on other edges can be treated in the same way.

APPENDIX E

DIFFERENCE EQUATION COEFFICIENTS RESULTING FROM USE OF THE FINITE ELEMENT SYNTHESIS APPROXIMATION METHOD IN TWO-DIMENSION

The GxG matrix coefficients resulting from the finite element synthesis method using bi-linear basis functions in two-dimensional multigroup diffusion theory are defined below.

In order to simplify the forms of the coefficients, it is convenient to define the following GxG matrices:

$$\mathbb{K}_{i,j}(x,y) = \psi^{*T}_{i,j}(x,y)\, \mathbb{A}_{i,j}(x,y) h_{xi} h_{yj}\, \psi_{i,j}(x,y)$$

$$\mathbb{L}^{X}_{i,j}(x,y) = \xi^{*T}_{i,j}(x,y)\, \mathbb{D}^{-1}_{i,j}(x,y) h_{xi} h_{yj}\, \xi_{i,j}(x,y)$$

$$\mathbb{L}^{Y}_{i,j}(x,y) = \eta^{*T}_{i,j}(x,y)\, \mathbb{D}^{-1}_{i,j}(x,y) h_{xi} h_{yj}\, \eta_{i,j}(x,y)$$

$$\mathbb{N}^{X}_{i,j}(x,y) = \xi^{*T}_{i,j}(x,y)\, \psi_{i,j}(x,y) h_{yj}$$

$$\mathbb{N}^{Y}_{i,j}(x,y) = \eta^{*T}_{i,j}(x,y)\, \psi_{i,j}(x,y) h_{xi}$$

$$\mathbb{M}^{X}_{i,j}(x,y) = \psi^{*T}_{i,j}(x,y)\, \xi_{i,j}(x,y) h_{yj}$$

$$\mathbb{M}^{Y}_{i,j}(x,y) = \psi^{*T}_{i,j}(x,y)\, \eta_{i,j}(x,y) h_{xi}$$

$$R^X_{i,j}(x,y) = \psi^{*T}_{i,j}(x,y)\, \mathbb{D}_{i,j}(x,y)\, \frac{h_{yj}}{h_{xi}}\, \psi_{i,j}(x,y)$$

$$R^Y_{i,j}(x,y) = \psi^{*T}_{i,j}(x,y)\, \mathbb{D}_{i,j}(x,y)\, \frac{h_{xi}}{h_{yj}}\, \psi_{i,j}(x,y)$$

for each region (i,j), and

$$S_{i,-j}(x) = \frac{h_{xi}}{h_{yj}}\, \psi^{*T}_{i,j}(x,1)\, \mathbb{D}_{i,j}(x,0)\, \psi_{i,j}(x,0)$$

$$S_{i,j-}(x) = \frac{h_{xi}}{h_{yj}}\, \psi^{*T}_{i,j}(x,0)\, \mathbb{D}_{i,j}(x,0)\, \psi_{i,j-1}(x,1)$$

$$S_{i,+j}(x) = \frac{h_{xi}}{h_{yj}}\, \psi^{*T}_{i,j+1}(x,0)\, \mathbb{D}_{i,j}(x,1)\, \psi_{i,j}(x,1)$$

$$S_{i,j+}(x) = \frac{h_{xi}}{h_{yj}}\, \psi^{*T}_{i,j}(x,1)\, \mathbb{D}_{i,j}(x,1)\, \psi_{i,j+1}(x,0)$$

for each horizontal region interface and

$$T_{-i,j}(y) = \frac{h_{yj}}{h_{xi}}\, \psi^{*T}_{i-1,j}(1,y)\, \mathbb{D}_{i,j}(0,y)\, \psi_{i,j}(0,y)$$

$$T_{i-,j}(y) = \frac{h_{yj}}{h_{xi}}\, \psi^{*T}_{i,j}(0,y)\, \mathbb{D}_{i,j}(0,y)\, \psi_{i-1,j}(1,y)$$

$$T_{+i,j}(y) = \frac{h_{yj}}{h_{xi}}\, \psi^{*T}_{i+1,j}(0,y)\, \mathbb{D}_{i,j}(1,y)\, \psi_{i,j}(1,y)$$

$$T_{i+,j}(y) = \frac{h_{yj}}{h_{xi}}\, \psi^{*T}_{i,j}(1,y)\, \mathbb{D}_{i,j}(1,y)\, \psi_{i+1,j}(0,y)$$

for each vertical region interface.

Also define the GxG matrix $\mathbb{E}_{i,j}(a,b;\ c,d)$ as

$$\mathbb{E}_{i,j}(a,b;\ c,d) = \int_0^1 dx \int_0^1 dy \Big\langle p_a(x)p_b(y)\{[\mathbb{K}_{i,j}(x,y) - \mathbb{L}^X_{i,j}(x,y) - \mathbb{L}^Y_{i,j}(x,y)]p_c(x)p_d(y) - \mathbb{N}^X_{i,j}(x,y)q_c(x)p_d(y) - \mathbb{N}^Y_{i,j}(x,y)p_c(x)q_d(y)\} + q_a(x)p_b(y)[\mathbb{M}^X_{i,j}(x,y)p_c(x)p_d(y) + \mathbb{R}^X_{i,j}(x,y)q_c(x)p_d(y)] + p_a(x)q_b(y)[\mathbb{M}^Y_{i,j}(x,y)p_c(x)p_c(y) + \mathbb{R}^Y_{i,j}(x,y)p_c(x)q_d(y)]\Big\rangle \qquad (E.1)$$

where a,b,c and d are equal to either 1 or 2 and

$$p_1(x) = (1-x)$$
$$p_2(x) = x$$
$$q_1(x) = -\frac{d}{dx}p_1(x) = 1$$
$$q_2(x) = -\frac{d}{dx}p_2(x) = -1$$

for each region (i,j), i = 1 to I, j = 1 to J. Then with the understanding that all nuclear constants outside the reactor region should be set equal to zero, we can write the matrix coefficients in the following form:

(i) Zero-current or Symmetry Boundary Conditions on All Four Boundaries

$$\underline{aa}_{i,j} = \psi^{*T^{-1}}_{i-1,j-1}(1)\, \mathbb{E}_{i-1,j-1}(2,2;\ 1,1)\ \psi^{-1}_{i-1,j-1}(0,0)$$

$$+ \frac{1}{2}\int_0^1 dy p_2(y)p_1(y)\{\psi^{*T^{-1}}_{i-1,j-1}(1,1)[\ \mathbb{R}^X_{i-1,j-1}(1,y)$$

$$- \mathbb{R}^X_{i-1,j-1}(0,y)]\psi^{-1}_{i-1,j-1}(0,0)$$

$$+ \psi^{*T^{-1}}_{i-1,j-1}(1,1)T_{i-1-,j-1}(y)\psi^{-1}_{i-2,j-1}(1,0)$$

$$- \psi^{*T^{-1}}_{i,j-1}(0,1)T_{+i-1,j-1}(y)\psi^{-1}_{i-1,j-1}(0,0)\}$$

$$+ \frac{1}{2}\int_0^1 dx p_2(x)p_1(x)\{\psi^{*T^{-1}}_{i-1,j-1}(1,1)[\mathbb{R}^Y_{i-1,j-1}(x,1)$$

$$- \mathbb{R}^Y_{i-1,j-1}(x,0)]\psi^{-1}_{i-1,j-1}(0,0)$$

$$+ \psi^{*T^{-1}}_{i-1,j-1}(1,1)S_{i-1,j-1-}(x)\psi^{-1}_{i-1,j-2}(0,1)$$

$$- \psi^{*T^{-1}}_{i,j-1}(1,0)S_{i-1,+j-1}(x)\psi^{-1}_{i-1,j-1}(0,0)\}$$

$$i = 2 \text{ to } I + 1,\ j = 2 \text{ to } J + 1$$

$$\underline{ab}_{i,j} = \psi^{*T^{-1}}_{i-1,j-1}(1,1)\ \mathbb{E}_{i-1,j-1}(2,2;1,2)\psi^{-1}_{i-1,j-1}(0,1)$$

$$+ \psi^{*T^{-1}}_{i-1,j}(1,0)\ \mathbb{E}_{i-1,j}(2,1;1,1)\psi^{-1}_{i-1,j}(0,0)$$

$$+ \frac{1}{2}\int_0^1 dy p_1(y)p_1(y)\{\psi^{*T^{-1}}_{i-1,j}(1,0)[\mathbb{R}^X_{i-1,j}(1,y)$$

$$- \mathbb{R}^X_{i-1,j}(0,y)]\psi^{-1}_{i-1,j}(0,0)$$

$$+ \psi^{*T^{-1}}_{i-1,j}(1,0)\ T_{i-1,j}(y)\psi^{-1}_{i-2,j}(1,0)$$

$$- \psi^{*T^{-1}}_{i,j}(0,0)T_{+i-1,j}(y)\psi^{-1}_{i-1,j}(0,0)\}$$

$$+ \frac{1}{2}\int_0^1 dy p_2(y)p_2(y)\{\psi^{*T^{-1}}_{i-1,j-1}(1,1)[\mathbb{R}^X_{i-1,j-1}(1,y)$$

$$- \mathbb{R}^X_{i-1,j-1}(0,y)]\psi^{-1}_{i-1,j-1}(0,1)$$

$$+ \psi^{*T^{-1}}_{i-1,j-1}(1,1)T_{i-1,j-1}(y)\psi^{-1}_{i-2,j-1}(1,1)$$

$$- \psi^{*T^{-1}}_{i,j-1}(0,1)T_{+i-1,j-1}(y)\psi^{-1}_{i-1,j-1}(0,1)\}$$

$$+ \frac{1}{2}\int_0^1 dx p_2(x)p_1(x)\{\psi^{*T^{-1}}_{i-1,j-1}(1,1)[S_{i-1,j}(x)$$

$$- S_{i-1,j-1+}(x)]\psi^{-1}_{i-1,j}(0,0)$$

$$+ \psi^{*T^{-1}}_{i-1,j}(1,0)[S_{i-1,+j-1}(x) - S_{i-1,j-}(x)]\psi^{-1}_{i-1,j-1}(0,1)\}$$

$$i = 2 \text{ to } I + 1,\ j = 1 \text{ to } J + 1$$

$$\underline{ac}_{i,j} = \psi^{*T^{-1}}_{i-1,j}(1,0)\, \mathbb{E}_{i-1,j}(2,1;1,2)\psi^{-1}_{i-1,j}(0,1)$$

$$+ \frac{1}{2}\int_0^1 dy p_1(y)p_2(y)\{\psi^{*T^{-1}}_{i-1,j}(1,0)[\, \mathbb{R}^X_{i-1,j}(1,y)$$

$$- \mathbb{R}^X_{i-1,j}(0,y)]\psi^{-1}_{i-1,j}(0,1)$$

$$+ \psi^{*T^{-1}}_{i-1,j}(1,0)T_{i-1-,j}(y)\psi^{-1}_{i-2,j}(1,1)$$

$$- \psi^{*T^{-1}}_{i,j}(0,0)T_{+i-1,j}(y)\psi^{-1}_{i-1,j}(0,1)\}$$

$$+ \frac{1}{2}\int_0^1 dx p_2(x)p_1(x)\{\psi^{*T^{-1}}_{i-1,j}(1,0)\ [\mathbb{R}^X_{i-1,j}(x,0)$$

$$- \mathbb{R}^Y_{i-1,j}(x,1)]\psi^{-1}_{i-1,j}(0,1)$$

$$+ \psi^{*T^{-1}}_{i-1,j}(1,0)_{S_{i-1,j+}}(x)\psi^{-1}_{i-1,j+1}(0,0)$$

$$- \psi^{*T^{-1}}_{i-1,j-1}(1,1)S_{i-1,j}(x)\psi^{-1}_{i-1,j}(0,1)\}$$

$$i = 2 \text{ to } I + 1,\ j = 1 \text{ to } J$$

$$\underline{ba}_{i,j} = \psi^{*T^{-1}}_{i-1,j-1}(1,1)\ \mathbb{E}_{i-1,j-1}(2,2;2,1)\psi^{-1}_{i-1,j-1}(1,0)$$

$$+ \psi^{*T^{-1}}_{i,j-1}(0,1)\ \mathbb{E}_{i,j-1}(1,2;1,1)\psi^{-1}_{i,j-1}(0,0)$$

$$+ \frac{1}{2}\int_0^1 dy p_2(y)p_1(y)\{\psi^{*T^{-1}}_{i-1,j-1}(1,1)\,[T_{-i,j-1}(y)$$

$$- T_{i-1+,j-1}(y)]\psi^{-1}_{i,j-1}(0,0)$$

$$+ \psi^{*T^{-1}}_{i,j-1}(0,1)[T_{+i-1,j-1}(y) - T_{i-,j-1}(y)]\psi^{-1}_{i-1,j-1}(1,0)\}$$

$$+ \frac{1}{2}\int_0^1 dx p_1(x)p_1(x)\{\psi^{*T^{-1}}_{i,j-1}(0,1)\ [\mathbb{R}^{Y}_{i,j-1}(x,1)$$

$$- \mathbb{R}^{Y}_{i,j-1}(x,0)]\psi^{-1}_{i,j-1}(0,0)$$

$$+ \psi^{*T^{-1}}_{i,j-1}(0,1)S_{i,j-1-}(x)\psi^{-1}_{i,j-2}(0,1)$$

$$- \psi^{*T^{-1}}_{i,j}(0,0)S_{i,+j-1}(x)\psi^{-1}_{i,j-1}(0,0)\}$$

$$+ \frac{1}{2}\int_0^1 dx p_2(x)p_2(x)\{\psi^{*T^{-1}}_{i-1,j-1}(1,1)\ [\mathbb{R}^{Y}_{i-1,j-1}(x,1)$$

$$- \mathbb{R}^{X}_{i-1,j-1}(x,0)]\psi^{-1}_{i-1,j-1}(1,0)$$

$$+ \psi^{*T^{-1}}_{i-1,j-1}(1,1)S_{i-1,j-1-}(x)\psi^{-1}_{i-1,j-2}(1,1)$$

$$- \psi^{*T^{-1}}_{i-1,j}(1,0)S_{i-1,+j-1}(x)\psi^{-1}_{i-1,j-1}(1,0)\}$$

$$i = 1 \text{ to } I + 1,\ j = 2 \text{ to } J + 1$$

$$\underline{bb}_{i,j} = \psi^{*T^{-1}}_{i,j}(0,0)\ \mathbb{E}_{i,j}(1,1;1,1)\psi^{-1}_{i,j}(0,0)$$

$$+ \psi^{*T^{-1}}_{i-1,j}(1,0)\ \mathbb{E}_{i-1,j}(2,1;2,1)\psi^{-1}_{i-1,j}(1,0)$$

$$+ \psi^{*T^{-1}}_{i-1,j-1}(1,1)\ \mathbb{E}_{i-1,j-1}(2,2;2,2)\psi^{-1}_{i-1,j-1}(1,1)$$

$$+ \psi^{*T^{-1}}_{i,j-1}(0,1)\ \mathbb{E}_{i,j-1}(1,2;1,2)\psi^{-1}_{i,j-1}(0,1)$$

$$+ \frac{1}{2}\int_0^1 dy p_1(y)p_1(y)\{\psi^{*T^{-1}}_{i,j}(0,0)[T_{+i-1,j}(y)$$

$$- T_{i-,j}(y)]\psi^{-1}_{i-1,j}(1,0)$$

$$+ \psi^{*T^{-1}}_{i-1,j}(1,0)[T_{-i,j}(y) - T_{i-1+,j}(y)]\psi^{-1}_{i,j}(0,0)\}$$

$$+ \frac{1}{2}\int_0^1 dy p_2(y)p_2(y)\{\psi^{*T^{-1}}_{i-1,j-1}(1,1)[T_{-i,j-1}(y)$$

$$- T_{i-1+,j-1}(y)]\psi^{-1}_{i,j-1}(0,1)$$

$$+ \psi^{*T^{-1}}_{i,j-1}(0,1)[T_{+i-1,j-1}(y) - T_{i-,j-1}(y)]\psi^{-1}_{i-1,j-1}(1,1)\}$$

$$+ \frac{1}{2}\int_0^1 dx p_1(x)p_1(x)\{\psi^{*T^{-1}}_{i,j-1}(0,1)[S_{i,j}(x)$$

$$- S_{i,j-1+}(x)]\ \psi^{-1}_{i,j}(0,0)$$

$$+ \psi^{*T^{-1}}_{i,j}(0,0)[S_{i,+j-1}(x)-S_{i,j-}(x)]\psi^{-1}_{i,j-1}(0,1)\}$$

$$+ \frac{1}{2}\int_0^1 dx p_2(x)p_2(x)\{\psi^{*T^{-1}}_{i-1,j-1}(1,1)[S_{i-1,-j}(x)$$

$$- S_{i-1,j-1+}(x)]\psi^{-1}_{i-1,j}(1,0)$$

$$+ \psi^{*T^{-1}}_{i-1,j}(1,0)[S_{i-1,+j-1}(x) - S_{i-1,j-}(x)]\psi^{-1}_{i-1,j-1}(1,1)\}$$

$$i = 1 \text{ to } I + 1,\ j = 1 \text{ to } J + 1$$

$$\underline{bc}_{i,j} = \psi^{*T^{-1}}_{i-1,j}(1,0)\ \mathbb{E}_{i-1,j}(2,1;2,2)\psi^{-1}_{i-1,j}(1,1)$$

$$+ \psi^{*T^{-1}}_{i,j}(0,0)\ \mathbb{E}_{i,j}(1,1;1,2)\psi^{-1}_{i,j}(0,1)$$

$$+ \frac{1}{2}\int_0^1 dy p_1(y)p_2(y)\{\psi^{*T^{-1}}_{i,j}(0,0)[T_{+i-1,j}(y)$$

$$- T_{i-,j}(y)]\psi^{-1}_{i-1,j}(1,1)$$

$$+ \psi^{*T^{-1}}_{i-1,j}(1,0)[T_{-i,j}(y)-T_{i+1+,j}(y)]\psi^{-1}_{i,j}(0,1)\}$$

$$+ \frac{1}{2}\int_0^1 dx p_1(x)p_1(x)\{\psi^{*T^{-1}}_{i,j}(0,0)[\mathbb{R}^Y_{i,j}(x,0)$$

$$- \mathbb{R}^Y_{i,j}(x,1)]\psi^{-1}_{i,j}(0,1)$$

$$+ \psi^{*T^{-1}}_{i,j}(0,0) S_{i,j+}(x) \psi^{-1}_{i,j+1}(0,0)$$

$$- \psi^{*T^{-1}}_{i,j-1}(0,1) S_{i,-j}(x) \psi^{-1}_{i,j}(0,1)\}$$

$$+ \frac{1}{2} \int_0^1 dx p_2(x) p_2(x) \{\psi^{*T^{-1}}_{i-1,j}(1,0) [\mathbb{R}^Y_{i-1,j}(x,0)$$

$$- \mathbb{R}^Y_{i-1,j}(x,1)] \psi^{-1}_{i-1,j-1}(1,1)$$

$$+ \psi^{*T^{-1}}_{i-1,j}(1,0) S_{i-1,j+}(x) \psi^{-1}_{i-1,j+1}(1,0)$$

$$- \psi^{*T^{-1}}_{i-1,j-1}(1,1) S_{i-1,-j}(x) \psi^{-1}_{i-1,j}(1,1)\}$$

$$i = 1 \text{ to } I + 1, \; j = 1 \text{ to } J$$

$$\underline{ca}_{i,j} = \psi^{*T^{-1}}_{i,j-1}(0,1) \, \mathbb{E}_{i,j-1}(1,2;2,1) \psi^{-1}_{i,j-1}(1,0)$$

$$+ \frac{1}{2} \int_0^1 dy p_2(y) p_1(y) \{\psi^{*T^{-1}}_{i,j-1}(0,1) [\mathbb{R}^X_{i,j-1}(0,y)$$

$$- \mathbb{R}^X_{i,j-1}(1,y)] \psi^{-1}_{i,j-1}(1,0)$$

$$+ \psi^{*T^{-1}}_{i,j-1}(0,1) T_{i+,j-1}(y) \psi^{-1}_{i+1,j-1}(0,0)$$

$$- \psi^{*T^{-1}}_{i-1,j-1}(1,1) T_{-i,j-1}(y) \psi^{-1}_{i,j-1}(1,0)\}$$

$$+ \frac{1}{2}\int_0^1 dx p_1(x)p_2(x)\{\psi^{*T^{-1}}_{i,j-1}(0,1)[\,\mathbb{R}^{Y}_{i,j-1}(x,1)$$

$$- \mathbb{R}^{Y}_{i,j-1}(x,0)]\psi^{-1}_{i,j-1}\,(1,0)$$

$$+ \psi^{*T^{-1}}_{i,j-1}(0,1)S_{i,j-1-}(x)\psi^{-1}_{i,j-2}(1,1)$$

$$-\psi^{*T^{-1}}_{i,j}(0,0)S_{i,+j-1}(x)\psi^{-1}_{i,j-1}(1,0)\}$$

$$i = 1 \text{ to } I,\ j = 2 \text{ to } J+1$$

$$\underline{cb}_{i,j} = \psi^{*T^{-1}}_{i,j}(0,0)\,\mathbb{E}_{i,j}(1,1;2,1)\psi^{-1}_{i,j}(1,0)$$

$$+ \psi^{*T^{-1}}_{i,j-1}(0,1)\,\mathbb{E}_{i,j-1}(1,2;2,2)\psi^{-1}_{i,j-1}(0,1)$$

$$+ \frac{1}{2}\int_0^1 dy p_1(y)p_1(y)\{\psi^{*T^{-1}}_{i,j}(0,0)[\mathbb{R}^{X}_{i,j}(0,y) - \mathbb{R}^{X}_{i,j}(1,y)]\,\psi^{-1}_{i,j}(1,0)$$

$$+ \psi^{*T^{-1}}_{i,j}(0,0)T_{i+,j}(y)\psi^{-1}_{i+1,j}(0,0)$$

$$+\psi^{*T^{-1}}_{i-1,j}(1,0)T_{-i,j}(y)\psi^{-1}_{i,j}(1,0)\}$$

$$+ \frac{1}{2}\int_0^1 dy p_2(y)p_2(y)\{\psi^{*T^{-1}}_{i,j-1}(0,1)[\,\mathbb{R}^{X}_{i,j-1}(0,y)$$

$$- \mathbb{R}^{X}_{i,j-1}(1,y)]\psi^{-1}_{i,j-1}(1,1)$$

$$+ \psi^{*T^{-1}}_{i,j-1}(0,1)T_{i+,j-1}(y)\psi^{-1}_{i+1,j-1}(0,1)$$

$$- \psi^{*T^{-1}}_{i-1,j-1}(1,1)T_{-i,j-1}(y)\psi^{-1}_{i,j-1}(1,1)\}$$

$$+ \frac{1}{2}\int_0^1 dx p_1(x)p_2(x)\{\psi^{*T^{-1}}_{i,j-1}(0,1)[S_{i,-j}(x)-S_{i,j-1+}(x)]\psi^{-1}_{i,j}(1,0)$$

$$+ \psi^{*T^{-1}}_{i,j}(0,0)[S_{i,+j-1}(x)-S_{i,j-}(x)]\psi^{-1}_{i,j-1}(1,1)\}$$

$$i = 1 \text{ to } I,\ j = 1 \text{ to } J + 1$$

$$\underline{cc}_{i,j} = \psi^{*T^{-1}}_{i,j}(0,0)\,\mathbb{E}_{i,j}(1,1;2,2)\psi^{-1}_{i,j}(1,1)$$

$$+ \frac{1}{2}\int_0^1 dy p_1(y)p_2(y)\{\psi^{*T^{-1}}_{i,j}(0,0)[\mathbb{R}^X_{i,j}(0,y)$$

$$- \mathbb{R}^X_{i,j}(1,y)]\psi^{-1}_{i,j}(1,1) + \psi^{*T^{-1}}_{i,j}(0,0)T_{i+,j}(y)\psi^{-1}_{i+1,j}(0,1)$$

$$- \psi^{*T^{-1}}_{i-1,j}(1,0)T_{-i,j}(y)\psi^{-1}_{i,j}(1,1)\}$$

$$+ \frac{1}{2}\int_0^1 dx p_1(x)p_2(x)\{\psi^{*T^{-1}}_{i,j}(0,0)\ [\mathbb{R}^Y_{i,j}(x,0)$$

$$- \mathbb{R}^Y_{i,j}(x,1)]\psi^{-1}_{i,j}(1,1) + \psi^{*T^{-1}}_{i,j}(0,0)S_{i,j+}(x)\psi^{-1}_{i,j+1}(1,0)$$

$$- \psi^{*T^{-1}}_{i,j-1}(0,1)S_{i,-j}(x)\psi^{-1}_{i,j}(1,1)\}$$

$$i = 1 \text{ to } I,\ j = 1 \text{ to } J$$

(ii) Zero Flux Boundary Condition on Certain Boundaries

If the left boundary has a zero-flux condition and the other three boundaries have symmetry conditions, then we should use the following equations:

$$\underline{bb}_{2,1}P_{2,1} + \underline{bc}_{2,1}P_{2,2} + \underline{cb}_{2,1}P_{3,1} + \underline{cc}_{2,1}P_{3,2} = 0$$

$$\underline{ba}_{2,j}P_{2,j-1} + \underline{bb}_{2,j}P_{2,j} + \underline{bc}_{2,j}P_{2,j+1} + \underline{ca}_{2,j}P_{3,j-1} + \underline{cb}_{2,j}P_{3,j} + \underline{cc}_{2,j}P_{3,j+1} = 0$$

; j = 2 to J

$$\underline{ba}_{2,J+1}P_{2,J} + \underline{bb}_{2,J+1}P_{2,J+1} + \underline{ca}_{2,J+1}P_{3,J} + \underline{cb}_{2,J+1}P_{3,J+1} = 0$$

$$\underline{ab}_{i,1}P_{i-1,1} + \underline{ac}_{i,1}P_{i-1,2} + \underline{bb}_{i,1}P_{i,1} + \underline{bc}_{i,1}P_{i,2} + \underline{cb}_{i,1}P_{i+1,1}$$

$$+ \underline{cc}_{i,1}P_{i+1,2} = 0; \quad i = 3 \text{ to } I + 1$$

$$\underline{aa}_{i,j}P_{i-1,j-1} + \underline{ab}_{i,j}P_{i-1,j} + \underline{ac}_{i,j}P_{i-1,j+1} + \underline{ba}_{i,j}P_{i,j-1} + \underline{bb}_{i,j}P_{i,j}$$

$$+ \underline{bc}_{i,j}P_{i,j+1} + \underline{ca}_{i,j}P_{i+1,j-1} + \underline{cb}_{i,j}P_{i+1,j} + \underline{cc}_{i,j}P_{i+1,j+1} = 0$$

; i = 3 to I + 1

j = 2 to J

$$\underline{aa}_{i,J+1}P_{i-1,J} + \underline{ab}_{i,J+1}P_{i-1,J+1} + \underline{ba}_{i,J+1}P_{i,J} + \underline{bb}_{i,J+1}P_{i,J+1}$$

$$+ \underline{ca}_{i,J+1}P_{i+1,J} + \underline{cb}_{i,J+1}P_{i+1,J+1} = 0; \quad i = 3 \text{ to } I + 1$$

where the matrix coefficients are defined the same way as in (i). The equations and coefficients for zero-flux conditions on other boundary or boundaries can be found similarly.

The implied zero-flux boundary conditions, as defined by trial functions Equations 4.11, will result in equations having the same forms as ordinary zero-flux conditions. However, the matrix coefficients must be changed by putting the appropriate modified basis functions, similar to Equations 4.12, in the corresponding regions.

APPENDIX F

LISTING OF THE COMPUTER PROGRAMS

FORTRAN listings of programs LIN1, LIN2, DOB1, DOB2, MAN1, and MAN2 are listed in only the first five copies of this report in the following six sections.